Åbo Akademi University

Erik Niemelä

Nanoparticles as Targeting System for Cancer Treatment

– From idea towards reality –

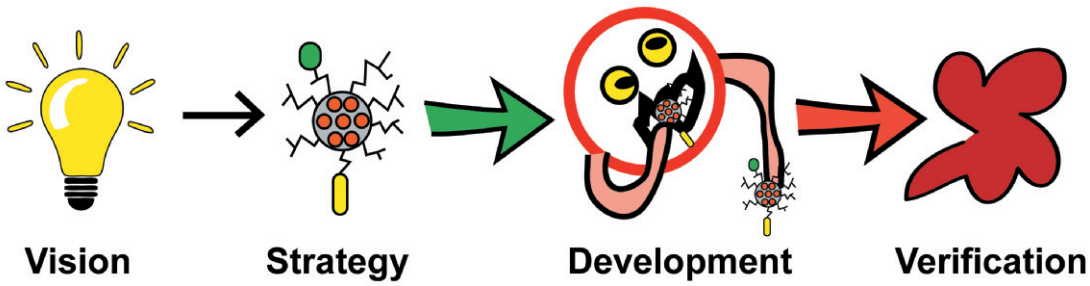

Erik Niemelä

Erik Niemelä graduated from Gymnasiet Grankulla Samskolan in 2006 and from Omnia media assistant school in 2008. He received his M.Sc. in Cell Biology from Åbo Akademi University in 2013. Since November 2013, he has been working as a graduate student in Professor John Eriksson's laboratory and co-supervised by Professor Jessica Rosenholm at the Faculty of Science and Engineering at Åbo Akademi University.

Cover image: "From idea towards reality"
By Erik Niemelä

Profile drawing by Ferdinand Rantakylä

Nanoparticles as Targeting System for Cancer Treatment

- From idea towards reality -

Erik Niemelä

Cell Biology
Faculty of Science and Engineering
Åbo Akademi University
Turku Bioscience Centre
University of Turku and Åbo Akademi University
Turku Doctoral Network in Molecular Biosciences
Åbo Akademi University
Turku, Finland
2019

From the Faculty of Science and Engineering, Cell Biology, Åbo Akademi University, Turku Bioscience Centre, University of Turku and Åbo Akademi University, Turku Doctoral Network in Molecular Biosciences (MolBio), Åbo Akademi University.

Supervised by
Professor John E. Eriksson
Faculty of Science and Engineering, Cell Biology, Åbo Akademi University,
Turku Bioscience Centre, University of Turku and Åbo Akademi University,
Turku, Finland

Co-supervised by
Professor Jessica M. Rosenholm
Faculty of Science and Engineering, Pharmaceutical Sciences Laboratory,
Åbo Akademi University,
Turku, Finland

Reviewed by
Associate Professor Hélder A. Santos
Drug Research Program, Faculty of Pharmacy, University of Helsinki
Helsinki Institute of Life Science, University of Helsinki,
Helsinki, Finland

and

Professor Gøril E. Flaten
Department of Pharmacy, The Arctic University of Norway,
Tromsø, Norway

Opponent
University Lecturer Róisín M. Owens
Department of Chemical Engineering and Biotechnology, University of Cambridge,
Cambridge, United Kingdom

ISBN 978-952-12-3854-3 (printed)
ISBN 978-952-12-3855-0 (digital)
Painosalama Oy – Turku, Finland 2019

To my dear family and friends

“Those who dare to fail miserably can achieve greatly”

John F. Kennedy

TABLE OF CONTENT

ABSTRACT

To be able to target cells of interest is one of the key aims in medicine today, because it could minimize side effects of drugs. This is of special importance in cancer therapies, were the treatment has serious side-effects on the patients healthy cells. Nanomedicine seeks to overcome this limitation by utilizing nanoparticles as drug carriers, as nanoparticles have shown considerable potential as targeted drug delivery systems and could thus be used in cancer treatment. The key is to figure out a novel way of targeting cells of interest; what are the differences in these cells that could be used as a Trojan horse for delivering the drug to the target tissue. The trick, however is to find what drug would benefit from being loaded to a nanoparticle carrier system. What drug incorporation method is plausible, what pore size can harbor that specific drug, what particle size would be optimal to be internalized without unspecific uptake? What kind of surface functionalization would yield the highest uptake in the cancer cell of interest and what could be the potential unwanted off-target effects?

In this thesis, we exploited the increased metabolism of cancer cells and high replication rate for designing mesoporous silica nanoparticles (MSNs) for targeted drug delivery. The faster a cell grows and divides, the higher the metabolism rate and DNA synthesis is, and thus, increased uptake of both glucose and folate molecules occurs. We used these cancer specific traits aiming for actively targeted drug delivery by either functionalizing the particle with sugar moieties, folic acid or its antagonist methotrexate. Subsequently, by loading the particles with molecules that intervene with processes that are more pronounced in cancer cells than healthy cells, it was possible to increase drug selectivity and efficacy even further.

In the first study, we loaded the particles with celastrol, which is an active molecule used in traditional Chinese medicine that has the ability to induce cell death in cancer cells that have a high rate of mitosis through destabilizing the mitotic spindle. In the second study, we utilized celastrol's ability in lower dosages to induce the heat shock response which could be beneficial in cells that suffer from protein aggregates, as increase in heat shock proteins can help remodel these aggregates back to their native form. This kind of targeted heat shock response could be beneficial for patients suffering from neurodegenerative diseases such as Alzheimer's and Parkinson's. In order to identify the cells that have induced the heat shock response, we created a tailor-made automated image analysis workflow based on the freely available BioImageXD software that can be used for numerous biological scenarios.

In the third and last study, we conjugated the nanoparticle with methotrexate (MTX) that acts as a folic acid antagonist and have been used in decades for chemotherapy; in this manner, we can create a targeting ligand that has an efficacy by itself. The benefit of using MTX as targeting ligand is that it opens the possibility to load the nanoparticle with a second active molecule that would further increase the efficacy of the treatment. This multidrug-loaded nanoparticle could be used for metastatic cancer therapy when conventional cancer treatments have a severe negative effect on the patient. The nanoparticle would seek the metastatic cell with the targeting ligand MTX, and then together with the second active molecule, in this case fingolimod (FTY720), induce apoptosis and stop the invading cancerous cell.

SAMMANFATTNING

Målstyrd läkemedelsbehandling och därmed minimeringen av biverkningar av läkemedel är viktiga forskningsområden inom medicin för tillfället. Minimeringen av biverkningarna är av särskild betydelse I samband med cancerterapier. Eftersom behandlingarna oftast har allvarliga biverkningar för patienten finns ett stort behov av nya och mer specifika behandlingsformer inom cancervård. Ett potentiellt sätt att uppnå målstyrd läkemedelsbehandling inom cancervård är att utnyttja nanopartiklar som läkemedelsbärare. Målsättningen är att läkemedlet upptas specifikt av cancercellerna och därmed minskar biverkningarna hos patienten. Nyckeln till att uppnå målstyrd läkemedelsbehandling är att hitta ett sätt att leverera läkemedlet specifikt åt cancercellerna med betydligt mindre upptagning hos de friska cellerna i resten av kroppen. Den avgörande frågan är, vilka unika egenskaper hos cancercellerna kan utnyttjas för att leverera läkemedlet specifikt till målvävnaderna. När det gäller nanopartiklar för målstyrd läkemedelsbehandling måste man även utreda vilka läkemedel som kunde dra nytta av att fyllas med eller konjugeras till en partikel, vilka läkemedelsintegreringsmetoder är möjliga samt vilken funktionalisering som ger upphov till största möjliga upptagning hos cancercellerna. Även partikel- och porstorleken har betydelse för upptagningen av läkemedlet. Dessutom är det viktigt att kartlägga de potentiella biverkningarna för att kunna föra vidare utvecklingen av nanopartiklar för målstyrd läkemedelsbehandling.

Denna avhandling innehåller tre akademiska studier där cancercellers avvikande egenskaper utnyttjas för att uppnå målstyrd läkemedelsbehandling. I den första studien utnyttjades cancercellers höga metabolism och ökade behov av socker. Genom att konjugera glukos till nanopartikeln levererades läkemedlet specifikt till de socker-hungriga cancercellerna. Nanopartikeln fylldes med läkemedlet celastrol som har förmågan att destabilisera mikrotubuli-nätverket i cancercellerna, vilket bidrar till att cancercellerna dör.

I den andra studien utnyttjades cancercellers tendens att uttrycka folsyra-receptorer på cellmembranet för att specifikt leverera små mängder celastrol till målcellerna för att aktivera den cellulära stressresponsen. Detta i sin tur ökar på mängden molekylära chaperoner som skyddar celler mot proteinaggregeringar genom att återställa proteinernas ursprungliga konfiguration. Proteinansamlingar är associerade med olika neurodegenerativa sjukdomar och därför kunde denna typ av behandling vara till nytta för patienter som lider av t.ex. Alzheimer och Parkinsons sjukdom. För att sedan identifiera vilka celler som aktiverat sin stressrespons skapade vi en skräddarsydd bildanalysmetod. Metoden är baserad på den fritt tillgängliga BioImageXD-programvaran och kunde användas för diverse olika biologiska scenarier. I den tredje och sista studien undersökte vi ifall den traditionella cytostatikan metotrexat (MTX), som är en folysra-antagonist, även kunde användas som målsökande ligand. Detta i sin tur möjliggör att partiklens inre kunde fyllas med ytterligarare ett läkemedel, i detta fall valdes molekylen fingolimod (FTY720) som tillsammans med cytostatikan skulle hämma cancercellers migration och inducera apoptos. Denna kombinatoriska nanopartikel skulle inte bara vara mer effektiv mot maligna tumörer än traditionell kemoterapi, utan patienten skulle också gynnas av betydligt lindrigare biverkningar.

LIST OF ORIGINAL PUBLICATIONS

I. **Niemelä E*, Desai D*, Nkizinkiko Y, Eriksson JE, Rosenholm JM.** Sugar-decorated mesoporous silica nanoparticles as delivery vehicles for the poorly soluble drug celastrol enables targeted induction of apoptosis in cancer cells. *Eur J Pharm Biopharm. 2015 Jul 14. pii: S0939-6411(15)00298-2. doi: 10.1016/j.ejpb.2015.07.009 (*equal contribution).*

II. **Niemelä E, Desai D, Lundsten E, Rosenholm JM, Kankanpää P, Eriksson JE.** Quantitative bioimage analytics enables measurement of targeted cellular stress response induced by celastrol-loaded nanoparticles. *Cell Stress Chaperones. 2019 May 11. doi: 10.1007/s12192-019-00999-9.*

III. **Niemelä E, Desai D, Niemi R, Milena D, Özliseli E, Kemppainen K, Rahman NA, Sahlgren C, Törnquist K, Eriksson JE, Rosenholm JM.** Nanoparticles carrying fingolimod and methotrexate enables targeted induction of apoptosis and immobilization of invasive thyroid cancer. *Submitted to European Journal of Pharmaceutics and Biopharmaceutics, 02.08.2019.*

LIST OF ADDITIONAL PUBLICATIONS

IV. **Sarfraz J, Borzenkov M, Niemelä E, Weinberger C, Törngren B, Rosqvist E, Collini M, Pallavicini P, Eriksson J, Peltonen J, Ihalainen P, Chirico G.** Photo-thermal and cytotoxic properties of inkjet-printed copper sulfide films on biocompatible latex coated substrates. *Appl Surf Sci. 2017 Nov 28;435:1087-1095. doi: 10.1016/j.apsusc.2017.11.203.*

V. **Rosqvist E, Niemelä E, Venu AP, Kummala R, Ihalainen P, Franz S, Eriksson JE, Peltonen J.** Human Dermal Fibroblast proliferation controlled by surface roughness of two-component nanostructured latex polymer coatings. *Colloids Surf B Biointerfaces. 2019 Feb 1;174:136-144. doi: 10.1016/j.colsurfb.2018.10.064.*

VI. **Rosqvist E*, Niemelä E*, Frisk J, Öhblom H, Koppolu R, Abdelkader H, Soto Véliz D, Mennillo M, Arun AP, Ihalainen P, Aubert M, Sandler N, Wilén C, Toivakka M, Eriksson JE, Österbacka R, Peltonen J.** A Low-cost Paper-Based Platform for Fast and Reliable Screening of Cellular Interactions with Materials. S*ubmission ready manuscript (*equal contribution).*

LIST OF PATENTS

I. **A transparent or semi-transparent nanostructured latex film for flexible and semi-transparent electronics for monitoring and manipulating cellular processes**, International Patent Application No. PCT/FI2016/050590, Filing Date: 26.08.2016.

II. **A nanostructured latex film for controlling and monitoring bacterial cell growth in food packaging**, U.S. Patent Application No. 16/033265, Filing Date: 12.07.2018.

CONTRIBUTION OF THE AUTHOR

I: The author performed the majority of the cell-based *in vitro* experiments including particle internalization and drug efficacy measurements by flow cytometry, western blot analysis for detecting the drug induced heat shock response, and confocal microscopy for detecting particle uptake in cancer cells quantified by image analysis software BioImageXD. D. Desai was responsible for the synthesis, functionalization and characterization of the mesoporous silica nanoparticle (MSN), as well as the glucose consumption assay and specific particle internalization by comparing particle localization in cancer cells versus normal fibroblasts utilizing confocal microscopy. Y. Nkizinkiko performed spectrophotometry for validating the particle internalization in target cells. The author together with D. Desai was responsible of analyzing the *in vitro* data and writing the first draft of the paper.

II: The author was responsible for most of the cell-based *in vitro* experiments including the drug induced nuclear stress bodies (nSBs) formation detected by confocal microscopy, particle internalization and toxicity by flow cytometry, western blot analysis for detecting the heat shock response. The image analysis by BioImageXD for quantifying the nSBs positive cell population was performed by the author under the supervision of P. Kankaanpää. E. Lundsten performed the heat shock experiment as well as the manual quantification of the nSBs positive population from the confocal images. D. Desai was responsible for the synthesis, functionalization and characterization of the MSN as well as the specific particle internalization in HeLa cells by confocal microscopy. The author was responsible of analyzing most of the *in vitro* data and writing the first draft of the paper.

III: The author was responsible for the majority of the cell-based *in vitro* experiments and executed the particle internalization and drug efficacy measurements by flow cytometry, western blot analysis for detecting the receptor expression in cancer cells and normal cells, confocal microscopy for detecting particle internalization in cancer cells versus normal cells. The author performed the drug efficacy studies using traditional cell counting and crystal violet whereas D. Desai performed the metabolic assays for validating the enhanced drug efficacy utilizing MSNs as carrier systems as well as the non-drug loaded particle toxicity. D. Desai was responsible for the synthesis, functionalization and characterization of the MSN and together with the author planned the drug efficacy experiment that was conducted together with the external experts using advanced label free imaging technique (Phasefocus VL21). R. Niemi performed together with E. Özliseli the *in vivo* experiments utilizing the chick chorioallantoic membrane (CAM) assay for evaluating the drug efficacy. The author together with M. Doroszko was responsible for the histological studies including sample preparation and staining as well as the acquisition of tumor images using Pannoramic 250 Slide Scanner. K. Kemppainen was responsible for the *in vitro* invasion assay showing the metastatic nature of the thyroid cancer cells. The author was responsible of analyzing most of the *in vitro* and *in vivo* data and writing the first draft of the paper.

SYMBOLS AND ABBREVIATIONS

A	Area
ABC	ATP-binding cassette
ACA	Acetic acid
AFM	Atomic force microscopy
APTES	(3-Aminopropyl)triethoxysilane
APTMS	(3-Aminopropyl)trimethoxysilane
ATP	Adenosine triphosphate
BBB	Blood-brain-barrier
Bcl-2	Anti-apoptotic B-cell lymphoma gene 2
BCS	Biopharmaceutical classification system
BIR	Baculovirus inhibitior of apoptosis protein repeat
CDC	Centers for Disease Control and Prevention
c-FLIP	Cellular FLICE-inhibitory proteins
CLSM	Confocal laser scanning microscopy
CME	Clathrin-mediated endocytosis
CTAB	Cetyltrimethylammonium bromide
CTAC	Cetyltrimethylammonium chloride
CvME	Caveolae-mediated endocytosis
d	Diameter
DDT	Dichlorodiphenyltrichloroethane
DED	Death effector domain
DISC	Death-inducing signaling complex
DLS	Dynamic Light Scattering
DMEM	Dulbecco's Modified Eagle's Medium
DNA	Deoxyribonucleic acid
DR	Death receptor
ECM	Extracellular matrix
EDD	Embryo development day
EGFR	Epidermal growth factor receptor
EMT	Epithelial-mesenchymal transition
EPR	Enhanced permeability and retention
ER	Estrogen receptor
ERK	Extracellular signal-regulated kinase
FA	Folic acid
FADD	Fas-associtated death domain
FBS	Fecal bovine serum
FDA	Food and drug administration
FGFR	Fibroblast growth factor receptors
FITC	Fluorescein isothiocyanate
GAaq	Glucuronic acid functionalization in aqeous condition
GAorg	Glucuronic acid functionalization in organic condition
Gluc	Glucose
GLUT	Glucose transporter
GMPs	Good Manufacturing Practices
GRAS	Generally recognized as safe

HD	Hydrodynamic diameter
HDAC	Histone deacetylases
HEPES	2-[4-(2-hydroxyethyl) piperazin-1-yl] ethanesulfonic acid buffer
HER2	Human epidermal growth factor receptor 2
HSP	Heat shock protein
HSR	Heat shock response
HSF1	Heat shock transcription factor 1
IAP	Inhibitors of apoptosis
IGF-1	Insulin-like growth factor 1 receptor
IPR	Intellectual property rights
i.v.	Intravenous
LB	Lipid bilayer
MMPs	Matrix metalloproteinases
MOMP	Mitochondrial outer membrane permeabilization
MSDS	Material Safety Data Sheet
MSN	Mesoporous silica nanoparticles
mTOR	Mammalian target of rapamycin
MTX	Methotrexate
NF-κB	Nuclear factor-κB
NIH	National Institutes of Health
PBS	Phosphate Buffer Saline
PDGFR	Platelet-derived growth factor receptors
PEG	Polyethylene glycol
PEI	Polyethyleneimine
pH	Potential hydrogen
PhD	Doctor of Philosophy
RAF	Rapidly Accelerated Fibrosarcoma
Rb	Retinoblastoma
RGD	Arginine-glycine-aspartic acid
R&D	Research and development
RNA	Ribonucleic acid
SAXD	Small angle X-ray diffraction
SEM	Scanning electron microscopy
TEM	Transmission electron microscopy
TEOS	Tetraethyl orthosilicate
TGA	Thermogravimetric analysis
TMOS	Tetramethyl orthosilicate
TNF	Tumor necrosis factor receptor superfamily
UV	Ultraviolet
USA	United States of America
VGFR	Vascular endothelial growth factor
WHO	World health organization
5-FU	5-fluorouracil

1. INTRODUCTION

Multicellular organisms that are built from trillions of cells need a delicate system to maintain cellular homeostasis, if this equilibrium is disrupted diseases are likely to occur. Manifested for example as accumulation of cells, due to lack of cell death is a prime cause for diseases such as cancer and uncontrolled clonal expansion of immune cells. On the other hand, excessive cell removal can lead to tissue loss that may develop to neurodegenerative diseases for example Huntington's and Alzheimer's disease or to a degenerative disorder of organs such as liver cirrhosis and muscular dystrophies.

The knowledge from death signaling and cell survival can be used to create new innovative and effective treatments towards diseases that are caused by disruption in the cell homeostasis. In the case of cancer, where the cells have desensitized themselves from apoptotic stimuli and hijacked the cell survival machinery, it is crucial to know what specific part of the cell homeostasis pathway needs to be targeted, as this would maximize the efficacy of the treatment and minimize the side effects of the drug. However, many drug compounds have either poor solubility or low permeability rendering them to problematic drug candidates with limited therapeutic efficacy. Nanomedicine seeks to overcome these limitations by utilizing material in the nanoscale as drug carrier that possesses the ability to encapsulate the drug and thereby preventing premature release in healthy tissues. Materials in the nanoscale can acquire unique properties for example increased chemical reactivity, electrical conductivity, magnetic properties and most importantly the surface area increases significantly providing a closer contact with the biological surrounding facilitating the reactions with the living material. Combining these acquired properties with the possibility to produce high loading degree man-made nanocarriers with tailor made ligand functionalization have opened a new dimension in drug development and diagnostics. However, there is no "holy grail" neither a "magic bullet" that would cure all diseases as different conditions have different genetic and phenotypic traits. For example, one effective targeting ligand towards a specific type of cancer would most likely not be effective towards a neurodegenerative disease. Furthermore, the nano-carrier itself needs to be biocompatible and biodegradable minimizing the adverse effect on the patents making the development of the drug carrier even more difficult. Not to mention the issues of upscaling the manufacturing procedure from an academic laboratory-developed nanoparticle to a cost effective largescale manufacturing plant. As well as the monetary problem of developing and patenting these drug innovations, as the accumulative costs of research and development goes up to several millions of dollars, money that are not necessary included in traditional research grant funding.

In spite of the many hurdles the development of nanomaterials are facing; there are some Food and Drug Administration (FDA) approved nanomedicine in the market showing that the efforts are not futile in the pursuit of targeted medicine. Especially amorphous silica nanoparticles have shown great potential to be used in biomedical applications due to high adsorption capacity, almost endless functionalization possibilities, biocompatible and simply because silica based materials are "generally recognized as safe" (GRAS) by the FDA.

2. REVIEW OF THE LITERATURE

2.1 Characteristics of cancer cells

The word 'cancer' originates from an observation over 2300 years ago by Hippocrates where the veins from breast tumors looked like the limbs of a crab, and from this observation the term *karkinoma* in Greek and later on the word *cancer* in Latin came from. Cancer is not one disease and should not be consider as such, rather realize that cancer is a group of over 100 diseases that develop over time from disruption in the cellular homeostasis (Cooper 2000, Broxmeyer 2004). Cancer can develop anywhere in the body and even though the basic processes of cancer development is the same, each cancer has its own unique set of features that depends on what cell type and genetic background it originates from (Hanahan & Weinberg 2000). The transformation towards a cancerous cell begins when a cell acquire an genetic or epigenetic change that lets the cell break free from the normal cell division and starts to proliferate abnormally (Figure 1). A genetic change can happen through an internal replication error during mitosis predisposed by specific hereditary traits or by spontaneous mutation caused by environmental factors e.g. radiation, ultraviolet (UV) light, tobacco smoke, carcinogens in diet or infectious disease (Anand *et al.* 2008). These mutations could either be a gain-of-function in a proto-oncogene functioning as a growth-stimulating signal such as H-Ras mutation or as a loss-of-function mutation in a tumor suppressor gene such as retinoblastoma (Rb) that normally functions as a brake in proliferation and activator of pro-apoptotic signaling pathways (Lee *et al.* 2010a, Ozaki & Nakagawara 2011, Hilgendorf *et al.* 2013).

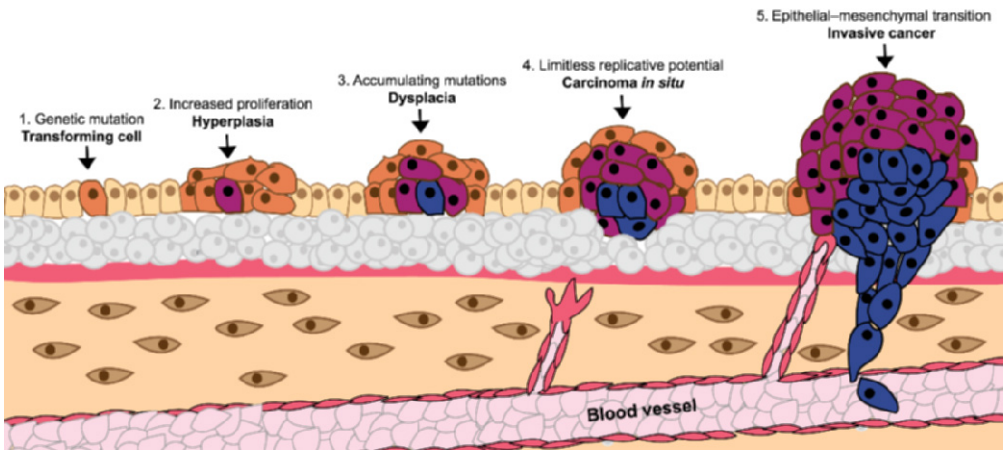

Figure 1. Schematic representation of tumor development. A malignant tumor develops over time, where the first mutation gives the cell growth advantage. The next stage starts by decreasing sensitivity to anti-growth signals by mutation in the Rb gene, then the transforming cell needs insulin like growth factors in order to grow and evade apoptosis. For the cancer to continue to grown and divide, limitless replicative potential needs to be achieved through activating the telomerase function for repairing shortening DNA strands. The excessive tumor growth results in deprivation of oxygen, circumvented by producing vascular endothelial growth factor for stimulating new blood vessels to grow towards the tumor. The last steps in cancer progression where the epithelial cells obtain a more mesenchymal phenotype and starts breaking down the surrounding tissue and invades the circulation and metastasize new locations in the body (adapted from Cooper 2000, Hanahan & Weinberg 2000).

In order for the transforming cell to continue to grow and eventually become a malignant tumor, several function needs to be acquired. For example, the cells ability for self-destruct (apoptosis) must be impaired often through p53 mutation, self-sufficiency in growth signals by mutated insulin-like growth factor 1 receptor (IGF-1). Furthermore, upregulated metabolism by constitutively active c-Myc, limitless replicative potential through upregulated telomerase expression, increased vascularization followed by tissue invasion and metastasis affecting organ functions that can be lethal (Hanahan & Weinberg 2000, Miller *et al.* 2012, Jafri *et al.* 2016). In more details, the excessive growth of the primary tumor results in deprivation of oxygen and nutrients, and to overcome this obstacle the cancer cells have to start producing vascular endothelial growth factor (VEGF) for stimulating new blood vessels to grow inside the tumor a process called angiogenesis (Carmeliet 2005, Goel & Mercurio 2013). In the next step in tumor progression, the cancer cells need to obtain migratory and invasive properties in order to metastasize other tissues. A developmental process called epithelial–mesenchymal transition (EMT) where the sheet-like epithelial cells that expressed E-cadherins starts taking more of an mesenchymal phenotype increasing the expression of N-cadherins, allowing the cancer cell to acquire mobility and coming loose from their neighboring cells (Kalluri & Weinberg 2009). This local invasion combined with the secretion of matrix metalloproteinases (MMPs) that breaks down the extracellular matrix (ECM) allows the cancer cell to enter the vasculature (Gialeli *et al.* 2010). After entry to the blood circulation, the cancer cells must evade the immune system, infiltrate tissues, and colonize new organs for successful metastasis and the formation of a secondary tumor (Chambers *et al.* 2002, Nguyen *et al.* 2009). All of these separate steps in cancer progression could potentially be utilized for cancer therapies if the details of what cellular signaling pathway is deregulated.

2.2 Conventional cancer therapeutics

Historically treatment of solid tumors has mainly relied on surgery, radiation and chemotherapy (Sudhakar 2009, Arruebo *et al.* 2011). Already over 2000 years ago surgeries have been used to remove skin abnormalities in similar manners as today, however recurrence of the tumor is not unusual when relying solely on surgery (Sudhakar 2009). The discovery of X-rays and radiation in the late 19th century by Rontgen and Becquerel paved the way for the development of radiotherapy and the first cured cancer case was in 1889. The clinical use of chemotherapy started in the 1930s based on the observations during the first and second world war that soldier exposed to mustard gas had decreased levels of leukocytes (Arruebo *et al.* 2011). The technological and clinical advances in the 1960s made it possible to develop a more sophisticated cancer treatment with instruments such as “Clinac 6” that used focused X-rays combined with chemotherapy for achieving higher success rates in curing cancer (Sudhakar 2009, Arruebo *et al.* 2011). Most of the traditional chemotherapy still in use today attacks the abrupted cellular homeostasis of cancer cells manifested by their increased proliferation and replication rate (Malhotra & Perry 2003). Normally such high replication rates are only seen in developmental stages and not in an adult body as most of the tissues and organs are already developed (Kermi *et al.* 2017). Therefore, using antimitotic drugs including taxanes (e.g. Taxol®) and vinca

alkaloids (e.g. Velban®) that intervenes with processes that are involved with cell division it is possible to eliminate tumors without lethal consequences to the adult post-mitotic cells (Seligmann & Twelves 2013). Other chemotherapies relies on inducing irreparable DNA damage for example alkylating agents and platinum drugs; as many cancers have impaired cell cycle checkpoints these cells enter mitosis regardless of the chromosomal damage followed by mitotic catastrophe (Castedo 2004, Nakanishi *et al.* 2006). Methotrexate (MTX) and 5-fluorouracil (5-FU) are antagonists that mimic building blocks essential for DNA synthesis thus preventing cell division in proliferating tumors (Goodsell 1999). Anthracycline are a class of antitumor antibiotics derived from the bacterium *Streptomyces peucetius var. caesius* from which doxorubicin and daunorubicin are the most common drugs discovered in the 1970s (Fujiwara *et al.* 1985, Thorn *et al.* 2011). The antitumor properties of these drugs involves inhibition of the enzyme topoisomerase II responsible of separating DNA strands during replication leading towards entangled chromosomes resulting in cell cycle arrest followed by apoptosis (Thorn *et al.* 2011). Other natural derived compounds frequently used in chemotherapy are bleomycin, enediynes, and mitomycin which cytotoxic mechanism involves the oxidative cleavage of DNA and RNA strands (Galm *et al.* 2005). Each treatment has their benefits and limitations and therefore cancer therapies relies often on combinatory treatment of surgery, radiotherapy and chemotherapy.

2.3 Challenges in traditional chemotherapy

Conventional chemotherapy have diverse side effects ranging from hair loss, weight loss, anemia and nausea to organ problems as the drug is systematically administered where it affects the whole body (O'Brien *et al.* 2006, Farokhzad & Langer 2009, Ramirez *et al.* 2009). The efficacy of drugs traditionally used in chemotherapy affects either cell proliferation or induces DNA damage that also damage healthy tissues especially cells that are under constant renewal such as hair follicles, epithelial cells of the intestine blood cells in the bone marrow and egg cells affecting fertility (Allan & Travis 2005, Blumenfeld 2012, Palumbo *et al.* 2013). Alkylating agents and platinum drugs which efficacy relies on inducing DNA damage in fast dividing cancer cells has the risk of mutating healthy cells or inducing irreparable chromosomal damage in normal tissues giving potential off-targeting effects (Allan & Travis 2005). In addition, cancer cells exhibit genomic instability as the mutation rate is significantly increased, which under selective pressure could result in resistance to the therapy administered (Gottesman *et al.* 2002). The molecular mechanisms behind cancer drug resistance include by not limited to; inhibition of drug import, increased drug efflux, increased ability to metabolize and detoxify the drug (Housman *et al.* 2014). For example, overexpression of the ATP-binding cassette (ABC) transporters in multi-resistant cancers enables transporting of drug molecules away from the intracellular compartment thus lowering the drug concentrations in these cancers to sub-lethal evading the effect of chemotherapy (Izquierdo *et al.* 1996). Combined with altered surrounding stromal tissue and dormant cancer stems cells that strengthen and rejuvenates the tumor, rendering the disease of cancer to a difficult one to combat (Papaccio *et al.* 2017, Landry *et al.* 2018). Therefore, modern chemotherapy often

contains a cocktail of many drugs that unfortunately also increases the risk of unwanted side effects for the patient (O'Brien *et al.* 2006, Hu *et al.* 2016).

Furthermore, the drug efficacy depends on the availability of the active substance inside the tumor cell influenced by the drug concentration in the blood plasma that relates to drug solubility in aqueous solution, as well as to the drug permeability allowing the molecule to pass biological membranes such as the cell membrane of the tumor. These two parameters, solubility and permeability, are evaluated in oral drug development using the standardized Biopharmaceutical Classification System (BCS; Figure 2; Benet 2012). A drug is considered highly soluble when the highest dose strength of an immediate release product is soluble in 250 ml or less of aqueous media where the pH ranges from 1 to 7.5. The drug permeability correlates directly to the lipophilicity of the compound, which can be calculated based on measurements of drug efflux across human intestinal membrane. A drug substance is considered highly permeable when over 90% of the compound is absorbed over the intestinal membrane and there is no evidence showing instability of the compound in the gastrointestinal tract (Amidon *et al.* 1995, Savjani *et al.* 2012). However, current trends in drug development are heading towards molecules that are more complex with greater lipophilicity and higher molecular weight resulting in low aqueous solubility. Issues related with poor water solubility such as suboptimal delivery of the drug and low bioavailability are some of the major reasons of failures in modern drug development. As around 90% of current drugs under development and 40% of approved drugs in the market are poorly water-soluble (Kalepua *et al.* 2015).

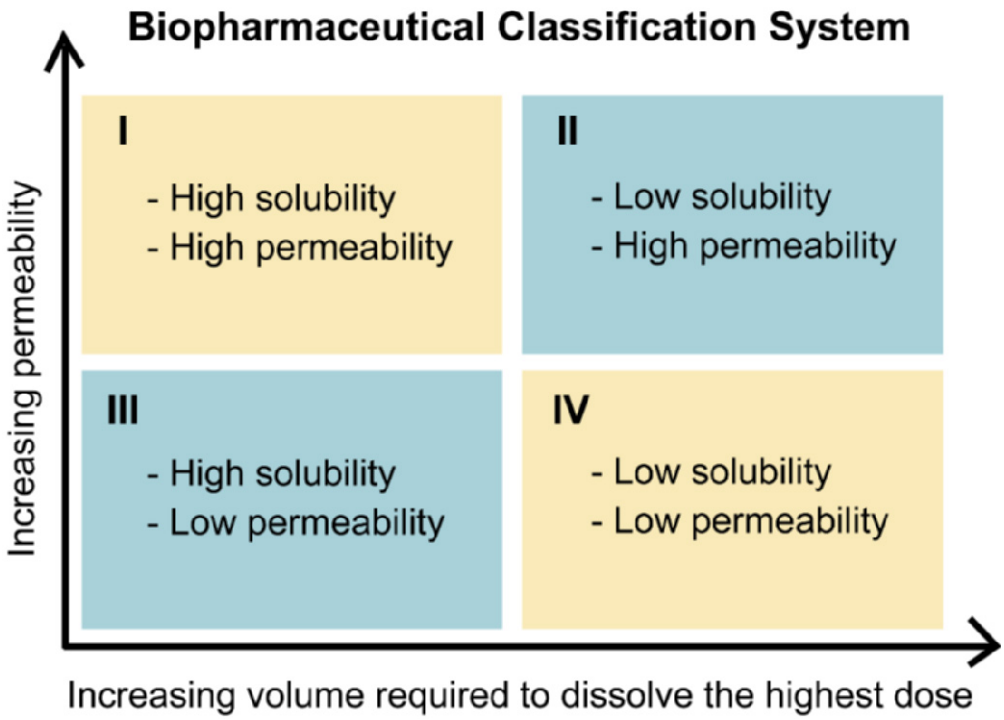

Figure 2. Biopharmaceutical Classification System (BCS; adapted from Benet 2012).

2.4 Towards targeted cancer therapies

Cancer therapeutics is headed towards personalized drug therapy and diagnostics where tailor made drug compounds are assigned to each individual patient for minimizing side effects and maximizing efficacy (Hanahan & Weinberg 2000). The first approved targeted cancer drug was tamoxifen in the 1970s, which effects is based on binding to the estrogen receptor (ER) blocking estrogens ability of stimulating ER-positive breast cancer cell growth (Yan *et al.* 2011). During the past decades, the discovery of oncogenes and tumor suppressor genes combined with the completion of the human genome has given insight in the mechanism of cancer development. There are more than 100 oncogenes and tumor suppressor genes known today that after mutation transforms a normal cell towards a cancerous one. Therefore, inhibiting the function of such mutated oncoproteins or tumor suppressor proteins by small-molecules or monoclonal antibodies for targeted therapy it would be possible stop fast dividing cancer cells without inducing undesirable side effects (Yan *et al.* 2011, Sun *et al.* 2017b). There are already some targeted therapies that have been approved by the Food and Drug Administration (FDA) for treatment of patients with different forms of cancers (Table 1). For example, small molecules e.g. pazopanib that inhibit the angiogenesis at the tumor site by targeting the vascular endothelial growth factor (VEGF) or by inhibiting tumor growth by drugs such as gefitinib that targets epidermal growth factor receptor (EGFR) or by regorafenib that binds to fibroblast growth factor receptor 2 (FGFR2; Table 1; Yan *et al.* 2011). The research and development (R&D) of monoclonal antibodies started around 1975 and the first market-approved antibody to be used for reducing the risk of kidney transplant rejection was Orthoclone OKT3 in 1986. Monoclonal antibodies to be used in cancer therapeutics include trastuzumab (Herceptin) that binds to the extracellular domain of the human epidermal growth factor receptor 2 (HER2) thus blocking its function slowing down the growth of malignant HER2 positive breast cancer cells (Hortobagyi 2001, Sun *et al.* 2017b). The drug-linked monocolonal antibody gemtuzumab functions as a cancer immunotherapy binding to CD-33 receptor expressed on myeloid leukemia cells while releasing the cargo calicheamicin (Padma 2015). There are also some attempts on stimulating the immune system to destroy the cancerous cell by vaccination; currently there is only one FDA approved vaccine named Sipuleucel-T manufactured by Dendreon (Butterfield 2015). Other targeted therapies includes prodrugs such as imatinib (Gleevec®) that are inactive derivate of the active drug molecules that have to undergo an enzymatic transformation to regenerate to its active form. Many enzymes are upregulated in cancer cells that can be targeted by prodrugs that are incorporated with appropriate substrates so that the upregulated enzyme(s) such as lysosomal proteases, ECM proteases and/or MMPs cleaves the prodrug at the tumor site to its active form and unleashes its cytotoxic effect (Giang *et al.* 2014, Padma 2015). Additionally, gene therapy might succeed in curing cancers by replacing the mutated oncogene such as p53 with the normal wild-type, attempts in gene therapy for head and neck cancer patents have shown to be beneficial (Bali *et al.* 2013). In the future, a tailored drug-cocktail for each mutated oncogene or tumor suppressor driven cancer might be the most efficient therapy as it is highly unlikely that one drug would cure them all due to the ever-changing cancer phenotype.

Table 1. FDA approved targeted cancer therapies 2003-2013 (adapted from Yan *et al.* 2011, Padma 2015, Sun *et al.* 2017b).

Compound	Company /Year	Type	Target(s)	Indication*
Ado-trastuzumab emtansine	Genentech /2013	Antibody	HER2	Breast cancer
Regorafenib	Bayer /2012	Drug	PDGFR, FGFR	Colorectal cancer /Stomach cancer
Denosumab	Amgen /2010	Antibody	TNFSF11	Bone metastases
Everolimus	Novartis /2009	Drug	mTOR	Renal cell carcinoma
Ofatumumab	Genmab /2009	Antibody	CD-20	Chronic lymphocytic leukemia
Pazopanib	GSK /2009	Drug	VGFR-1, -2, -3, c-kit, PDGFR	Renal cell carcinoma
Romidepsin	Gloucester /2009	Drug	HDAC	Cutaneous T cell lymphoma
Lapatinib	GSK /2007	Drug	HER2/EGFR	Breast cancer
Nilotinib	Novartis /2007	Small molecule	BCR-ABL	Chronic myelogenous leukemia
Temsirolimus	Wyeth /2007	Drug	mTOR	Renal cell carcinoma
Dasatinib	Bristol-Myers Squibb /2006	Drug	Src, BCR-ABL	Chronic myeloid leukemia
Panitumumab	Amgen /2006	Antibody	EGFR	Colorectal carcinoma
Sunitinib malate	Pfizer /2006	Small molecule	VGFRs, PDGFR	Gastrointestinal stromal tumor
Vorinostat	Merck /2006	Drug	HDAC	Cutaneous T-cell lymphoma
Sorafenib Tosylate	Bayer /2005	Drug	RAF, VEGFR-2, -3, PDGFR-b, c-kit	Renal cell carcinoma
Bevacizumab	Genentech /2004	Antibody	VEGF	Colorectal cancer
Cetuximab	ImClone Systems /2004	Antibody	EGFR	Colorectal cancer
Erlotinib Hydrochloride	OSI Pharms /2004	Drug	EGFR	Non-small cell lung cancer
Bortezomib	Millennium Pharms /2003	Drug	Proteasome	Multiple myeloma
Gefitinib	AstraZeneca /2003	Drug	EGFR	Non-small cell lung cancer
Tositumomab	Corixa Corporation /2003	Antibody	CD-20	Non-Hodgkin's lymphoma

2.5 Regulation of programmed cell death

Apoptosis is the term that was first used by Kerr, Wyllie and Currie in 1972 to describe programmed cell death in eukaryotes for maintaining cell populations in tissues (Kerr *et al.* 1972). Eukaryotic cells have two major apoptotic pathways, the intrinsic pathway and the extrinsic pathway (Figure 3) The intrinsic pathway is activated by cellular stresses; such as radiation, oxidative stress and cytotoxic drugs leading towards mitochondrial membrane leakage, DNA damage and finally cell death (Elmore 2007, Kroemer *et al.* 2009). If the cell stress is non-lethal, the anti-apoptotic B-cell lymphoma gene 2 (Bcl-2) family proteins blocks the intrinsic apoptotic stimuli (Hongmei 2012). However if the trauma is irreparable, the intrinsic pro-apoptotic proteins Bax and Bak are activated leading to mitochondrial outer membrane permeabilization (MOMP) that allows the leakage of electron carrier protein called cytochrome c. This accumulation of cytochrome c in the cytosol promotes apoptosome formation and activation of initiator caspases which in turn activates executioner caspases that ultimately leads to apoptosis (Elmore 2007, Hongmei 2012).

The extrinsic apoptotic pathway is mediated by death receptors (DRs) that are members of the tumor necrosis factor receptor superfamily (TNF; Elmore 2007). There are over twenty DRs and of them, eight has the ability to induce apoptosis, of which Fas/CD95-receptor is one of the best characterized (Aggarwal 2003). When the death ligand binds to the DR; a conformational change takes place in the intracellular region of the receptor leading to recruitment of an adaptor protein named Fas-associtated death domain (FADD). Together creates a platform for death effector domain (DED)-containg proteins to bind and form death-inducing signaling complex (DISC). When the initiator procaspase is recruited to the DISC, the procaspase is cleaved to its active form and then released to the cytosol where the active caspase initiates the apoptotic proteolytic cascade (Aggarwal 2003 Boatright *et al.* 2003, Elmore 2007). Ultimately leading towards cell death, which is manifested by nuclear and cytoplasmic condensation, plasma membrane blebbing and DNA fragmentation (Kroemer *et al.* 2009, Hongmei 2012). These cell fragments are called apoptotic bodies and are then engulfed by professional phagocytes thereby preventing the inflammatory response (Nagata 2018). Necrosis is traditionally defined as uncontrolled cell death, where the cells have undergone an accident leading towards membrane swelling and cell rapture resulting to release of cellular content, which causes a local inflammation in the surrounding tissues (Kroemer *et al.* 2009). However, evidence are accumulating that necrosis can even occur in a more controlled manner, nowadays defined as necroptosis (Golstein & Kroemer 2007). There are other forms of cell death, such as anchorage-dependent programmed cell death called anoikis where the cell have lost its cell to matrix interaction or by cornification of keratinocytes which is necessary for the formation of the epidermis (Kroemer *et al.* 2009). Drugs such as Taxol® disrupt microtubule formation during cell division killing the cell through mitotic catastrophe (Denisenko *et al.* 2016). Macrophages that have a bacterial infections might die through pyroptosis which is an inflammation reaction driven by caspase-1 (Galluzzi *et al.* 2012, Kroemer *et al.* 2009). The balance between different pathways of controlled or uncontrolled cell death depends on the nature and severity of the death stimulus and cell type.

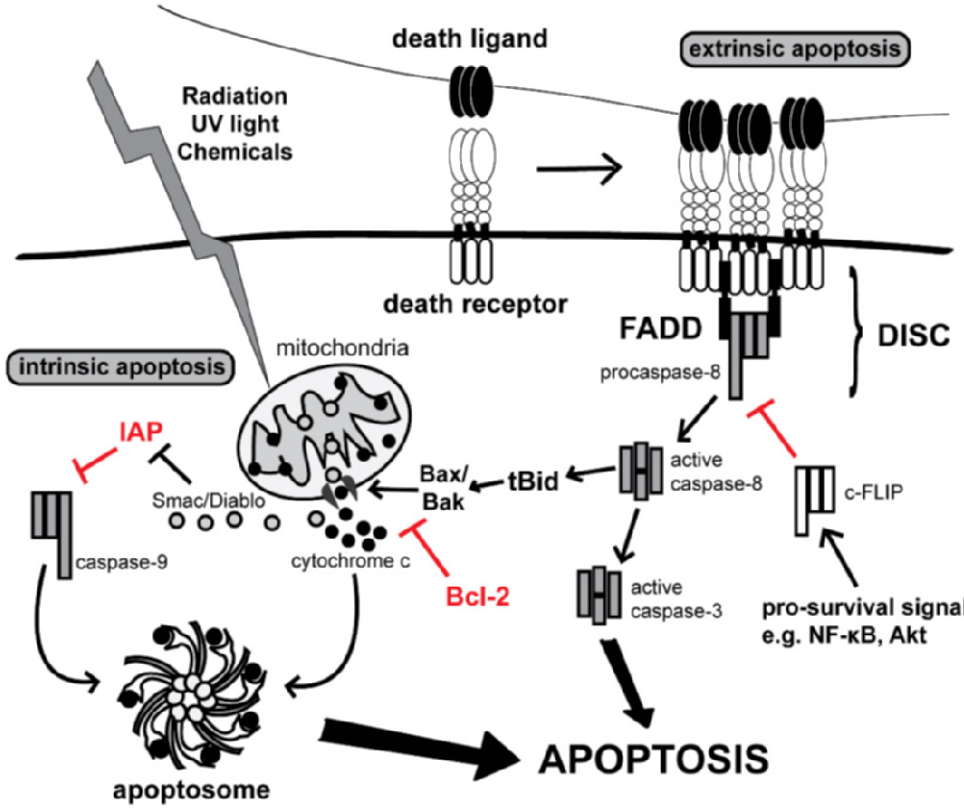

Figure 3. Schematic representation of the apoptotic signaling pathway. Programmed cell death can be initiated by either extrinsic or intrinsic stimulus. The extrinsic apoptosis is activated by death ligand binding to death receptor (DR) leading to the formation of a death inducing signaling complex (DISC). The intracellular death domain facilitates the cleavage and activation of the initiator caspase-8, which in turn activates downstream executioner caspases that starts the cleavage of cellular compartments leading towards apoptosis. However, by receiving pro-survival signals it is possible for the cell to prevent the extrinsic apoptotic signaling cascade by blocking the activation of the initiation caspase by cellular FLICE-inhibitory proteins (c-FLIP) binding to the DISC. The pro-apoptotic proteins Bax and Bak together with the anti-apoptotic Bcl-2 proteins balance the apoptotic stimuli by regulating the integrity of the mitochondrial membrane. The intrinsic apoptotic signaling pathways activates by irreparable cellular damage resulted from radiation, chemicals, UV light or pathogens that leads to mitochondrial outer membrane permeabilization (MOMP). Followed by the release of cytochrome c that promotes APAF-1 oligomerisation and the formation of the apoptosome, which serves as a platform for caspase-9 and together strengthens the apoptotic cascade. The inhibitors of apoptosis proteins (IAPs) can block the activation of caspase-9 and thus preventing the formation of the apoptosme, however, Smac/Diablo can, after leaking out of the mitochondria block the IAPs so that the apoptotic pathway may still prevail.

2.5.1 Caspases are the executors of apoptosis

All eukaryotic cells have the possibility of self-destruction, in other words programmed cells death in which cysteine-dependent aspartate proteases called caspases are the main executors (Kroemer *et al.* 2009). These caspases are synthesized as inactive procaspases which upon apoptotic stimuli are then dimerized in close proximity to each other leading to a proteolytic cleavage resulting in an active initiator caspase (caspase-2, -8, -9, -10), amplifying the apoptotic stimuli (Elmore 2007). These stimulated initiation caspases proteolytically activates in turn the downstream executioner caspases (caspase-3, -6, -7) that are responsible for the cleavage of cellular compartments leading toward apoptosis (Hongmei 2012). Caspase-1 on the other hand is the part of the inflammasome complex that promotes cytokine maturation and secretion, induced by bacterial infection (Franchi *et al.* 2009). The main objective in these sequential signaling cascades is that it function as an amplification from the original death stimuli (Elmore 2007). However, in order to maintain cellular homeostasis it is crucial that the apoptotic stimuli is kept under strict control otherwise the cell might start to transform to an immortal cancer cell (Elmore 2007, Lee *et al.* 2010a, Hongmei 2012).

2.5.2 Inhibitors of apoptosis regulates cellular homeostasis

The pro-apoptotic stimulus can also be inhibited or modulated by cellular FLICE-inhibitory proteins (c-FLIP), that are another DED-containing protein homologues to caspas-8 and capsase-10, however lacking the catalytic domain (Fuentes-Prior & Salvesen 2004, Safa 2012). Therefore FLIP function is reduced to recruitment to the DISC and from there regulate DR-mediated apoptosis by directly binding to the initiator caspase without its activation functioning as a death signaling antagonist (Moubarak *et al.* 2010). There are three mammalian FLIP isoforms, two short isoforms named c-$FLIP_S$ and c-$FLIP_R$, which are potent caspase inhibitors and one long isoform named c-$FLIP_L$ that functions are still not completely understood (Irmler *et al.* 1997, Safa 2012). When c-$FLIP_L$ is overexpressed it competes with procaspase-8 for the DED binding sites of FADD, inhibiting the DR-induced apoptosis. However, heterodimerisation of caspase-8 and c-$FLIP_L$ has shown to cause partial processing of the caspase resulting in a molecule that can induce pro-survival signaling pathways (Bagnoli *et al.* 2010). Studies have shown that c-$FLIP_L$ can activate Akt, extracellular signal-regulated kinase (ERK) and the nuclear factor-κB (NF-κB) transcription factors pathways, thereby stimulation of cell growth, differentiation and replication (Safa 2012). On the other hand, activation of the NF-KB or Akt pathway correlates with an increased expression of $FLIP_L$ showing a complex crosstalk between death signaling and cell survival signaling pathways (Micheau *et al.* 2001, Wang *et al.* 2008, Urbano *et al.* 2014). Furthermore, knock-out mice lacking the $FLIP_L$ are more sensitive to extrinsic apoptotic stimulus, as cells derived from these animals are primed towards cell death (Yeh *et al.* 2000). Recent studies have shown that cancer cell can benefit from overexpressing $FLIP_L$ making them death receptor ligand TRIAL resistant (Sun *et al.* 2017a). Another important protein family that controls caspase activity are the inhibitors of apoptosis (IAP; Gyrd-Hansen & Meier 2010). These IAPs are proteins defined by having a baculovirus inhibitior of apoptosis protein repeat (BIR) domain that enables binding and inhibition of caspases. In mammalian cells, XIAP is the only

IAP that is able to directly bind and inhibit caspase activity; whereas cIAP1 and cIAP2 functions more as scaffolds interacting with caspases not inhibiting (Eckelman *et al.* 2006). Cells lacking XIAP are more sensitive to apoptotic stimulus; on the other hand cancer cells overexpressing IAPs can tolerate sever conditions, such as nutrient depravation, DNA damage and hypoxia without activating the apoptotic cascade (Gyrd-Hansen & Meier 2010, Elmore 2007). Understanding such crosstalk between two opposite cellular processes will unravel important features of cell homeostasis and cancer progression, with mechanisms enabling fast switches from survival to death or the other way around. Therefore, creating drugs that would specifically target cellular switches have become attractive drug candidates for cancer treatment (Dubrez *et al.* 2013).

2.6 Nanomedicine for personalized therapy

Cancer and cardiovascular disease is the number one cause of death in the western-world and the World Health Organization (WHO) estimated that there will be over 15 million new cases of cancer worldwide in 2020 (Wicki *et al.* 2015). In Finland there was around 34 122 new cancer cases in the year 2016 and the mortality rate was around one third of the affected population (Finnish Cancer Registry 2016). In the United States of America the ratio is quite similar as there was around 1 596 670 diagnoses and 571 950 deaths from cancer in 2011 (Steichen *et al.* 2013). One of the major challenges in current cancer treatment is the lack of drug accumulation in target tissues and the dose-related toxicity as the administration of chemotherapy often include high systemic exposure leading towards unwanted side-effects (Allan & Travis 2005, Wicki *et al.* 2015). The therapeutic index is a term that describes how much drug is needed for the therapeutic effect compared to the dosage that causes toxicity (Muller & Milton 2012). Therefore, the development of targeted drug delivery systems are required in order to increase the therapeutic window and therefore reduce the side-effects of administered drugs (Meijerman *et al.* 2008, Copple *et al.* 2014).

Nanomedicine is an emerging interdisciplinary field where nanotechnology and medicine combines in the pursuit of developing nanomaterials that could be used for personalized diagnostics, treatment, prevention and delivery of drug molecules to target tissue (Seigneuric *et al.* 2010, Rivera Gil *et al.* 2010 Kluenker *et al.* 2018). Nanoparticles have shown great potential as drug delivery vehicles due to low toxicity, high drug loading capacity, potential of bypassing biological barriers and tailor-made surface functionalization (Wagner *et al.* 2006, Seigneuric *et al.* 2010). Furthermore, nanoparticles can prolong the drug dissolution at the target site in order to obtain optimal therapeutic efficacy by keeping the drug molecule encapsulated and thereby preventing premature release (Sun *et al.* 2015). Functionalized nanoparticles with targeting ligands can be used for specific cell type internalization and thereby increase the therapeutic index and lowering the off-target effects (Tsai *et al.* 2009, Rosenholm *et al.* 2009, Zhang *et al.* 2018). There are thousands of publications on different nanoparticles for targeted drug delivery of both liposomal, polymeric and inorganic nanoparticles. However, there are only a few FDA clinically approved nanomedicine on the market such as Abraxane®, Doxil®, Lipoplatin®, Marqibo® (Venditto & Szoka 2013). This could at least partly be explained by manufacturing challenges such as upscaling of the production in a cost effective way, limited

available toxicity data on nanomaterials as well as bottlenecks in keeping the nanocarrier in a well-dispersed homogenous suspension (Wagner *et al.* 2006, Crookes-Goodson *et al.* 2008, Wicki *et al.* 2015). Some might even say that collaboration between academia and industry is still in their "infancy" and needs to be further developed in the pursuit of creating targeted drug systems that can be used in the clinics (Venditto & Szoka 2013).

2.6.1 Definition of nanomaterials

The definition of nanomaterials lies in the dimensions of the object being between 0.2 nm to 100 nm, which is less than 0.0001 mm and as a reference a human hair is about 0.1 mm in width (Lidén 2011). However, this definition is not absolute as there are different opinions regarding the dimensions of nanomaterials depending on what guidelines are being used (Maynard 2011). Regardless of the exact definition of these nanomaterials, quantum effects begin to dominate the properties of materials that have dimension less than 100 nm (Shrader-Frechette 2007, Karlsson *et al.* 2009). These tiny materials have different properties than their bulk counterpart, and one of the key reasons is because they have a larger surface area to volume ratio. Thus, allowing nanomaterials to be more reactive on both biological and chemical substances, which may be desirable, however also giving potentially adverse reactions (Chen *et al.* 2005, Chen *et al* 2006). Desirable properties of nanomaterials are that otherwise a non-reactive material becomes reactive when produced in the nanoscale. These materials can gain new properties such as conductivity, oxidation potential, increased strength, optical transparency and magnetism. Qualities that are important in many different consumer products, for example, in sunscreen, cosmetics, CD players, hard discs and as protective coatings (Shrader-Frechette 2007). In nanomedicine it is important that these new materials are biocompatible and biodegradable as they would be used as targeted drug delivery systems or for diagnostic purpose, or even as a combinatory, teragnostic approach (Guo & Tan 2009, Jain 2012, Kluenker *et al.* 2018).

2.6.2 Regulations of nanomaterials

The regulation of nanomaterials is not a straight forward task, as the definition of nanomaterial is not standardized and may vary depending on what guidelines are being used (Lidén 2011, Maynard 2011). In the current Regulation of the European Parliament and of the Council of Europe on the Registration, Evaluation, Authorization and Restriction of Chemicals (REACH 2006) the word "nano" simply do not exist as a definition, which in turn causes some difficulties in categorizing these new materials in the European Union (EU) under the current regulations (Kimbrell 2009). The European Commission has chosen to make use of existing legislation to regulate nanomaterial the so-called "incremental approach", whereas the materials composition itself is the defining factor, regardless of the physical dimension of the material (Franco *et al.* 2007). Even though nanomaterials might have completely different properties than its bulk counterpart, for example gaining magnetic or oxidative properties (Shrader-Frechette 2007, Kroll *et al.* 2009). One possible reason for this approach is due to the reality that a change in legislation in such a way that nanomaterials would have a more extensive regulation is both technically demanding and politically problematic (Kimbrell 2007, Franco *et al.* 2007). The commission has

acknowledged that some adjustments needs to be made in REACH annexis in order to give a more specific framework regarding the requirements of nanomaterials and their risk assessments (Lidén 2011, Maynard 2011).

An investigation done by Franco and colleagues in 2007 on the subject of how effective nanomaterials are regulated; showed that there are clear gaps in the legislation during that time as some nanomaterials were incorrectly classified in the Material Safety Data Sheets (MSDSs). The study evaluated the applicable regulations along the life cycle of three different products containing carbon nanoparticles; a badminton racket, a lubricant and a baseball club (Franco *et al.* 2007). One of the problems in the regulation of nanomaterials appears to be that the current methods available are sometimes insufficient to analyze and classify these new materials and their chemical and physiological properties (Kroll *et al.* 2009). Due to these uncertainties and the lack of toxicological data available, it becomes difficult to apply many of the current environmental laws to certain nanomaterials, such as the case with carbon nanotubes (Karlsson *et al.* 2008, 2009). The study done by Franco *et al.* 2007 shows that it is often unclear whether nanomaterials are covered by the current legislation, which could lead to exposure to nanomaterials by either employers or consumers without their consent. This in turn rises the ethical questing about nanotechnology in the workplace, as there is still lack of clarity regarding the regulation of nanomaterials and the risk it may pose to workers (Schulte & Salamanca-Buentello 2007). History has shown that "miracle materials" such as asbestos, mercury and dichlorodiphenyltrichloroethane (DDT) have serious health effects and probably some nanomaterials will also have adverse effect on both the environment and humans (Bartrip 2004, Kimbrell 2009).

Nanomedicine on the other hand is under more strict supervision and regulation as its purpose is to either enhance the efficacy or reduce the toxicity of its agents that will be in clinical use (Crookes-Goodson *et al.* 2008). However, there is a clear need of harmonization regarding the regulations of nanomedicine as one regulatory agency might categorize a product as a medical devices and another agency might categorize the product as a medicinal product. In the EU the regulation applied depends largely on does the product contains at least one component in the nano-size (1-1000 nm) and is it purposely designed for clinical applications (Bremer-Hoffmann *et al.* 2018). The US Food and Drug Administration (FDA) has chosen a more case-by-case approach for the use of nanomaterials in products, according with specific legal standards that are applicable for each type of product (Pillai 2014, Bobo *et al.* 2016). Already in 2016, there was around 51 FDA approved nanomedicine and another 77 products in clinical trials, and many of them are formulations made of micsells, liposomes or inorganic and metallic particles (Bobo *et al.* 2016). The trend in nanomedicine is going towards more complex materials that include actively targeting carriers and multi-functional theranostics that will further blur the boundaries of material categories making it even harder to classify these new materials (Pillai 2014, Bobo *et al.* 2016). In one study, regulatory agencies were asked to define which physiochemical properties is considered relevant for the preclinical characterization of nanomedicine that are not applicable to other pharmaceutical classes and based on

these answers; size and stability matters the most whereas density, surface charge and surface chemistry were less relevant (Figure 4; Bremer-Hoffmann *et al.* 2018).

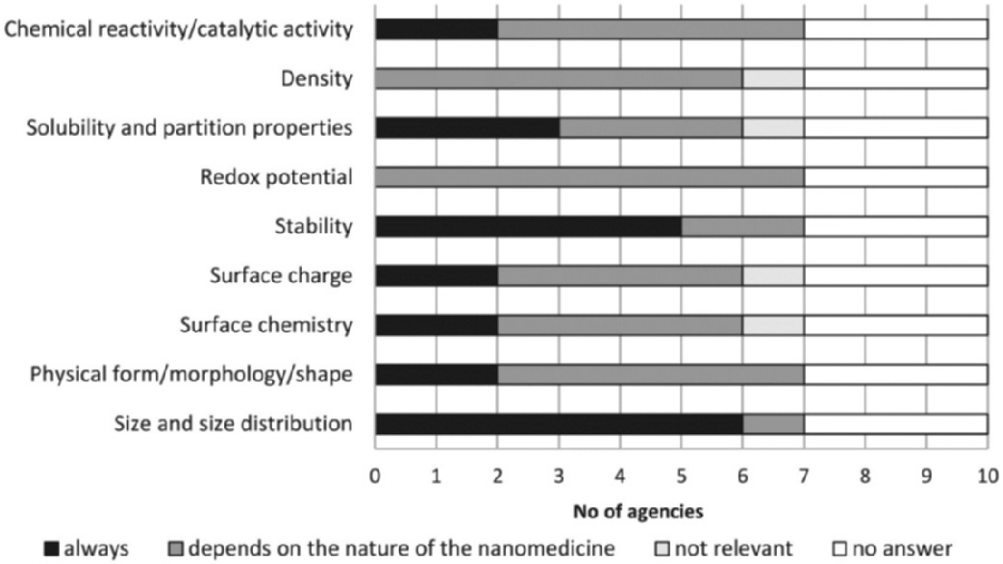

Figure 4. Relevance of physicochemical parameters for preclinical characterization of nanomedicine (adapted from Bremer-Hoffmann *et al.* 2018).

2.6.3 Toxicity and environmental effects of nanoparticles

Nanomaterials small dimensions make them more reactive than their bulk counterparts, they can penetrate deeper in to tissues and they can bind to protein and DNA, consequently there is an increased risk of toxicity and unwanted effects when using materials in the nanoscale (Shrader-Frechette 2007). However, the toxicity of nanoparticles does not entirely depend on the size, rather the combination of the physicochemical properties of the particle which depends on what materials are being used as well as the surface functionalization (Kroll *et al.* 2011). The increasing use of nanomaterials in pharmaceutics and consumer products causes nanomaterials to accumulate in the environment, where these new materials can have adverse reaction on the environment and on humans that can be hard to predict (Karlsson *et al.* 2009, Kroll *et al.* 2009). One of the contributing factors of nanoparticle accumulating in nature is due to the insufficient purification methods current wastewater treatment plants utilize. Most of the nanomaterials being consumed by human's ends up in the sewage, from which they are not properly separated before released to the environment. The problem lies in the small size of nanomaterials as they do not settle down properly in aqueous solution and therefore cannot be sediment by gravity; as sedimentation is the current method to separate inorganic material from wastewater (Brar *et al.* 2010). The next step in the purification process is based on microorganisms that absorb the organic compounds, thus cleaning the sewage water even further. However, some of these nanoparticles have the ability to inhibit bacteria's growth and reduce their metabolism, which may degrade the purification capacity of the treatment plant even further (Brar *et al.* 2010, Ikuma *et al.* 2015).

For example, some nanoparticles are proven to be more toxic to different bacterium than the original bulk materials (Bondarenko *et al.* 2013). In Jiang *et al.* 2009 study, three different bacterium (*Bacillus subtilis, Escherichia coli and Pseudomonas fluorescens*) were used to investigate the toxicity of nano-scaled aluminum, silicon, titanium and zinc oxides. The result showed that nanoparticles made of zinc oxide were the most toxic as they killed 100% of all three bacterium. The aluminum oxide and silicon dioxide nanoparticles had both around 50% viability for all three bacterium. The bulk particles of aluminum oxide and silicon dioxide themselves were not toxic for the bacteria as no significant reduction in viability were detected when compared to the non-treated control samples. All bacterial samples that were given nanoparticles had a significantly lower viability compared to than of the untreated control samples. The only bulk material that had an effect was zinc oxide as it showed significant reduction in the viability of all three bacterial species (Jiang *et al.* 2009). Zinc oxide is a highly oxidative material as bulk and not surprisingly giving rise to some toxicity to the bacterium (Weibel *et al.* 2014). However, not all nanoparticles are toxic; for example aluminum and silica based nanoparticles are usually consider non-toxic to cells and safe for human consumption (Jiang *et al.* 2009, Harrison 2009, Kettiger *et al.* 2015). One should always remember that its is the dose that matters; as eating too much salt (sodium) for example could be dangerous for humans as well as drinking too much water (Yamashiro *et al.* 2013, Ha 2014).

Furthermore, “bare” nanoparticles that are not functionalized are in generally more toxic to eukaryotic cells compared to e.g. coated metal particles that releases less harmful ions and functionalized particles are less prone to aggregation that can cause protein denaturation and DNA damage (Perreault *et al.* 2014, Srivastava *et al.* 2015, Huang *et al.* 2017). Environmental and toxicological studies of different sized particles shows that some nanoparticles are toxic to bacteria, algae, invertebrates and mammals (Handy 2008). Especially zinc oxide nanoparticles have been proved to be highly toxic for the fresh water flea *Daphnia magna*, whereas aluminum based nanoparticles were least harmful to the water flea (Zhu *et al.* 2009). In addition, *D. magna* could absorb nanoparticles that were accumulated in the digestive system, enabling the nanoparticles to be transferred to the next trophic level (Zhu *et al.* 2010). In the experiment performed by Zhu *et al.* 2010 the fresh water flea was exposed to titanium dioxide nanoparticles for one day and then the *D. magna* was transferred to an aquarium to be consumed by Zebrafishes as food. The result showed that the nanoparticle could be taken up by the fresh water flea which was transferred to the next tropic level detected as particle accumulation in the Zebrafish (Zhu *et al.* 2009, 2010). Taken together, nanoparticles can be toxic to animals and humans and that they can be transferred from lower trophic level to higher levels, indicating that some precautions in the development of nanomaterials are warranted. However the toxicity of these materials should not be generalized, as the size by itself is not the only affecting factor, rather consider each combination of the material with its specific surface charge, porosity, density and functionalization on a case-by-case manner (Kroll *et al.* 2011, Pillai 2014, Srivastava *et al.* 2015).

2.6.4 Mesoporous silica nanoparticles as targeted drug delivery

Inorganic silica based nanoparticles have been receiving increasing attention in the field of targeted drug delivery systems because they are considered non-toxic and biocompatible as silica degrades in aqueous environment to different species of silica acid and ultimately gets excreted via the urine (Hao *et al.* 2012, Kettiger *et al.* 2015). There are roughly two ways of producing nanomaterials; either the top-down or the bottom-up approach where both methods have their benefits and downfalls (Hoffmann *et al.* 2006, Guo & Tan 2009). The top-down approach starts with building materials that have larger dimensions than the final product which means in practice that the materials undergoes physical stresses in order to be reduced in size. This in turn might lead to surface imperfections as well as the top-down method is not cost efficient as some of the raw materials goes to waste during production (Guo & Tan 2009). The bottom-up method starts by introducing smaller building blocks in solution which then transforms to the final product, leading to less defects in a more cost- and material-efficient way (Huang *et al.* 2008). However, scaling up the bottom-up methods remains a major challenge, as variations in pH, temperature and mixing ratios may influence the structure of the final product (Desai 2012). There are different bottom-up methods such as co-precipitation, template synthesis and sol-gel method where the building blocks are often copolymers, colloids and liquid crystals (Brinker & Scherer 1990, Huang *et al.* 2008, Guo & Tan 2009). Synthesis of moderate size (250-300 nm) porous silica nanoparticles by the sol-gel method has some clear advantages as it enables delicate control of particle dimensions, which has a clear therapeutic benefit as smaller particles tend to be unspecifically internalized and larger particles tend to aggregate in biological systems (Rosenholm *et al.* 2006, 2008, 2009, Shang *et al.* 2014).

Mesoporous silica nanoparticles (MSNs) are unique in the way that they have tunable ordered repetitive mesostructures of pores in the range of 2-10 nm and that these particles can be synthetized in various sizes and shapes (Liu *et al.* 2015, Kresge *et al.* 1992). Mesoporous silica materials were first discovered in the early 1990s by Mobile Oil Company using surfactants as structure directing agents together with inorganic materials that can be deposited through hydrolysis and condensation using the sol-gel method (Kresge *et al.* 1992, Beck *et al.* 1992). The porous silica structures are revealed after the removal of the surfactant by either chemical extraction or thermal calcination. In short, the synthesis contains four main components: source of silica, structure-directing agent (surfactants), solvent (often methanol or ethanol), and a catalyst (often sodium). The formation depends on two main phenomena: the ability of the surfactant to form micelles in liquid and the ability of the inorganic material (silica) to condensate in order to form stable structures (Hoffman *et al.* 2006, Wan & Zhao 2007). The shape and size of the micelles defines the size of the particles whereas the mesoporous are mostly governed by the surfactant used and its concentration as well as pH, temperature and presence of other components (Ducheyne *et al.* 2015). Rendering the variation of different MSNs that can be produced to astronomical and therefore numerous variables need to be taken in account for when designing and synthetizing MSNs for targeted drug delivery systems. In the pharmaceutical industry, Good Manufacturing Practices (GMPs)

guidelines have been developed for the production of medicinal products that will be used by humans in order for the final product to be consistent and safe (Adamo *et al.* 2012, Gouveia *et al.* 2015). There are laboratory products in the market containing nanoparticles that have been produced using GMPs, for example, NanoParticle Fluorescent Calibration Slide (Grace Bio-Labs inc., Bend, Oregon, USA) designed to be used for microarrays scanners. However, highly detailed protocol standards are not always feasible in academic laboratory conditions that might account for some variation in the synthetized product (Desai 2012, Baer *et al.* 2018).

2.6.5 Targeting strategies for MSNs

Targeting approached can be classified in to either active or passive targeting. In the passive targeting, non-functionalized particles would quickly be removed from the blood circulation by macrophages through the process of opsonization, where the particles accumulate in the liver and spleen for clearance (Owens & Peppas 2006). This accumulation can be utilized when treating hepatic and spleen disorders such as liver fibrosis, hepatocellular carcinomas or Hodgkin's and non-Hodgkin's lymphomas (Hillaireau & Couvreur 2009). Non-functionalized particles have also been observed to accumulate at tumor sites elsewhere in the body, due to enhanced permeability and retention effect (EPR) which is a consequence of leaky and fenestrated blood vessels around majority of tumors (Gerlowski & Jain 1986, Matsumura & Maeda 1986). However, passive targeting that utilizes the EPR effect might not be sufficient in all cancer cases combined with the possible off-targeting effects that might have a negative impact on the patient's wellbeing (Bae & Park 2011, Bazak *et al.* 2014). Therefore, functionalizing the particle surface with an active targeting ligand could further enhance the drug accumulation at the target site and minimize possible side effects (Bae & Park 2011). Such functionalization can be achieved by covalently attaching a cancer specific targeting ligand in order to increase the particle endocytosis in the tumor cells with minimal uptake in healthy cells (Figure 5; Rosenholm *et al.* 2006, 2008a&b, 2009a&b, 2010).

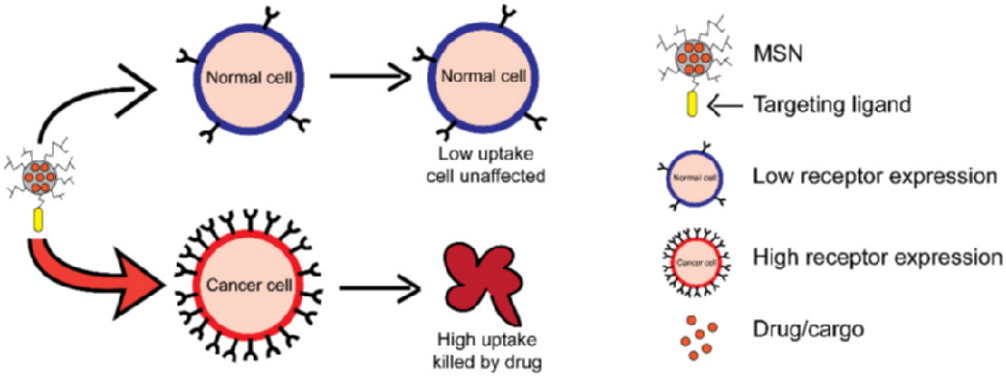

Figure 5. Schematic representation of the key concept of MSNs targeted drug delivery. Utilizing cancer specific traits such as high folate receptor or glucose transporter expression in order to have increased particle internalization in target cells with minimal uptake in healthy cells for minimizing side effects of the drug. Improved efficacy can be achieved by using drugs that intervenes more pronounced in cancer cells than healthy cells, for example, celastrol that kills fast dividing cells through destabilizing the mitotic spindle.

For example, one common trait of many cancer cells are that they express folate receptors in much higher amounts than most normal tissues (Parker *et al.* 2005). Therefore utilizing folic acid as a small molecule targeting ligand, which is a synthetically produced vitamin B9, it is possible to achieve targeted drug delivery towards folate receptor expressing tumors (Leamon & Low 2001, Leamon & Reddy 2004). Cancer cells with high folate receptor expression would internalize these nanoparticles through receptor-mediated endocytosis and as a consequence they would internalize much higher amounts of drug-loaded particles than the healthy cells; giving rise to high drug concentrations at the tumor site with potentially lower off-target effects (Rosenholm *et al.* 2009, Rosenholm *et al.* 2010a&b, Porta *et al.* 2013). Other small molecules that can be utilized for targeting strategies are for example, carbohydrates designed for interacting with lectin receptors at the surface of cells (Carrillo-Conde *et al.* 2011). Sugar targeting strategies may include; mannose- or galactose-functionalized particles that can be internalized through mannose or asialoglycoprotein receptor-mediated endocytosis by macrophages or with glucose (Gluc) conjugated particles through glucose transporters (GLUT) that are commonly overexpressed in cancer cells (Brevet *et al.* 2009, Sonoke *et al.* 2011, Gary-Bobo *et al.* 2012, Li *et al.* 2014). Active targeting strategies might also include covalently attaching peptides, antibodies and nucleic acid based aptamers to the nanoparticle surface (Kue *et al.* 2016). Targeting peptides such as arginine-glycerin-aspartic acid (RGD) can be used for binding with αυβ3 integrin receptor at the tumor cell surface in order to archive targeted drug delivery (Xiao *et al.* 2014). However, using small molecules for targeting ligands have some advantages over peptides and antibodies due to their stability, ease of conjugation, and relative low cost (Kue *et al.* 2016).

Antibodies on the other hand has the benefit of targeting specific antigens at the tumor cell surface giving rise to higher specificity than small molecules (Fosgerau & Hoffmann 2015). Folate for example, which is abundant in the diet, can compete with the ligand-modified delivery vehicle when circulating in the bloodstream and therefore lower the desired efficacy (Attarwala 2010). Anti-HER2 monoclonal antibody conjugated MSNs have been developed for targeting breast cancer cells as well as an anti-EGFR functionalized particle for the treatment of an EGFR mutated lung cancer (Tsai *et al.* 2009, Wang *et al.* 2016). However, some of the major drawback from antibody based targeted drug delivery systems is due to the potential unwanted immunologic reaction, as well as the risk of the ligand being degraded in the body combined with the difficulty in conjugating the antibody to the delivery system at the desired amino acid site (Tsai *et al.* 2009, Wang *et al.* 2016). Aptamers on the other hand are therapeutic oligonucleotides that are built of single stranded DNA or RNA, which forms three-dimensional structures with high affinity and specificity towards proteins in similar manners as monoclonal antibodies. There are some length limitations of these aptamers as sequences longer than 60 nucleotides are not feasible to produce under the current methods and this can lead to some restrictions in what protein can be targeted (Ray & White 2010). Due to these pros and cons of different targeting strategies, active targeting that utilizes small molecules could be considered as the first choice to start with in an academic project as it would most likely be cheaper and easier to execute.

2.6.6 Cellular internalization and interaction of MSNs

Each living cell is surrounded by a lipid bilayer (LB) called the cell membrane that protects and separates the cell from the surrounding (Wilbrandt 1935). The cell membrane functions as a semi-permeable membrane that allows diffusion of small molecules and lipophilic signaling molecules and together with its receptors and transporters maintains the cells chemical composition (Goñi 2014). The size, shape and charge of the extracellular molecule determines which internalization pathway will be employed by the cell which is also the case for nanoparticles (Verma & Stellacci 2010, Albanese *et al.* 2012). Larger particles are internalized via phagocytosis, whereas particles of moderate size of a few hundred nm can be taken up by several mechanisms whereas small particles of around 10 nm are more likely to unspecifically penetrate the cell membrane (Figure 6; Kou *et al.* 2013). The amount of particles internalized may vary depending on the cell type being investigated and particle size and form, for example, HeLa cells seems to favor spherically shaped 50 nm sized MSNs whereas human melanoma cells favor rod shaped particles of 420 nm size (Lu *et al.* 2009, Barua & Mitragotri 2014). The surface charge of the nanoparticles influences the uptake kinetics as positively charged particles are usually internalized in higher quantities than negatively charged (Chung *et al.* 2007). The surface charge of the particles also seems to determine the intracellular distribution; as positively charged particles possesses the ability to escape endosomes whereas acidic or negative/neutrally charged particles usually retains in lysosomes designated for degradation (Yue *et al.* 2011, Baltazar *et al.* 2012). The undelaying mechanism of this endosomal escape is probably due to of the extra positive charge of the nanoparticle is being balanced by chloride ions influx that results in an increased ionic strength. This in turn leads to increase volume of water inside the endosome followed by swelling and finally rupture of the membrane, a phenomenon known as "proton-sponge" effect that results in the escape of the nanoparticle from the endosome (Godbey *et al.* 1999, Rosenholm *et al.* 2009, Varkouhi *et al.* 2011).

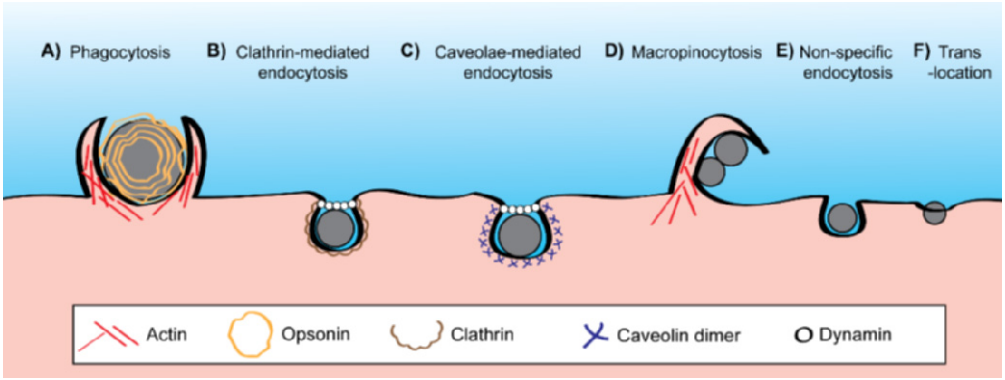

Figure 6. Schematic representation of nanoparticle internalization pathways. a) Larger particles are internalized via phagocytosis mostly by macrophages through actin-based mechanism. Moderate sized nanoparticles can be internalized through different mechanism for example; b) Clathrin-mediated endocytosis, c) caveolae-mediated endocytosis or d) by engulfing particles and the extracellular milieu by macropinocytosis. There are other e) non-specific internalizations that are clathrin and caveolin independent and tiny particles can unspecifically pass through membranes by f) trans-location (adapted from Hillaireau & Couvreur 2009, Kou *et al.* 2013).

The particles surface balance between hydrophobicity and hydrophilicity plays an important role in stability and internalization. Hydrophobic particles encourage internalization as the cell membrane is made of lipids having high affinity towards each other (Nam *et al.* 2009). However, for the particle to be dispersed in aqueous solution such as in the blood stream and to be released to the cytoplasm it is equally important to have hydrophilic properties, as highly hydrophobic particles tend to aggregates and stay at the cell surface (Samadi Moghaddam *et al.* 2015). Therefore, by functionalizing the inorganic hydrophobic MSN with organic water-soluble polymer such as polyethyleneimine (PEI) or polyethylene glycol (PEG) it is possible to match these criteria for optimal internalization and intracellular distribution (Rosenholm *et al.* 2009, Lee *et al.* 2010b).

2.6.7 Biocompatibility and bio-distribution of MSNs

In order to evaluate the potential clinical use of MSNs as targeted drug delivery systems it is imperative to study not only efficacy or cellular internalization but also the biocompability and bio-distribution both *in vitro* and *in vivo.* As one of the main challenges in targeted drug delivery is to achieve sufficient amount of drug to the target tissue with minimal off-targeting effects (Sanhai *et al.* 2008, Bae & Park 2011). This is of special importance in cancer therapies, were the treatment has serious side-effects on the patients such as hair loss, weight loss, anemia, general nausea and pain (Farokhzad & Langer 2009, Ramirez *et al.* 2009). MSNs have shown considerable potential as drug carrier due to high loading capacity and low toxicity as silica-based materials are biodegradable and therefore generally considered safe (Harrison 2009). By intravenous (i.v.) injections, it is possible to administer directly to the bloodstream where the nanoparticles can either use passive targeting or utilize active targeting in order to seek the tumor cells (Fu *et al.* 2013). With systemic administration, it is possible to bypass some of the hurdles orally ingested drugs might encounter such as, as low pH, enzymes that might metabolize the drug and an intestinal layer that needs to be penetrated (Jain 1999, Sriraman *et al.* 2014). However, nanoparticles in the bloodstream will be covered in plasma proteins (opsonins) that favor phagocytosis by macrophages in the spleen and liver that might limit the amount of particles reaching the target site (Owens & Peppas 2006). Systemic administration might also lead to accumulation of the drug molecule in healthy tissues and organs leading to unwanted side effects (Palumbo *et al.* 2013). Furthermore, if the tumors resides in the brain the particle most also penetrate the blood-brain-barrier (BBB) which can be a challenge, as macromolecules in general are not allowed to enter the brain (Ballabh *et al.* 2004). In order to overcome such obstacles; both the administration route and the nanoparticle design should carefully be considered in order for the cargo to be released at the target site. Studies done on healthy mice shows that the bio-distribution after i.v. injection of MSNs accumulates in the liver, kidney and urine bladder whereas some of the particles were excreted through the renal route (Liu *et al.* 2013, Fu *et al.* 2013). However, a sick tumor bearing mice phenotype is different from a healthy mouse, consequently MSNs accumulates in the tumor area due to the EPR effect of the leaky and fenestrated blood vessels (Matsumura & Maeda 1986, Park & Park 2016). Particles with a hydrodynamic diameter (HD) of a few nm are so small that they can pass the glomerulus in the kidneys and therefore be cleared from the

circulation via the urine (Figure 7; Barua & Mitragotri 2014, Shang *et al.* 2014). Particles larger than 8 nm cannot easily pass through the glomerulus in the kidney as the fenestrations are in the size range of 2-8 nm; however rod-shaped particles with a diameter less than 6 nm can still pass through due to their elongated shape. The renal clearance can be enchanted even with larger particles if the material composition is biodegradable so that the nanoparticle can dissociate into small clearable fragments (Liu *et al.* 2013). On the other hand, particles larger than 200 nm are at risk of being phagocytosed by macrophages in the liver that could influence the final bio-distribution (Hillaireau & Couvreur 2009, Owens & Peppas 2006). Functionalization plays also an important role as PEGylated MSNs with the intermediate size of 70 nm where phagocytosed by macrophages in the liver, spleen and lungs (Lee *et al.* 2010b). Another mice study showed that injected PEI functionalized MSNs accumulated at the tumor site with around 10%, whereas the liver accumulated around 27%, and the lungs had about 15%, with ~14% in the spleen and that the kidneys had around 4% of the circulating particles (Park & Park 2016). Therefore, functionalization, material composition, degradation profile and size do matter for targeted drug delivery and that the desired accumulation at the tumor site can be further increased by adding an active targeting ligand at the surface of the MSNs.

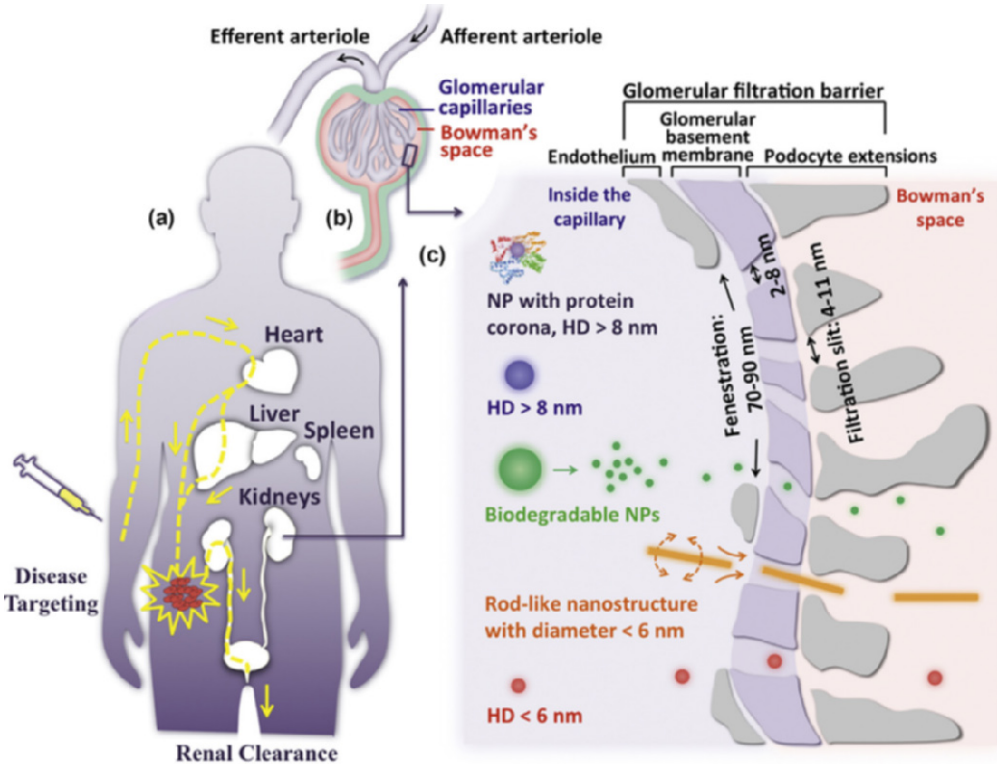

Figure 7. Schematic representation of ideal targeting strategy. a) Clinical use of clearable nanoparticles where the diseased tissue specifically internalizes the particles and the off-targeting particles are rapidly cleared from the circulation through renal clearance. b) Structure of the kidney corpuscle where c) glomerular filtration is a nano scale phenomenon. The capillary wall inside the glomerulus is made of three layers: fenestrated endothelium, glomerular basement membrane and podocyte extensions of epithelial cells (Liu *et al.* 2013).

2.6.8 Drug incorporation and drug release of MSNs

Mesoporous silica nanoparticles have shown considerable potential as targeted drug delivery systems because of their unique properties e.g. high loading degrees of drug molecules, controlled drug release kinetics and the possibility of various targeting ligand functionalization (Liong *et al.* 2008, Wang 2009, Vivero-Escoto *et al.* 2010). By loading drugs inside the porous structures of the particles it is possible to have controlled intracellular release of hydrophobic cargo that otherwise would not have reached to the target tissues that could have resulted in a premature release (Vallet-Regí *et al.* 2007, Kwon *et al.* 2013, Bharti *et al.* 2015). Several factors influence drug loading and release kinetics of MSNs such as particle morphology, pore size, chemical composition, functionalization, physiological environment, and the properties of the drug being incorporated to the particle as well as the drug loading method. (Rosenholm *et al.* 2008a, Hao *et al.* 2012, Vallet-Regí *et al.* 2017 Zhou *et al.* 2018).

Currently, the two most common methods for drug loading to the MSNs is either by physical adsorption of a highly saturated drug solution to the porous surface or by covalently conjugating the molecule to the particle surface (Popat *et al.* 2011). The process of impregnating the drug molecule to the pore walls can be facilitated by selecting a solvent that has low affinity to the drug, thus favoring the drug adsorption towards the silica material (Rosenholm & Lindén 2008, Andersson *et al.* 2004). For example, by using a hydrophobic solvent such as cyclohexane with a hydrophobic drug or an aqueous solution for water-soluble drugs (Rosenholm *et al.* 2009, Rosenholm & Lindén 2008). Furthermore, the charge of both the drug molecule and MSNs surface influences drug adsorption. The non-functionalized MSNs have a negative charge and will attract positively charged drug molecules as the PEI functionalized particles have a positive charge which will allow loading of negatively charged drug molecules (Andersson *et al.* 2004). By covalently conjugating a drug molecule in the porous structure it is possible to have an enzymatic driven drug release inside the cells without undesired leaking during the journey to the target site (Mortera *et al.* 2009, Popat *et al.* 2012, Yuan *et al.* 2013). However, careful considerations need to be accounted for when covalently attaching drug molecules on the particle as this might allosterically change the configuration of the molecule to its inactive form (Yuan *et al.* 2013). The drug inside the MSNs can also be released by simple diffusion, temperature-driven release, pH driven or photo-induced release (Figure 8). The release mechanism and kinetics of MSNs depends on drug solubility and particle properties, for example, water-soluble drugs are mainly released by diffusion, whereas hydrophobic drugs are usually released by degradation of the carrier (Costa and Lobo 2001, von Haartman *et al.* 2016). Spherical nanoparticles have shown to have faster dissolution rates than rod shaped particles, which is due to their relative larger outer surface area (Hao *et al.* 2012). Furthermore, the endosomal release of the drug-loaded nanoparticle can be facilitated by the proton-sponge effect (Godbey *et al.* 1999, Varkouhi *et al.* 2011). Particle functionalization plays also an important role in drug dissolution from the nanoparticles; for example, PEI branching have been shown to function as a “molecular gate” preventing premature release of drug molecule outside target cells (Zhou *et al.* 2018, Rosenholm *et al.* 2008b, Mamaeva *et al.* 2016).

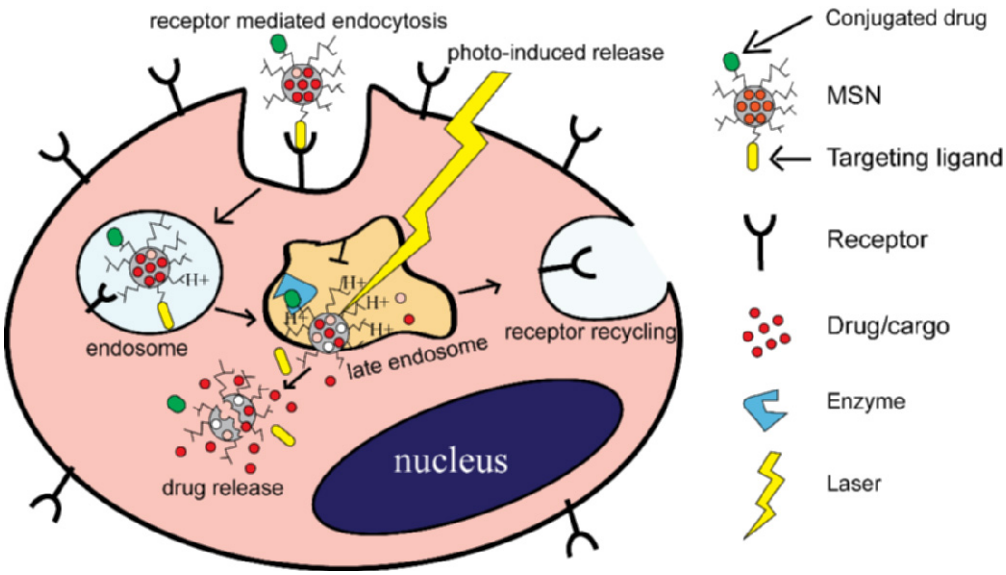

Figure 8. Schematic presentation showing receptor mediated particle internalization and different drug release mechanisms from MSNs. The drug cargo can be released through simple diffusion in the case of water-soluble drugs or as a consequent of a decrease of pH in the late endosome resulting in an endosomal release of the drug carrier or by photo-release induced by an external laser or by degradation in the lysosome or by erosion of the particle.

In addition, drug-loading degree can influence the release kinetics; having a high loading-degree increases the formation of crystalline form of the drug inside the particle (Popat *et al.* 2011). As drugs in the crystalline form have lower dissolution rate than drugs in the amorphous form, therefore having the molecule in the non-crystalline form might be of interest for increasing drug efficacy (Maghsoodi 2015). Furthermore, pore size plays an important role as pores smaller than 10 nm in diameter confines the drug molecule inside the particle preventing crystallization of the molecule, therefore keeping the drug in an amorphous state (Zhou *et al.* 2018). It is due to these highly variable design possibilities of MSNs and their high drug loading capabilities that makes them potential drug delivery systems for various diseases and conditions.

2.7 Celastrol - a natural compound as potential drug candidate

Natural compounds have lately received attention in the pharmaceutical field due to limitations of synthetized drug molecules that currently can be manufactured. For example, cost efficiently synthetizing complex chiral molecules in larger quantities, is still a challenge (Atanasov *et al.* 2015). Natural compounds on the other hand, can be very complex molecules made by living organism that are evolutionary optimized for having a biological functions or activity (Beutler 2009). The natural compound celastrol is a pentacyclic triterpene extracted from the traditional Chinese medicinal plant Thunder God Vine (*Tripterygium wilfordii Hook.F.*) that have been used for centuries against fewer, rheumatics and other inflammations (Westerheide *et al.* 2004, Salminen *et al.* 2010). Celastrol has the ability of manipulating cellular homeostasis depending on the amount being administered and what cell type is affected (Figure

9). Celastrol reacts to the nucleophilic thiol groups of the amino acid cysteine forming covalent Michael adducts, thereby changing the structure and function of the protein (Salminen *et al.* 2010). In lower concentration, celastrol activates the cellular heat shock response (HSR) in similar manners as heat stress by turning on the heat shock transcription factor 1 (HSF1), which leads to the increased expression of molecular chaperones called heat shock proteins (HSPs; Chow *et al.* 2007, Westerheide *et al.* 2004). Molecular chaperons are important in protein quality control and folding, as well as in the protection of cells from different forms of proteotoxic stress, such as heat shock, oxidative stress, heavy metals and chemicals (Westerheide *et al.* 2004, Trott *et al.* 2008). Many neurodegenerative diseases, such as Huntington's and Kennedy's disease, are characterized by protein aggregates that have a toxic effect on cells. These polyglutamine aggregates are also considered the underlying cause for the initiation and progression of other neurodegenerative diseases such as Alzheimer's and Parkinson's disease (Adachi *et al.* 2009, Leak *et al.* 2014). The 70-kDa heat shock protein (Hsp70) assist a wide range of protein folding processes such as the assembly of newly synthesized proteins as well as the refolding of misfolded proteins (Mayer & Bukau 2005). An increase in expression of molecular chaperones has been found to reduce the toxicity of protein aggregates and therefore up-regulation of molecular chaperones is of pharmacological interest in treating diseases characterized by accelerated protein aggregation (Dubey *et al.* 2015). However, recent studies done on yeast has shown that the molecular chaperone Hsp70 functions as an negative feedback loop of its transcription factor HSF1, where a sudden increase in the expression of Hsp70 as an consequence of proteotoxic stress leads to the deactivation of HSF1 turning off the transcription of the molecular chaperone (Krakowiak *et al.* 2018). Therefore, pharmacologically activating the heat shock response by an steady release kinetics without triggering the negative feedback loop could be beneficial in treating diseases associated with protein aggregates such as Alzheimer's and Parkinson's.

Celastrol have recently gained medical interest as a possible therapeutics to be used for inducing the heat shock response (Cascão *et al.* 2017). However, the therapeutic window for the use of celastrol is narrow, because of low water solubility and due to higher concentrations induces toxicity by intervening with cell division (Li *et al.* 2012). Celastrols ability to induce cell death is through destabilizing the mitotic spindle of dividing cells and by disrupting topoisomerase II function that ultimately leads to DNA fragmentation and cell death (Jo *et al.* 2010). However, by targeted drug delivery, it would be possible to increasing the local concentration of celastrol in cancer cells with high cell division in order to kill these fast growing cells through mitotic catastrophe (Piras & Piras 1975). On the other hand, chemically inducing the heat shock response in neuronal cells of Alzhaimers patients it would be possible protects the brain from accumulating further harmful protein aggregates (Salminen *et al.* 2010, Cascão *et al.* 2017). Taking together, targeting celastrol to specific cell types by carrier systems could significantly lower the amount of drug concentration needed to be administered to the patients for inducing desired kinetics of the heat shock response and consequently minimize the associated toxic effects.

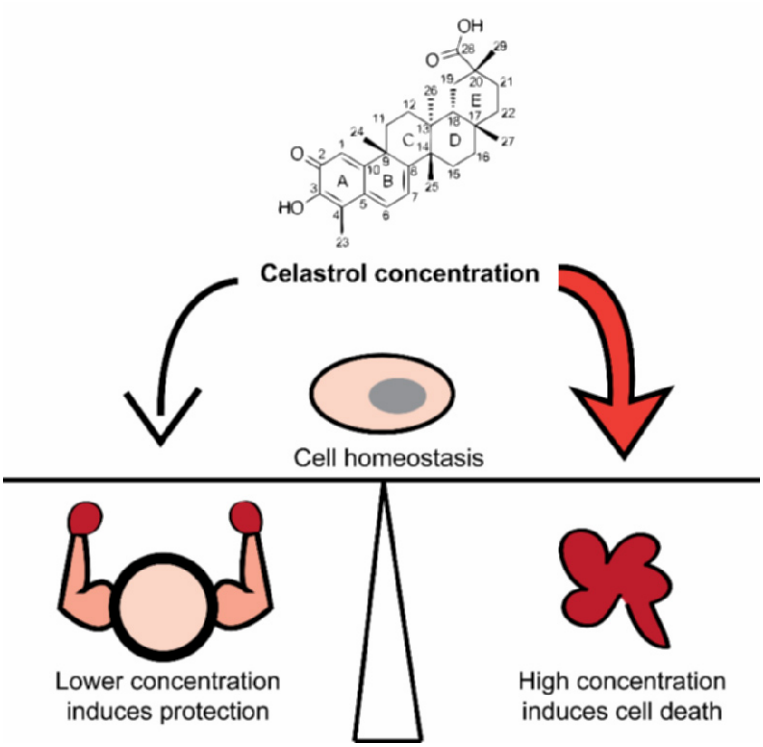

Figure 9. Celastrols unique property of modulating cellular homeostasis. Low concentrations induces the heat shock response increasing the amount of molecular chaperones thus protects the cells from harmful protein aggregates. High concentrations of celastrol in dividing cells destabilize the microtubule leading to mitotic catastrophe and cell death. Therefore, targeting celastrol to specific cell types by carrier systems could be beneficial in diseases that originate from proteotoxic stresses.

2.8 Quantitative bioimage analytics for personalized diagnostics

Historically Antony van Leeuwenhoek (1632-1723) is considered one of the pioneers in the field of microcopy where he gave detailed descriptions of protozoans in different environments with his hand made microscope (Lane 2015). In the past, microscopy was a qualitative method; however as the digitalization made several advances also in digital microscopy it is nowadays possible to also extract quantitative information from qualitative images (Nat Methods 2012). Today, bioimaging has grown to become one of the key methodologies in biomedical research. New imaging techniques emerges that uses ever-higher resolution combined with faster than before throughput measurements producing large multidimensional images (Kankaanpää *et al.* 2012). However, manual quantification still often used in order to transform the vast arrays of image data produced into meaningful information. Nowadays there are numerous general image analysis software's available, however it is often necessary to develop tailor made analytical workflows for each specific biological purpose which can be challenging as most cell biologist do not have an programming background (Nat Methods 2012, Kankaanpää *et al.* 2012, Carpenter *et al.* 2012).

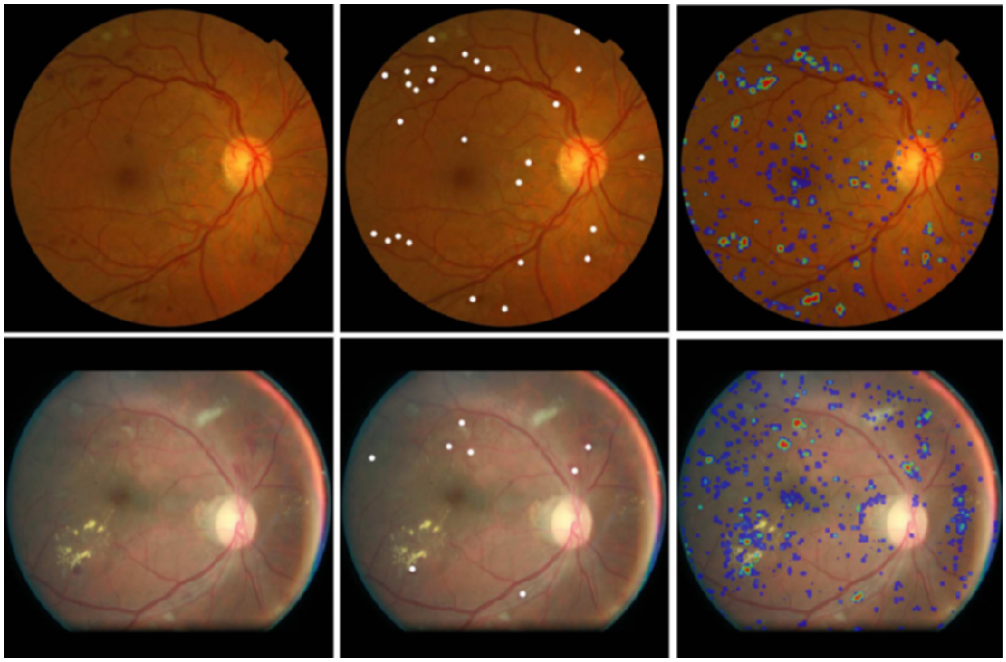

Figure 10. Automated image analysis for identifying hemorrhage centers in human retinas. The left column depicts an example of color fundus images of a human retina taken from the Kaggle dataset. The middle column shows reference hemorrhage center locations depicted as white dots. The right column shows pixel probability maps obtained by deep learning network architectures image analysis (Van Grinsven *et al.* 2015).

There are a few user-friendly image analysis software available such as ImageJ, Fiji, CellProfiler, BioImageXD and Icy that can be implemented without advanced programming skills in order to acquire quantitative data (Hartig 2013, Eliceiri *et al.* 2012). Computerized image analysis can also gain new information, such as size distribution, intensity quantifications and co-localization that would manually be too laborious to execute. BioImageXD for example, supports true 3D data analysis that include flexible visualization and easy-to-use batch processing that requires no programming skills (Kankaanpää *et al.* 2012). BioImageXD has been used in many publications within the biomedical research field ranging from virology and nanoparticle internalization to cancer medicine and drug development (Upla *et al.* 2004, Karjalainen *et al.* 2008, Sukumaran *et al.* 2012). Such computerized image quantification workflows could also open up possibilities for automated diagnostics and personalized medicine to fight against different forms of diseases such as cancer and neurodegenerative disorders (Kim *et al.* 2011, Oxtoby *et al.* 2017). For example, it would be possible to analyze the amount of protein aggregates in brain tissue or the relative amount of heat shock proteins expressed in traumatized organs such as the heart or liver. There are already some image analysis currently used in clinics, for example, identifying anatomical changes in mammography of patient with possible breast cancer. The method is based on texture analysis of mammograms where the clinician have selected the region of interest, then the computer automatically discriminates between benign and malignant clusters based on the preset classification schemes (Kim *et al.* 2011). In another study, automated image analysis was used in

combination with computer learning in order to identify hemorrhage centers in human retinas (Figure 10). Demonstrating that in the future, it would be possible of combining automated image analysis with deep learning of clinical data for even faster personalized diagnostics with less need of human operation and interpretation (Van Grinsven *et al.* 2015).

2.9 Funding and patenting challenges in academic research

Funding opportunities in the United states of America (USA) has changed during the past 50 years from previously mostly federal funded research to a more mixed source of finance with also business-funded basis (Edwards & Roy 2017). This has led to a hypercompetitive environment for academics seeking funding from government agencies such as National Institutes of Health (NIH), Centers for Disease Control and Prevention (CDC) that creates pressure for researchers to "cut corners" leading towards possible unethical behavior. Because of the increased competition and the demise of academic positions, many PhD graduates are selecting careers elsewhere in government or in industry (Abbott *et al.* 2010, Stephan 2012a&b, Edwards & Roy 2017). Obtaining funding is also an age-related problem as young scientists with novel ideas might be rejected, as these new ideas might not fit in the current accepted view. This happened to the Nobel Prize winners Drs. Barry Marshall and Robin Warren in the 1980s when they tried presenting their findings that ulceration is primarily an infectious disease at a gastroenterology meeting in Australia, as their abstract was rejected because at that time ulcers were believed to be a result from stress (Shuchman 2018).

During the last decades, revolutionary advances in gene therapy, stem cell research, proteomics, genomics and nanotechnology have shown that there is a need of reconstructing traditional basic science and clinical research in order to facilitate translational research that would give rise to novel effective therapeutics (Homer-Vanniasinkam & Tsui 2012). The academic culture need to start valuing patenting and commercialization activity as important merit for career advancement as publishing and teaching. As industrial research laboratories are in a decline in the US and universities need to play a more central role in technology transfer for facilitating new discoveries and inventions (Sanberg *et al.* 2014). The US Department of Commerce's report in 2012 lists that there is a need to "speed the movement of ideas from basic science labs to commercial application". Innovations are crucial in the modern knowledge-centered economic growth of welfare countries with high salaries and raw material shortage combined with an ageing population and its associated problems (Mainzer 2011, Lunenfeld 2013, Sanberg *et al.* 2014). Therefore, integration of different scientific fields with medicine is crucial in order to response to transdisciplinary global problems. The Carl von Linde-Academy in Germany is prime example of such innovation center; distinguished for its combination of natural science, medicine, and life sciences platforms with interdisciplinary research projects and courses across all faculties. The mission of the Carl von Linde-Academy is to find and support creative potentials of the university, a vision strongly supported by the German state and society (Mainzer 2011).

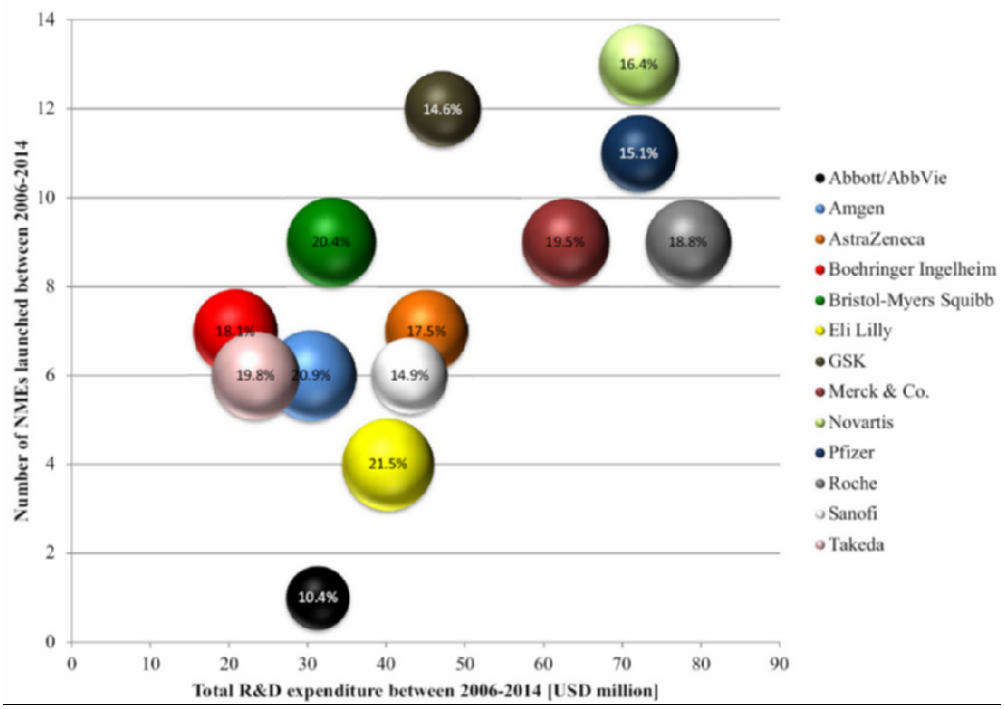

Figure 11. Research and development (R&D) efficiencies of research-based pharmaceutical companies during the years 2006–2014. Total number of new molecular entities (NMEs) approved by the Food and Drug Administration (FDA) compared to the total R&D expenditure per company. The size of the bubble illustrates the R&D intensity calculated from R&D expenditure divided with total sales shown in percentages. Calculation that the accumulative cost per approved drug is approximately 3 billion USD (Schuhmacher *et al.* 2016).

One could argue that the main goal of biomedical research is to ensure that inventions such as a new therapy, device or method would be clinically implemented as the initial motivation for the researcher often is based on trying to solve a problem and cancer is one prime example of such situation (Heus *et al.* 2017). However, the development of an invention can be very expensive, for example, clinical testing of a drug typically have an accumulative cost of millions of US dollars and therefore it is crucial to protect intellectual property rights (IPR) in order to have a fair return of the initial investment (Figure 11; Heus *et al.* 2017, Schuhmacher *et al.* 2016). The historical cost per approved drug has gone from 1 billion US dollars to today's estimation of more than 3 billion dollars (Schuhmacher *et al.* 2016). Aspects that is not generally acknowledged among academic researchers as their model of operation differs from the business model of a pharmaceutic company, and as an consequents universities often have little founding left for product development and patenting (Heus *et al.* 2017). In the US it is estimated that 1 million dollars of federal funding give rise to 10 new publication but only 0.2 new patents, rendering the impact of state funded research to relatively small (Jacob & Lefgren 2011). On the other hand, funding agencies are starting to place emphasis also on translational research as separate funding entities are being developed; NIH's National Center for Advancing Translational Sciences is one example that will help universities build long-term

partnerships with industry (Sanberg *et al.* 2014). Therefore, supporting interdisciplinary PhD programs with integrated IPR funding combined with an established industrial network could facilitate innovations and create new effective therapies that could benefit patients and society as the cost of R&D is in millions (Figure 12; Hammerstedt & Blach 2008).

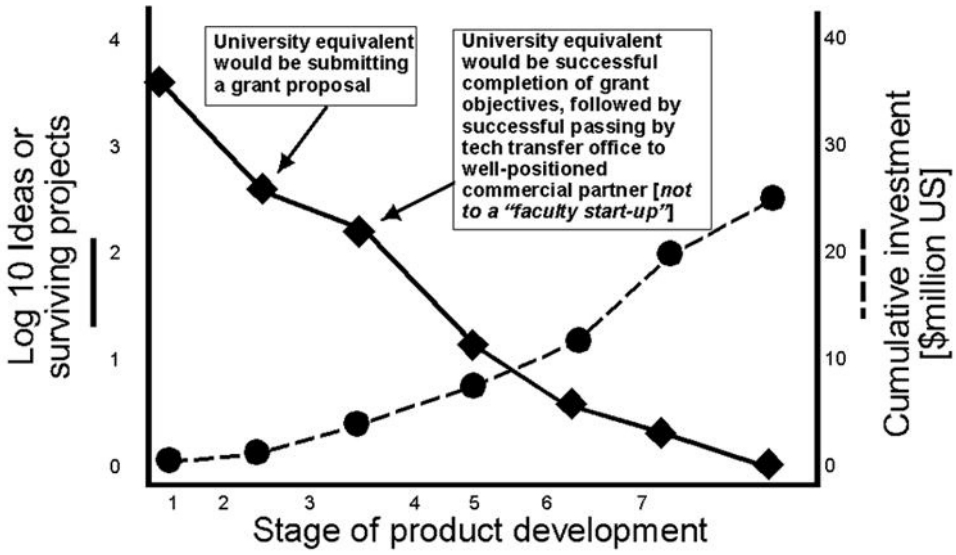

Figure 12. Graphic representation of the relative progress of original academic ideas through product development to final profit making product (Hammerstedt & Blach 2008).

3. AIM OF THE STUDY

The collective aim of this thesis was to create new innovative drug delivery systems that could be used in the future to fight cancer, and to develop imaging modalities for detecting the drug efficacy in target cells. Mesoporous silica nanoparticles (MSN) were chosen as delivery system owing to their high loading capabiliaty of hydrophobic molecules and due to their modular design with endless functionalization possibilities. By combining John Eriksson's labs experience in cell death and survial with Kid Törnqvist's group's cell signaling knowledge together with Jessica Rosenholm's BioNanoMaterials group it was possible to create MSNs for targeted drug delivery that can be used for controlling the cellular homeostasis. Furthermore, this collaboration has opened up the possibility of evaluating different targeting strategies and their efficacy towards cancer cells.

The first specific aim was to exploit cancer cells increased metabolism in order to achieve targeted drug delivery. Since cancerous cells have much faster metabolic rate than most normal healthy cells they take up glucose at significantly higher rates, potentially allowing for selective internalization of glucose-conjugated nanoparticles. By loading the nanoparticle with celastrol, an active ingredient of the traditional Chinese medicinal plant Tripterygium Wilfordii, it should be possible to specifically target cancer cells and induces apoptosis (***I***).

The second specific aim was to achieve target selectivity by functionalizing the nanoparticles surface with folic acid (FA), as many cancer cells have high folate receptor (FR) expression and previous studies have shown considerable particle internalization through FR-mediated endocytosis. The nanoparticles were also loaded with the poorly water-soluble drug celastrol that has the ability in lower dosages to activate the heat shock response and induce the formation of nuclear stress bodies (nSBs). The response, in this study the formation of nSBs, was quantified with our tailor-made analytical tool that uses BioImageXD; an open source software for evaluating the target specificity of these drug-loaded nanoparticles compared to freely administered celastrol (***II***).

The third specific aim was to create a multidrug-loaded nanoparticle that targets cancer cells by utilizing an active targeting ligand combined with a second drug loaded inside the particle. The idea is to use an active ligand on the surface of the nanoparticle as well as load the particle with an anti-proliferating molecule fingolimod (FTY720) that works by inhibiting the phosphorylation of sphingosine and thereby blocks the production of the bioactive molecule sphingosine 1-phosphate (S1P), which is important for cell growth, survival and migration. The active ligand methotrexate (MTX) is a chemotherapy agent that has been used for decades; MTX ultimately blocks the synthesis of thymine and purine nucleotides leading to cell death. This multidrug-loaded nanoparticle could be used for metastatic cancer treatment when conventional cancer treatments have a severe negative effect on the patient. As the nanoparticle would first seek the metastatic cell with the targeting ligand MTX and then together with the second active molecule FTY720 destroy the cancerous cell (***III***).

4. MATERIALS AND METHODS

This section contains the main aspects of the materials and methods used in this thesis, however the details can be found in the original publications and manuscripts (***I-III***).

4.1. Synthesis of mesoporous silica nanoparticles

The mesoporous silica nanoparticle (MSN) core and the polyethyleneimine (PEI) coating were synthesized according to our previously published protocols (Nakamura *et al.* 2007, Rosenholm *et al.* 2006, 2008a&b, 2009, 2010a&b). In our standardized procedure, 1.19 g of tetramethoxysilane (TMOS) was mixed with 3-aminopropyltrimethoxysilane (APS) in an alkaline solution with an H_2O: MeOH ratio of 60:40, containing the structure-directing agent cetyltrimethyl ammonium chloride (CTACl). In order to make the particles inherently fluorescent, 250 µl of a solution containing fluorescein isothiocyanate (FITC) in dimethylformamide (DMF; 1 mg/ml) was added to the siliane mixture. The resulting alkaline synthesis solution has a molar ratio of 0.9 TMOS: 0.1 APS: 1.27 CTACl: 0.26 NaOH: 1439 MeOH: 2560 H2O. The solution was kept overnight at room temperature under constant stir and then the precipitate was collected by centrifugation, washed with deionized water and ethanol. Then the particles were dried *in vacuo* and the structure-directing agent was removed by repeated ultrasonic treatment in acidic ethanol. The polyethyleneimine, PEI, branching was grown by adding aziridine under constant stir in a toluene acetic acid solution overnight, thereafter the particles were centrifuged, washed and vacuum dried and stored for further processing and analysis (***I-III***).

4.2. Functionalization and characterization of MSN

The particle system comprising of a mesoporous silica core and PEI branching layer was further functionalized by either sugar motifs, FA or MTX according to procedures written in the publication and manuscripts (***I-III***). The mesoscopic ordering of the MSN was detected by powder-XRD using a Kratky compact small-angle system (M. Braun, Austria), the particle size and morphology was determined by scanning electron microscopy (JSM-6335F, Jeol Ltd., Japan). The hydrodynamic size of the particles was determined by dynamic light scattering (ZetaSizer NanoZS, Malvern Instruments Ltd., UK) and the mesoporosity by nitrogen sorption measurements (ASAP 2010 sorptometer, Micromeritics, USA). Thermogravimetric analysis (TGA, STA 449 F1 Jupiter, Netzsch GmbH & Co, Germany) was utilized in order to estimate the amount of PEI, sugar motifs, FA or MTX functionalized to the particle. To find out the amount of drug loading in the MSNs, samples were first dispersed in ethanol for complete drug elution. The drug concentration was determined by UV/vis spectroscopy measurements at a wavelength of 425 nm.

4.3. Image analysis based size distribution of MSNs

In order to quantify the specific size distribution of the synthetized MSNs, transmission electron microscope (TEM; JEM 1400-Plus, JEOL Ltd., Tokyo, Japan) operating at 120 kV with a LaB6 filament and a 2 k ×2 k CCD camera was utilized in conjunction with ImageJ for post image processing (Souza *et al.* 2016, Rueden *et al.* 2017). First, the scale bar was manually set by the calibration data of each image, and then the acquired image was blurred with Gaussian smooth set at 5.00 for minimizing

detection of artifacts from being registered as individual particles (Underwood & Gorham 2017). Automatic thresholding was then used to divide the image into foreground (MSNs) and background, which is based on IsoData algorithm (Ridler & Calvard 1978). Then, "Analyze particles" was used to identify and measure the area of each individual MSNs (Rueden *et al.* 2017, Underwood & Gorham 2017). Utilizing the formula $d = 2\sqrt{A}/\pi$, it was possible to calculate the diameter (d) of each MSN from the area (A), producing quantifiable size distributions of the MSNs from the TEM images. Objects smaller than 100 nm was considered artifacts or fragments and objects bigger than 400 nm were particle aggregates and were therefore excluded from the analysis. At least three representative images were acquired from three independent experiments (#batches) of synthetized MSNs. The error bars represent plus minus the standard deviation of the mean (±SD) of each particle batch and the number (n) represent how many individual MSNs were analyzed. Frequency distribution was used for representing the size distributions of the total MSNs populations from the quantified TEM images.

4.4. Glucose consumption in normal versus cancerous cells

The glucose consumption of normal MEF (mouse embryonic fibroblast) versus cancerous HeLa (cervical cancer cells) and A549 (lung epithelial carcinomas) cells were studied using a Glucose (GO) Assay kit (Sigma-Aldrich, St. Louis, MO, USA). First, 10^5 cells of each cell line were seeded separately in 6 well plates and the cells were allowed to adhere overnight. Then the used cell medium was changed with 2 ml of unused Dulbecco's Modified Eagle's medium (DMEM) and the cells were allowed to consume nutrients for 24 hours. The glucose consumption were then detected at 540 nm using Hidex Sense Beta Plus microplate reader (Hidex Oy, Turku, Finland). The glucose concentration in each sample medium was then calculated using a glucose standard curve, and then the obtained glucose amount was subtracted from the measured glucose concentration in the unused cell medium containing 45.93 μg/ml glucose in order to calculate the glucose consumption in each cell line (***I***).

4.5. Specific MSNs uptake in cancer cells

For the *in vitro* uptake studies the cancerous target cells that were cultured and used were follicular thyroid carcinoma cells (ML-1) and cervical cancer cells (HeLa). The non-target cells were mouse embryonic fibroblasts (MEF) cells and normal human primary thyroid follicular epithelial cells (Nthy-ori 3-1) or lung epithelial carcinomas (A549). The amount of endocytosed particles inside the cell population was analyzed by BD FacsCalibur flow cytometer (FL-I; BD Pharmingen, USA) and the data was quantified and analyzed using BD CellQuest Pro™ software. For specific particle endocytosis studies confocal microscopy Zeiss LSM510 META (Carl Zeiss Microscopy GmbH, Jena, Germany) were used to measure FITC intensity inside cells. The extracellular fluorescence was quenched with trypan blue and the cell membrane was labaled with rhodamine-lectin (Vector Laboratories, Burlingame, California, USA). The imgages was taken with 63/100× oil objective using 488 nm excitation and 500–550 nm emission for detecting the FITC channel, 405 nm excitation with 420–480 nm emission for detecting the DAPI channel and for detecting the rhodamine-lectin an excitation of 543 nm with emission filter of 570–600 nm (***I-III***).

4.6. Image quantification of internalized MSNs

In order to quantify specific particle internalization in the selected cell lines; confocal microscopy was employed in combination with image analysis. Cells were incubated with 30 µg/ml glucose conjugated inherent FITC fluorescent MSNs for 3 hours. The extracellular fluorescent signal was quenched by trypan blue incubation and then the cells were fixed, mounted on slides in VECTASHIELD® Mounting Media containing 4', 6-diamidino-2-phenylindole dihydrochloride (DAPI; Vector Laboratories, Burlingame, CA, USA). Particle internalization was detected using a Zeiss LSM510 META confocal microscope (Carl Zeiss Microscopy GmbH, Jena, Germany) with 63x oil objective utilizing 405 nm excitation for the DAPI fluorescent stain and 488 nm excitation for the FITC molecule. The particle internalization was quantified with BioImageXD 1.0RC3 software (Kankaanpää *et al.* 2012). To count the cell numbers per image the DAPI channel was used in order to separate the cell nucleus from the background. Then the average normalized FITC intensity was measured and divided by the total cell number giving a value of FITC intensity per cell (***I***).

4.7. Efficacy of drug-loaded MSNs

In order to measure the drug-loaded nanoparticle efficacy compared to the free drug *in vitro*, DNA fragmentation was measured as a hallmark for apoptotic cells (***I-III***). The method involves detection of the apoptotic cell's DNA as it starts to fragment and these DNA fragments can then bind to propidium iodide (PI). The DNA bound PI causes a change in its excitation wavelength that can be detected and quantified by flow cytometry (Nicoletti *et al.* 1991). To verify the toxicity and efficacy of the different treatments; WST-1 cell viability assay (Roche Applied Science, Upper Bavaria, Germany) and crystal violet was utilized, for counting and monitoring cells Bürker chamber was used with Brightfield microscopes (Thomas *et al.* 2004).

4.8. Target validation of drug-loaded MSNs

For drug target validation immunofluorescence analysis was employed. HeLa or A549 cells were grown on sterile coverslips under either control conditions, heat shocked, or treated with celastrol or celastrol-loaded MSNs. Cells were washed, fixed, permeabilized and then incubated with blocking solution for 1 hour. Samples were kept overnight in cold with rabbit anti-HSF1 antibody (1:400 dilution; Holmberg *et al.* 2000), washed and then incubated with the secondary goat anti-rabbit antibodies in a dilution of 1:5000 (Alexa™ 546, Molecular Probes, Eugene, Oregon, USA) in room temperature for 1 hour. The samples were mounted and the DNA was stained with VECTASHIELD® Mounting Media containing DAPI (Vector Laboratories, USA). Images where acquired using a Zeiss LSM510 Meta scanning confocal microscope equipped with the SP2 (version 3.2) software and Plan-Apochromat 63x/1.4 Oil DIC objective, utilizing 405/488 nm and 543/560 nm excitation/emission wavelengths. Images was further processed and analyzed using BioImageXD software, the DAPI channel was employed for identifying and segmenting the cell nucleus. For detecting the nuclear stress bodies the HSF1 channel was segmented using dynamic thresholding. Object co-localization was used to analyze the nSBs inside the separated cell nucleus, which in turn made it possible to determine the size and numbers of nSBs-positive cells within the sample population (***II***).

4.9. Western blot analysis

Western blot analysis was utilized in order to validate both the downstream effects of celastrol as well as to estimate folate receptor (FR) expression levels in the selected cell lines (***I-III***). Cells of interest were grown in control conditions for estimating the FR expression or incubated with increasing amounts of celastrol or celastrol-loaded MSNs for measuring the heat shock response. Whole cells samples were lysed with laemmli buffer containing β-mercaptoethanol and the proteins were denaturated at 95°C for 10 minutes. Proteins were separated by 10% SDS-PAGE and transferred to nitrocellulose membranes. Heat shock protein 70 (Hsp70) were detected with primary antibody Hsp70 (StressGen Biotechnologies Inc., Collegeville, PA, USA) at 1:10000 dilution, folate receptor alpha antibody (FOLR1; Lifespan Biosciences Inc., Seattle, WA, USA) was used at 1:1000 dilution and as loading control anti-β-actin antibody (Sigma-Aldrich, St. Louis, MO, USA) was used at 1:1000 dilution or anti-Hsc70 (StressGen Biotechnologies Corp., Victoria, Canada) at 1:10000 dilution. Horseradish peroxidase conjugated secondary antibodies (GE healthcare, Buckinghamshire, UK) were detected using enhanced chemiluminescence (Amersham Biosciences Corp., Piscataway, NJ, USA). Densitometry of the western blot result was performed using imageJ and normalized to the loading control (Hartig 2013).

4.10. Advanced imaging techniques

To quantify morphological changes in the ML-1 thyroid cancer cells given the combination drug treatment of MTX or FTY720. Cells were grown on sterile 6-well plate and administered either drug cocktail or drug-loaded MSN using 0.219 μM MTX and 4.05 μM FTY720 concentrations. The samples were imaged using the VL21 instrument (Phasefocus Ltd, Sheffield, UK) with 20x magnification using 20 minutes intervals per region of interest (ROI) for a duration of 72 hours. The aim of the investigation was to identify apoptotic phenotypes in the ML-1 cells administered either free drug cocktail or drug-loaded MSNs using advanced image analysis performed by experts from Phasefocus Ltd (***III***).

4.11. *In vitro* invasion assay

To validate the inhibitory effect of the combinatory drug treatment of MTX and FTY720 on cancer cell motility, Boyden chamber invasion experiments were conducted with Transwell Permeable Support inserts with 8 μm pore size (Corning Inc; Corning, NY, USA; Kramer *et al.* 2013, Justus *et al.* 2014). Inserts were coated with human collagen IV thereafter cells were added into the upper well that contained cell culture medium with 10% FBS, as chemoattractant in the lower well a 20% FBS containing medium was used. The concentration of MTX and FTY720 were as follows: the low dosage was 0.13 μM MTX and 2.43 μM FTY720, the high dosage was 0.438 μM MTX and 8.10 μM FTY720 and the test substances were present in both wells. Cells were allowed to invade for 7 hours and then the cells were fixed with paraformaldehyde and stained with crystal violet for visualization and counting using light microscopy (***III***).

4.12. *In vivo* drug efficacy studies

To determine the nanoparticle delivery efficacy *in vivo* using human-derived xenografts in a cost effective way, the chicken chorioallantoic membrane (CAM) model was utilized (***III***; Zeisser-Labouèbe *et al.* 2004). Fertilized chicken eggs were cleaned with 70% ethanol and placed in a 140/200 Rural incubator (FIEM srl, Guanzate, Italy) with the narrow apex down for the first three days at 37°C and with a relative humidity of around 65%. On embryo development day (EDD) three a few mm wide hole were made on the apical side (narrow apex) of the eggshells and the puncture was sealed with adhesive tape. Then the eggs were left in the incubator at static mode for five more days with the narrow apex upwards. ML-1 cells were grown in complete Dulbecco's modified eagle's medium (DMEM), harvested and re-suspended at an density of 1 x 10^6 cells per 10 µl in serum-free media and mixed with equal amount of Matrigel (Growth Factor Reduced Basement Membrane Matrix; Corning) at EDD 8. In parallel, the hole in the eggshells was enlarged with pliers to 2-3 cm and 20 µl of cell suspension was inoculated in a plastic O-rings near major blood vessels at the CAM. In order to protect the embryo, a plastic film was used to seal the opening of the eggshell and the eggs were returned to the incubator and kept at static mode until next step of procedure. At EDD 9 the MTX and FTY720 drug cocktail and multidrug-loaded MSNs were suspended in physiological HEPES buffer at pH 7.2 to concentrations ranging from 1-10 µg of FTY720 / 30 µl (33.3-333.3 µg/ml) and 0.1-1 µg MTX / 30 µl (3.3-33.3 µg/ml) and the treatment volume was 30 µl per egg. The forming tumors were imaged on each day that follows until EDD 12, at which point the solid tumors are excised and weighed as an end point measurement in order to validate the tumor mass. Then the tumors were fixed in paraformaldehyde and stored in paraffin embedded blocks that were cut for further histological preparations.

4.13. Immunohistochemistry of tumor samples

The paraformaldehyde fixed and paraffin embedded tumors were cut into 4 µm sections and immunohistochemically stained with antibodies and reagents listed in the article (***III***). In brief, antigens were retrieved using high-temperature in Tris-EDTA buffer (pH 9), washed in TBS with 0.1% Tween20 (TBST; Sigma-Aldrich, Saint Louis, MO), blocked in 3% BSA (Sigma-Aldrich) in TBST for 1 hour at room temperature then incubated overnight with the primary antibody. On the next day, slides were washed 3x with TBST, incubated with secondary antibody for 30 min, washed three times in TBST and visualized using Liquid DAB+ Substrate Chromogen System (Dako, Glostrup, Denmark). Slides were scanned by Pannoramic 250 Slide Scanner (3DHISTECH Ltd., Budapest, Hungary).

4.14. Statistical analysis

Statistical significance between samples was determined by One-way analysis of variance with Bonferroni post hoc test or Tukey's multiple comparisons test, using GraphPad Prism® 5.0 or 6.0 (San Diego, California, USA). If the p-value was less than 0.05 the data was considered significantly different. The error bars represent plus minus the standard error of the mean (±SEM) or standard deviation (±SD) and the number (n) of samples is indicated in the figure legends (***I-III***).

5. RESULTS AND DISCUSSION

5.1. Mesoporous silica nanoparticles as targeting systems

This thesis contains proof-of-concept on how to target specific cell populations by functionalized drug-loaded nanoparticles. Enabling significantly less off-target effects when administering different compounds such as celastrol, MTX and FTY720 as the drug is accumulated and retained in the cells of interest (***I-III***). Cancer cells were chosen as model system because of cancer being one of the main cause of death in the western world, and many of the cytostatic drugs still in use were developed decades ago with substantial side effects on the patients (Allan & Travis 2005, Wicki *et al.* 2015). Consequently, there is a high demand of developing new forms of cancer treatment with minimal off-target effects, and nanoparticles have shown considerable potential as targeted drug delivery systems (Meijerman *et al.* 2008, Vivero-Escoto *et al.* 2010). Nanoparticle-based drug delivery systems can easily be adapted to specific internalization pathways for different organs and disease conditions by changing the targeting ligand and surface functionalization (Bae & Park 2011). For instance, cancer cells growth advantages is also their biggest disadvantage, as most cancer cells have an increased metabolism and cell division that can be utilized as targeting strategies (Malhotra & Perry 2003, Zhang & Yang 2013). These cancer specific traits are the basis of the studied targeting pathways; as either Gluc, FA or MTX conjugated nanoparticles were synthetized in this thesis. The second step in designing the delivery system is to choose what kind of materials should be used for the particle core, so that the drug of interest can be loaded to the carrier with desired release kinetics without premature release. In addition, the size of the particles needs to be considered, as large particles tend to aggregate in biological systems and tiny nanoparticles can spontaneously penetrate the cell membrane leading towards unspecific internalization in healthy cells (Verma & Stellacci 2010, Albanese *et al.* 2012). The surface functionalization influence also particle toxicity and particle internalization as well as drug release kinetics (Yue *et al.* 2011, Baltazar *et al.* 2012). Due to these demanding requirements, MSNs of modular design in the size range of 250-300 nm were synthetized and evaluated for the use as targeting delivery system for cancer cells.

5.2. Characterization of the synthetized MSNs

The MSNs were synthetized according to the procedure described in the materials methods section, based on similar protocols used in previous studies (Rosenholm *et al.* 2006, 2008a&b, 2009). Four different batches of synthetized MSNs were characterized in this thesis by different methods in order to compare possible variations of these particles (***I-III***). Electron microscopy was utilized in order to confirm the average particle size, monodispersity, morphology and the mesoscopic ordering (Figure 13). The transmission electron microscopy (TEM) reveals that these MSNs have similar porous structure with radially aligned mesopores, and that the average particle size based on the image analysis was around 208 d.nm (Figure 13). The particle size distribution shows that from the 118 analyzed particles around 100 particles were in the size range of 160 – 280 d.nm, verifying a homogenous particle population (Figure 13f). From the scanning electron microscopy (SEM), it was possible to confirm that the average diameter of the particles was indeed around 200-300 d.nm and that the whole particle population had similar morphology (Figure 13d).

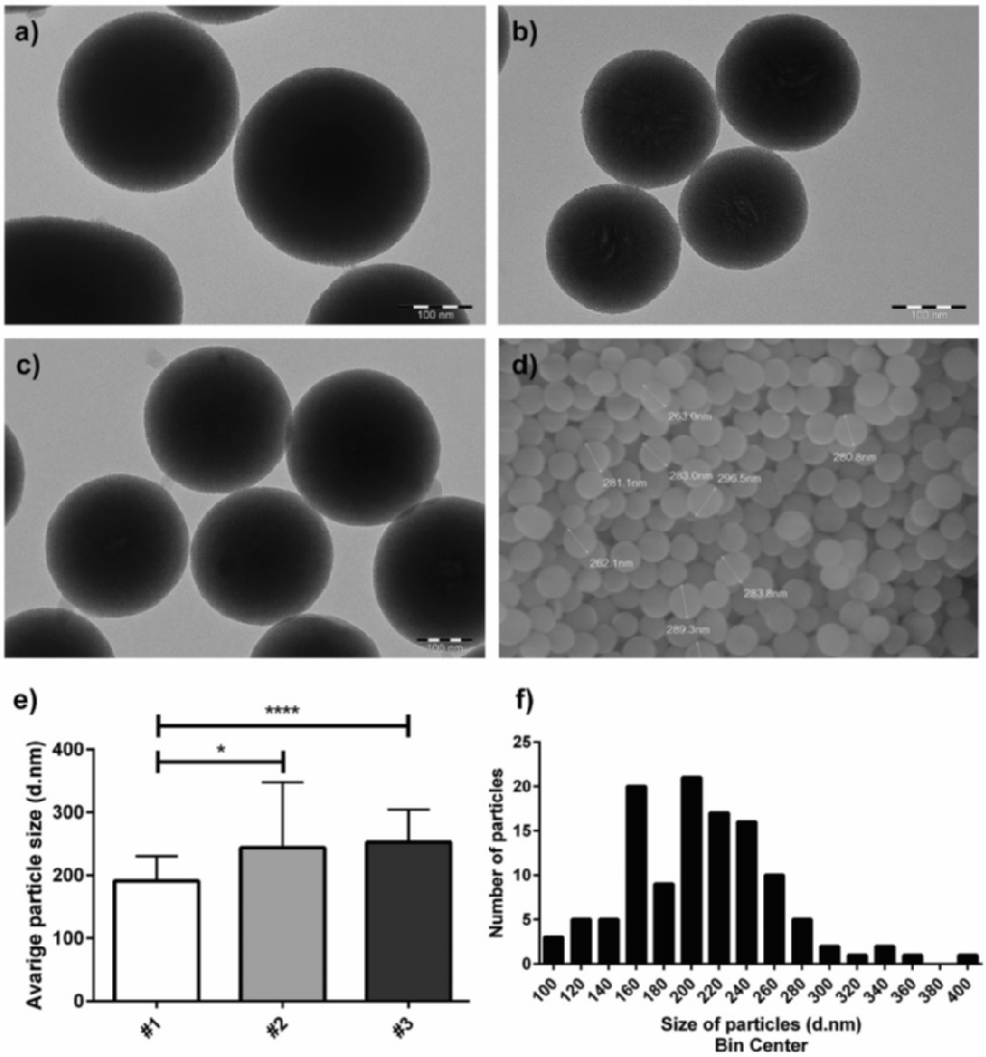

Figure 13. Characterization and size estimation of MSNs. a) TEM image of synthetized MSNs from batch #1, b) TEM image of synthetized MSNs from batch #2, c) TEM image of synthetized MSNs from batch #3, d) SEM image of synthetized MSNs from batch #4, e) image quantification of size difference (d.nm) between batches, f) size distribution (d.nm) in the whole MSN population. Total amount of MSN quantified (n=118), error bars represents mean ± SD, * $P \leq 0.05$, **** $P \leq 0.0001$. Size distribution of objects in diameter (d.nm) and scale bar in images a-c are 100 nm.

Intriguingly, some particle size variations were detected between the synthesis batches (Figure 13a-e). However, when comparing the average size of each batch to the size distribution of the whole particle population, the variation is within the highly probable (~85 %) average size range of 180 – 280 d.nm (Figure 13). It is know that differences in temperature, pH, relative humidity, type of surfactant used and surfactant concentration could affect the shape and size of the synthesized particles (Wan & Zhao 2007, Desai 2012, Ducheyne *et al.* 2015, Donald *et al.* 2016, Baer *et al.* 2018). That could at least partly explain the minor variations in particle size

between batches as the particles were synthetized at different time points and in different facilities that could influence external factors. The zeta potential and hydrodynamic size of the synthetized particles were measured with dynamic light scattering in HEPES buffer at physiological pH 7.2. The "bare" non-functionalized particle shoved lower zeta potential than the PEI branched particles as well as ligand conjugated particles, indicating successful functionalization (Table 2). The hydrodynamic size confirmed full redispersibility of all 4 synthetized particle batches as well as an indication that the first batch of particles had the smallest diameter, which corresponds to the TEM images as well as the quantification (Table 2 & Figure 13). To determine surface area, pore size and pore volume, N_2-sorption measurements was performed and the arrangement and size of the mesopores was detected with small angle X-ray (SAXRD) and the pore width of all analyzed particles were in the range of 3 – 3.5 nm in size (Table 2). In addition, thermogravimetric analysis (TGA) was used to determine the organic content of the PEI branched particles and the amount of functionalized targeting ligand on the particles surface used in this thesis (Rosenholm *et al.* 2009). Based on the TGA analysis, batch number 4 had less PEI branching than batch #1, whereas batch #2 and #3 were quite similar in terms of PEI content. Differences in particle functionalization/charge influence internalization as generally positively charged particles tend to be taken up in larger quantities, however the ligand functionalization influences the overall net charge that was similar in all particles.

Table 2. Physiochemical characterization of synthetized MSNs (*I-III*).

Synthesized Particles (# batch number)	**#1**	**#2**	**#3**	**#4**
Targeting ligand (abbreviation)	**n/a**	**FAaq**	**MTXaq**	**GAorg**
Hydrodynamic size of MSN (d.nm)	243	n/a	n/a	341
Hydrodynamic size of PEI-MSN (d.nm)	384	396	488	490
Hydrodynamic size of ligand-PEI-MSN (d.nm)	n/a	451	373	447
Zeta potential of MSN (mV)	-26.3	-2.4	n/a	-5.5
Zeta potential of PEI-MSN (mV)	28.3	41.2	57.0	50.3
Zeta potential of ligand-PEI-MSN (mV)	n/a	53.1	54.0	52.4
Fluorescence intensity of MSN (520 nm)	956	n/a	n/a	840
Fluorescence intensity of PEI-MSN (520 nm)	432	n/a	292	439
Fluorescence intensity of ligand-PEI-MSN (520 nm)	n/a	n/a	168	385
Organic content of PEI-MSN (weight %)	33	34	34	24
Targeting ligand content (weight %)	n/a	~1	2.10	0.95
Pore volume of MSN (cc/g)	1.856	n/a	0.754	0.833
Pore width of MSN (nm)	4.093	n/a	3.537	3.537
Pore volume of PEI-MSN (cc/g)	0.821	n/a	0.305	0.281
Pore width of PEI-MSN (nm)	3.537	n/a	3.179	3.06
Drug of interest	**n/a**	**Celastrol**	**FTY720**	**Celastrol**
Drug loading degree (%)	n/a	4.10	27.86	2.57

5.3. Functionalization influence drug loading and release kinetics

In this thesis, different drug molecules were loaded or conjugated to ligand functionalized MSNs in order to evaluate the drug delivery potential of these carrier systems (***I-III***). The loading degree inside the particle with the hydrophobic drug celastrol was between 2.57 – 4.1 % of weight depending on batch variations, whereas the drug FTY720 could be loaded to 27.8 – 33.2 weight percentage depending on the functionalization of the particle (Table 2). However, as celastrol was the focus of this thesis, the drug release kinetics were further studied utilizing UV/vis spectroscopy. The *in vitro* release kinetics of both free celastrol and celastrol-loaded MSNs was done in HEPES buffer at 7.2 pH for simulating physiological conditions. Already after 48 hours, the free celastrol had dissolved to a degree of 50 % in the aqueous solution, which is not desirable for intracellular drug delivery as the drug should be released at the target site and not prematurely (Figure 14). The non-functionalized particles showed also rapid release kinetics as after 6 hours around 20 % was released from the carrier, whereafter the release curve stagnated (Figure 14). The rapid release could be explained by excessive drug molecules on the surface of the particles that are almost immediately dissolved in the solution. The functionalized particles does not exhibit the same rapid release kinetics, which demonstrates that that PEI branching does indeed function as an "molecular gate" preventing premature release of the drug preventing the possible drug interaction with healthy cells (Zhou *et al.* 2018). Drug release kinetics of functionalized MSNs depends also on drug solubility, environmental conditions and the degradation properties of the silica material used in the particle (von Haartman *et al.* 2016, Hao *et al.* 2012). The slow release kinetic is beneficial in intracellular drug delivery as it can take several hours for the particle to reach target tissues and can remain there for days (Yu *et al.* 2016, Park & Park 2016).

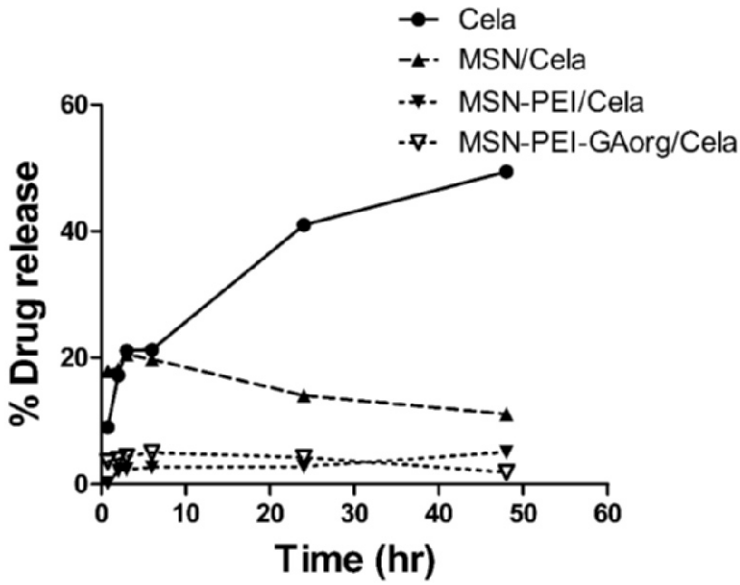

Figure 14. Hydrophobic drug release kinetics. Release/dissolution kinetics of free celastrol, celastrol-loaded control MSNs, celastrol-loaded MSN-PEI and celastrol-loaded MSN-PEI-GAorg in HEPES buffer (pH 7.2) for a duration of 48 hours (adapted from ***I***).

5.4. Functionalization affects particle toxicity

In this part, the *in vitro* toxicity of different surface functionalization was investigated in order to evaluate the potential application of these MSNs as carrier systems. The toxicity results from lower particle concentrations (up to 10 ug/ml) shows no significant difference compared to the control (***I-III***). Higher particle concentrations (30 µg/ml) for 24 hours was studied in HeLa cells using propidium iodide (PI) staining and the apoptotic population was measured by flow cytometry. The results shows that non-functionalized particles are indeed more toxic to cells compared to functionalized particles (Figure 15). The slightly more toxic effect could be a result of non-functionalized particle tendency to aggregate in aqueous solution, which inside the cell would results in DNA damage detected by flow cytometry (Nicoletti *et al.* 1991, Shang *et al.* 2014). Other studies have shown that non-functionalized particles are more toxic to cells than functionalized particles (Chung *et al.* 2007, Lee *et al.* 2010b). On the other hand, positively charged nanoparticles are considered more toxic to cells as they tend to interact with negatively charged proteins and DNA (Fröhlich 2012). The PEI itself have shown to be toxic when freely administered to cells, however no significant cytotoxicity have been reported when using PEI functionalized MSNs in previous studies (Desai *et al.* 2014, Kettiger *et al.* 2015). Indicating that the possible PEI toxicity can be suppressed when made in a larger construct such as a PEI branched MSN (Figure 15). The possible toxicity of functionalized nanoparticles should therefore be evaluated on a case-by-case basis, as looking separately on each component can give a misleading interpretation.

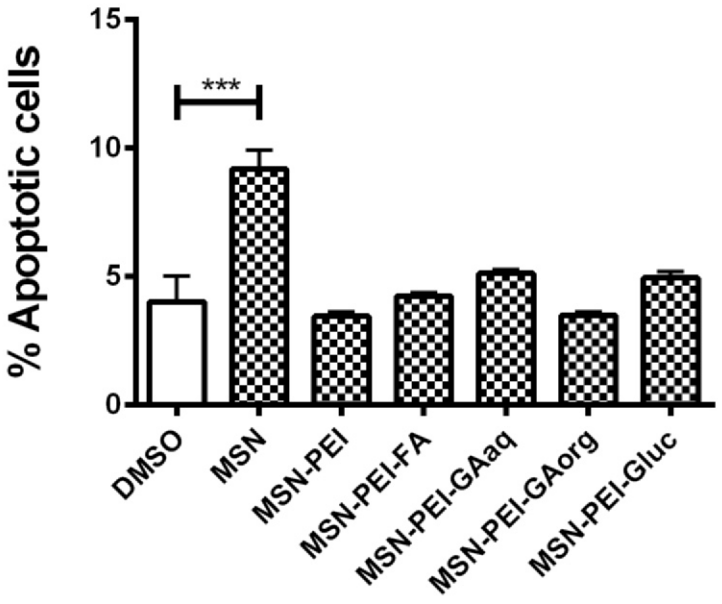

Figure 15. Toxic effect of different functionalized MSNs at 30 µg/ml measured after 24 hours incubation with HeLa cells using PI staining. Non-functionalized particles shows significant toxicity compared to vehicle control (DMSO 1.2% w/v) and functionalized particles. Error bars represent ± SEM (n≥3), *** P ≤ 0.001 (adapted from supp. file ***I***).

5.5. Glucose consumption as targeting strategy in cancer cells

One of the most important aspects in targeted drug delivery is figuring out a way of achieving high drug accumulation in target tissue with minimal off-target effects. This is possible when utilizing differences in the cells of interest as a "Trojan horse" for targeting specific cell populations. One of the hallmarks of cancer is their tendency for accelerated cell growth followed by an increased metabolic activity. Cancer cells have an altered metabolism, whereas normal cells generate adenosine triphosphate (ATP) by aerobic respiration by complete oxidation of glucose molecules in the mitochondria. Cancer cells on the other hand generates ATP through glycolysis that consumes significantly more sugars per generated ATP molecule, producing lactates as a by product (Zhang & Yang 2013, Liberti & Locasale 2016). However, glycolysis has its benefits, as it is 10-100 times faster than aerobic respiration and hypothetically this increased glucose consumption gives cancer cells an additional carbon source for anabolic processes needed for the rapid cell proliferation (Liberti & Locasale 2016). Therefore, Glucose assay kit was utilized in order to verify these metabolic differences in cancerous HeLa and A549 cells compared to normal MEF. The assay show that both HeLa and A549 cancer cells consume significantly more glucose than normal MEF cells (Figure 16). De facto, HeLa cells consumes over twice as much glucose after 24 hours than MEF cells. This elevated cancer cell metabolism was utilized as a targeting strategy for drug delivery in this thesis by conjugating sugar moieties on the surface of these MSNs (***I***).

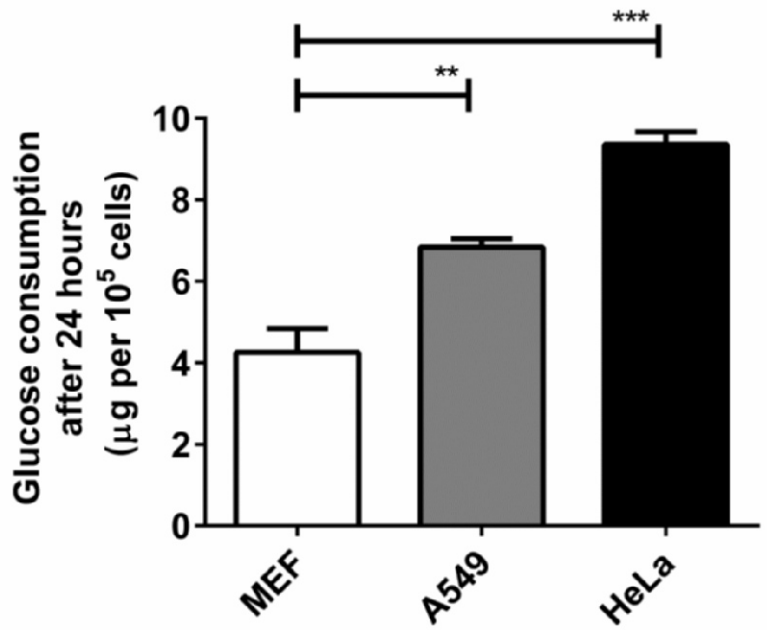

Figure 16. Glucose consumption in MEF, A549 and HeLa cells after 24 hours. The cancer cells have significantly higher glucose consumption than MEF cells seen after 24 hours incubation in complete DMEM. Error bars represent ± SEM (n=3), ** $P \leq 0.01$, *** $P \leq 0.001$ (adapted from supp. file ***I***).

5.6. Functionalization affects particle internalization

In order to investigate the effect of particle functionalization and targeting ligand conjugation on cellular internalization, both flow cytometry and confocal microscopy was utilized. First two different cancer cells (HeLa and A549) with high metabolism compered to normal MEF cells was utilized to provide proof of concept that cancer specific internalization can be achieved with sugar moieties on the particle surface (Figure 17&18). Intriguingly, when conjugating sugar molecules directly on the "bare" particle surface there were no significant increase in particle uptake in either cancer cell lines. Only when conjugating the targeting ligand to PEI branched particles an increased internalization was observed. We could speculate that a certain net positive charge is necessary for particle internalization as the PEI functionalized particles themselves had an increased internalization compared to bare particles, and that the PEI branching is essential for the further increased efficacy of the targeting ligand (Figure 18 & Table 2). However, it was not possible to distinguish which sugar targeting ligand was the most efficient in the terms of uptake percentages in the cancer cells. Therefore, normalized mean fluorescence intensity was calculated from 10 000 cells against each functionalized particle fluorescence which provided the information that the MSN-PEI-GA_{org} had the highest uptake in cancer cells (Figure 18b&d). The functionalized particle uptake in normal MEF cells was around four times lower compared to that of the cancer cells demonstrating selective internalization (Figure 17). In order to confirm that the particles were taken up by the cancer cells and not aggregated on the cell membrane, confocal microscopy was employed. The cell nucleus was stained with DAPI, the cell membrane stained with rhodamine-lectin and the FITC fluorescent particles visualized inside the cell; thus confirming particle internalization (***I***). Furthermore, confocal images of HeLa cells administered with the different targeting ligand quantified using BioImageXD showed significantly higher internalization of the MSN-PEI-GA_{org} validating the selected targeting motif (***I***).

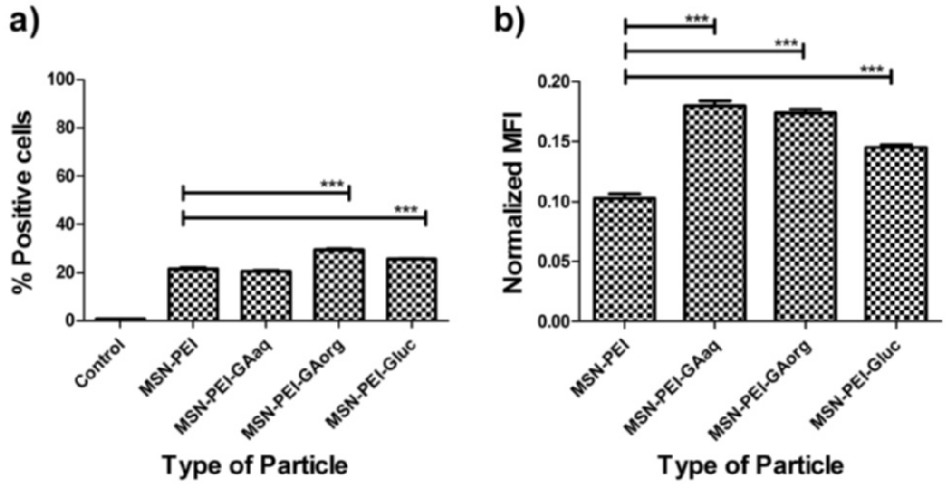

Figure 17. Flow cytometry quantification of MSNs internalization in MEF cells after 3 hours incubation. a) Mean % of FITC positive cells using 5 µg/ml of nanoparticles or control. b) Normalized mean fluorescence intensity resulting from particle uptake in MEF cells. Error bars represent ± SEM (n≥4), *** $P \leq 0.001$ (***I***).

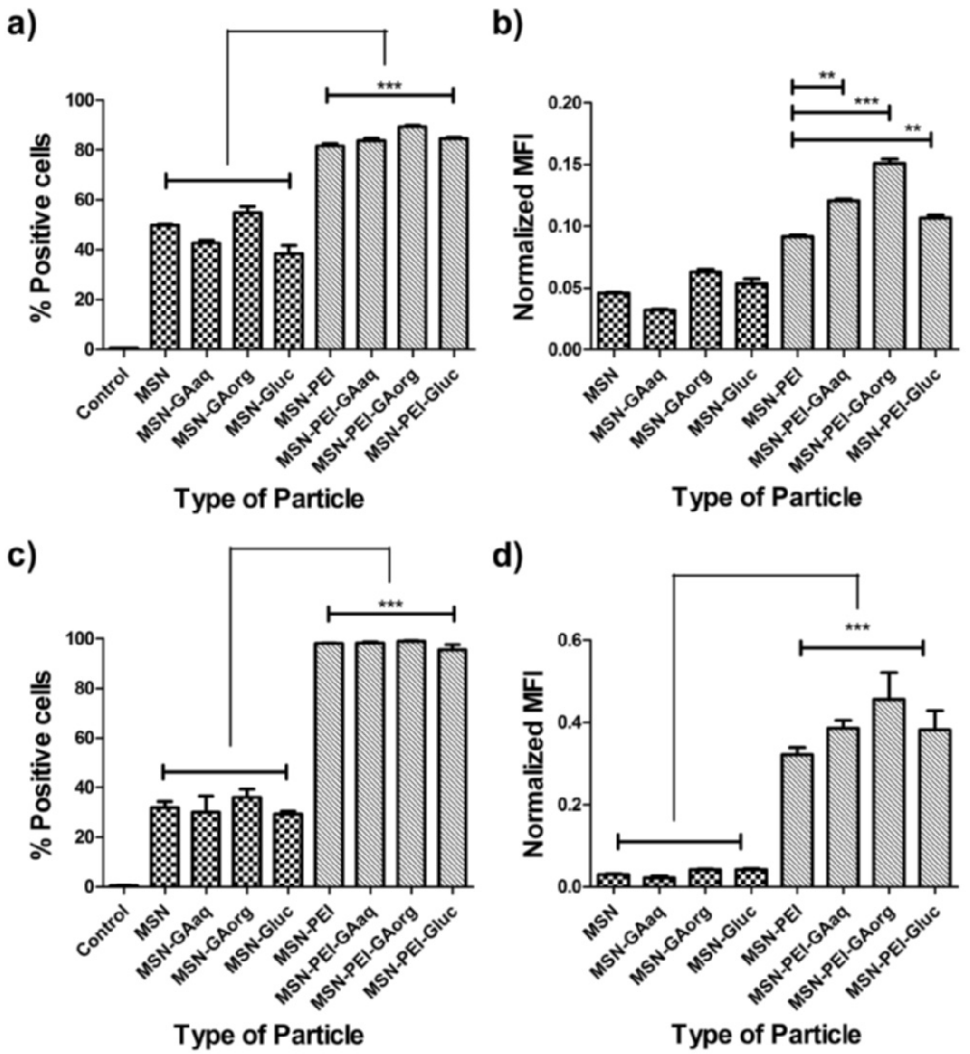

Figure 18. Flow cytometry quantification of the cellular internalization of MSNs in two different cancer cells after 3 hours incubation. a) Mean % of FITC positive HeLa cells using 5 μg/ml of nanoparticles or control. b) Normalized mean fluorescence intensity resulting from particle uptake in HeLa cells. c) Mean % of FITC positive A549 cells using 5 μg/ml of nanoparticles. d) Normalized mean fluorescence intensity resulting from particle uptake in A549 cells. Error bars represent ± SEM (n≥4), ** $P \leq 0.01$, *** $P \leq 0.001$ (***I***).

5.7. Folic acid targeting towards folate receptor expressing cells

Another cancer specific trait that can be utilized as targeting strategy is by conjugating folic acid (FA) on the particle surface, as many cancer cell have a tendency of overexpressing folate receptors (FR) on the cell membrane, consequently allowing for receptor-mediated endocytosis (Leamon & Low 2001, Leamon & Reddy 2004, Rosenholm *et al.* 2009). In this part of the study, HeLa cells was chosen as the cancer cell model as they express folate receptors in high quantities, whereas A549 cells were selected in this case as the "non-cancerous" cell model as they have negligible amounts of FR at their cell membrane (***II***; Parker *et al.* 2012). The flow cytometry results shows that FA-PEI-MSN are internalized in significantly higher amounts in HeLa cells than A549 cells, as the uptake difference is ten-fold higher in target cells compared to off-target cells (Figure 19a). To validate successful particle endocytosis, confocal microscopy was utilized and the fluorescent particles are seen as green dots inside the cell membrane visualized in magenta (Figure 19b). However, some healthy cells do express FR and could thus internalize FA conjugated particles giving rise to potential off-target effects (Parker *et al.* 2005, O'Shannessy *et al.* 20015). Therefore, we studied also cells that originates from the thyroid gland that express variable amount of FR for evaluating some of the FA targeting pitfalls (Weber *et al.* 2013, Shen *et al.* 2015). The cells used were thyroid follicular cancer cells (ML-1) and normal thyroid cells (Nthy-ori 3-1) and HeLa cells as the FR positive cell line which is known to internalize FA conjugated MSNs (***III***).

The quantification of the western blot results shows that both thyroid cell lines do express FR (Figure 20). However, there are significantly lower expression levels in the normal thyroid cells that functions as the basis for this targeted drug delivery strategy towards thyroid cancer cells (Figure 20b). The flow cytometry result shows that the FA-PEI-MSN are internalized in higher amounts in the cancerous thyroid cells (ML-1) compared to the normal thyroid cell (Nthy-ori 3-1) indicating that receptor expression levels are not the only affecting factor in particle internalization (Figure 20). The confocal images verifies that these FA conjugated nanoparticles are indeed internalized by cancerous thyroid cells and that normal thyroid cells only internalize low amounts of particles (Figure 20d&e). Receptor turnover is known to affect antibody internalization kinetics and, therefore, the FR turnover rate could potentially influence particle internalization (Paulos *et al.* 2004). However, such aspect would need to be further studied to know the effect of receptor turnover on particle internalization. Furthermore, mathematical models can be used for estimating the optimal nanoparticle size and the density of the targeting ligand on the surface on the particle for effective binding to cell specific receptor clustering on the cell membrane (Gonzalez-Rodriguez & Barakat 2015). Therefore, it is possible that the observed higher internalization in the thyroid cancer cells is due to rapid receptor turnover and/or matching particle targeting ligand/receptor clustering on the cancerous cells compared to the normal cells that also express FR at their cell membrane (***III***).

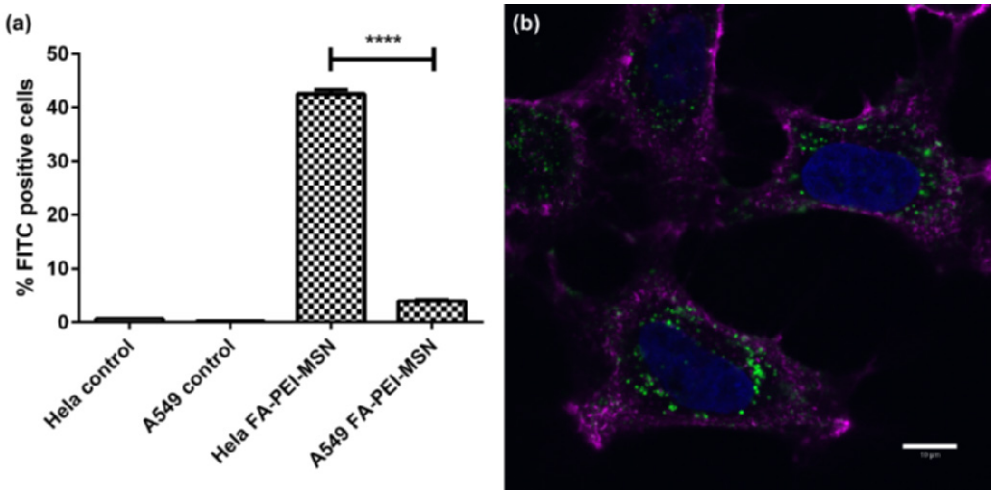

Figure 19. Cellular uptake of FA-PEI-MSNs in cells after 3 hours incubation. a) Flow cytometry quantification showing mean % of FITC positive HeLa and A549 cells using 1 µg/ml of nanoparticles or untreated cells (control), error bars represent ± SEM (n≥4), **** P ≤ 0.0001. b) Confocal microscopy images of FA-PEI-MSN endocytosis in HeLa cells at 10 µg/ml concentrations, using DAPI nuclear staining (blue), rhodamine-lectin plasma membrane staining (magenta) and particles conjugated with FITC (green), scale bar 10 µm (***II***).

Even though there is particle internalization in normal thyroid cells; this would not pose any major concern in the case of thyroid cancer, as surgical removal of the thyroid is the mostly used treatment method (Clark *et al.* 1988). The real off-target risk is the other tissues that express FR, which are the proximal tubules of the kidney, the choroid plexus, intestinal brush-border membranes, pneumocytes in the lung and placental tissue (Parker *et al.* 2012). However, in the case of intravenous injection of nanoparticles with FA targeting ligand to the blood stream, the possible off-target effects would be minor. This is because the theoretical internalization at the intestine would only be feasible if the carrier would be ingested orally, and entering the brain would require penetrating the blood brain barrier, which is highly unlikely for macromolecules or, in this case nanoparticles with a size over 200 nm (Ballabh *et al.* 2004). Particle accumulation in the lungs is also unlikely as folate-based radiodiagnostic agents when administered intravenously to patients do not accumulate in the lungs despite of their high FR expression. One possible explanation for this phenomenon could be that the apically oriented FRs in the lung epithelium are not in contact with the circulating blood and therefore, the injected folate-derived imaging agents cannot accumulate in the lung tissue (Parker *et al.* 2012). The FR expression in placenta during pregnancy could pose a potential threat for the embryo when administering folate-targeting nanomedicines. However, conventional chemotherapy for pregnant women poses already a threat for the embryo and should therefore only be given under special circumstances e.g. under later stages of the pregnancy in order to reduce the risk of birth defects (Esposito *et al. 2016*). Therefore, the most likely affected organ would be the kidneys, as FR are highly expressed in the proximal tubule where its function is to filter small molecules and proteins from the urine (Eshbach & Weisz 2016). Fortunately, our nanocarrier system is designed to be relatively large and cannot directly pass the glomerulus and therefore, our particle

would remain in the blood circulation and would not enter the proximal tubule where potential off-target internalization could occur (He *et al.* 2011, Liu *et al.* 2013). *Summa summarum,* developing targeting strategies is a complicated task, where the characters of the cell of interest needs to be carefully considered in order to create an carrier system that matches the criterion of the living organism for optimal internalization and drug retention in target tissues.

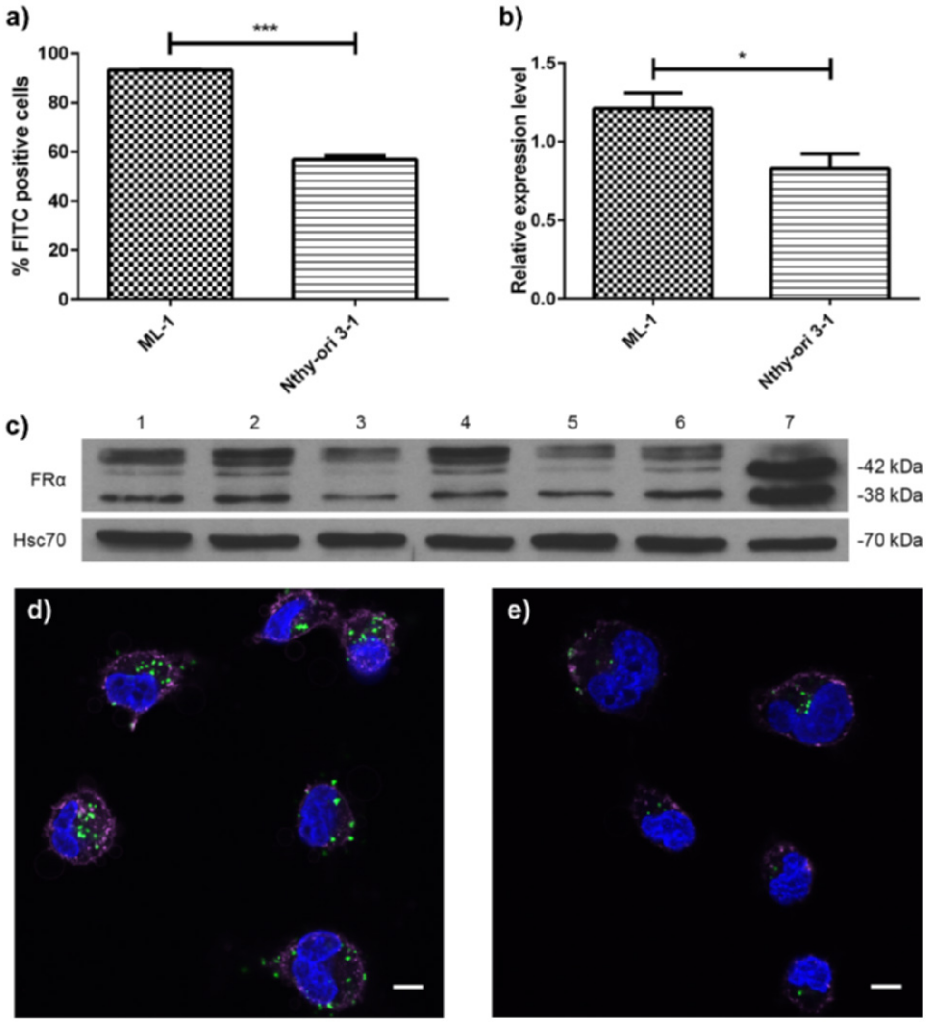

Figure 20. ***In vitro*** **uptake efficasy of folic acid conjugated nanoparticles.** a) Flow cytometry quantification of cellular uptake of FA-PEI-MSNs shown as % FITC positive cells using 1.5 µg/ml of nanoparticles in ML-1 cell compared to Nthy-ori 3-1 cells after 4 hours incubation. b) Quantification of FRα protein levels in Nthy-ori 3-1 cells and ML-1 cells. c) Folate receptor protein expression in Nthy-ori 3-1 cells (1,3,5), ML-1 cells (2,4,6), and HeLa cells (7) as a FRα positive control. Confocal microscopy images of MSN-PEI-FR endocytosis in d) ML-1 cells and e) Nthy-ori 3-1 at 1.5 µg/ml for 4 hours with scale bar of 10 µm. Error bars represent ± SEM (n≥3), * $P \leq 0.05$, *** $P \leq 0.001$ (***III***).

5.8. Particle toxicity depends also on cell type

Particle toxicity is not only dose, material or functionalization dependent; the toxic effect varies also with what cell type is being affected and the amount of particles are internalized in that specific tissue (***I-III***). In order to study the potential unwanted/off-target effect of these PEI functionalized MSNs in normal versus malignant cells; we utilized follicular thyroid carcinoma cells (ML-1) and normal human primary thyroid follicular epithelial cells (Nthy-ori 3-1) at concentrations up to 60 µg/ml for 72 hours (***III)***. In order to detect more subtle changes in the cellular homeostasis resulting from administering these non-drug loaded MSNs, we utilized a metabolic viability assay (WST-1; Guertler *et al.* 2011). It is known that silica materials are generally considered safe and significant toxicity of MSNs are only detectable when using non-functionalized particles in high doses, where the toxicity is most likely caused by particle aggregation and not the particle composition (Srivastava *et al.* 2015, Paatero *et al.* 2017). The viability assay shows that normal thyroid cells are more susceptible compared their cancerous counterparts to possible effects of MSNs when high enough doses are given (60 µg/ml) for prolonged durations (72 hours; Figure 21). There is less variation in the cell viability when administering different concentrations of MSNs to ML-1 cells compared to the Nthy-ori 3-1 cells. The normal thyroid cells shows variation in viability depending on the amount of particles administered; 6 – 24 µg/ml gives higher viability compared to the negative control (no treatment) whereas 60 µg/ml decreases viability. When comparing the two cell lines viability using two-way ANOVA the results shows that there is a significant difference when administering these MSNs for prolonged exposures. A moderate amount of particles (6 – 24 µg/ml) gives an metabolic advantage to the normal thyroid cells and high concentrations (60 µg/ml) gives an negative effect on the normal cells, whereas the cancerous cells only shows minor variation in different concentrations (Figure 21).

The efficacy of different drug-loaded nanoparticles is a well-studied subject; however, the metabolic effect of non-drug loaded MSNs has on cells is a less studied matter. One study done by Huang and collages showed that increasing amounts of MSN with prolonged exposure actually increases cell viability detected by MTT assay in human malignant melanoma (A375) cells. The promoted proliferation could be through an oxidative mechanism where the increasing amount of particles increases oxidation leading towards the inhibition of NF-kB activation and upregulation of Bcl-2 expression (Huang *et al.* 2010). The Bcl-2 protein represent anti-apoptotic proteins that shifts the cellular homeostasis toward survival, which could be the explanation of the increased proliferation detected in these A375 cancerous cells (Elmore 2007, Huang *et al.* 2010, Hongmei 2012). However, our viability data shows that that normal cells on the other hand has a limit on the proliferation effect of PEI-MSNs as high concentration lowers the metabolic rate of Nthy-ori 3-1 cells (Figure 21). Therefore, it is hard to predict the effect different nanoparticles has on each specific cell line as the metabolic state and protein expression pattern of different tissues varies. Not to mention cancerous cells versus normal cells can have quite different phenotype and genotype that can greatly affect the outcome of different treatment forms (Lee *et al.* 2010a, Ozaki & Nakagawara 2011, Hilgendorf *et al.* 2013, Paatero *et al.* 2017).

Furthermore, the negative effect detected in these healthy cells is quite artificial, as most of the intravenously administered particles in potential patients would spread out to the whole body, and only a few percent of the particles tend to accumulate at target sites and even less to possible healthy cells (Bae & Park 2011). Especially when using active targeting as most healthy cells do not overexpress FR or glucose transporters (GLUT) and would thus not internalize FA/Gluc conjugated MSNs and, therefore, the negative effect at healthy tissue of the carrier itself would remain minute (Parker *et al.* 2005, Liberti & Locasale 2016). Furthermore, these *in vitro* studies are made in a closed artificial platform where particle accumulation would be far higher than in the *in vivo* situation where these particles would partially be degraded and cleared from circulation by the liver and kidneys and thus, particle concentration at possible off-target sites woulde be considerably lower in man (Owens & Peppas 2006, Park & Park 2016, Del Agua *et al.* 2018). Taken together, it is important to study particle toxicity first *in vitro*, then equally important is to study the possible off-target effect *in vivo* for understanding such complex interaction between the carrier material and the living organism for going forward in the product development and twoards clinical trials.

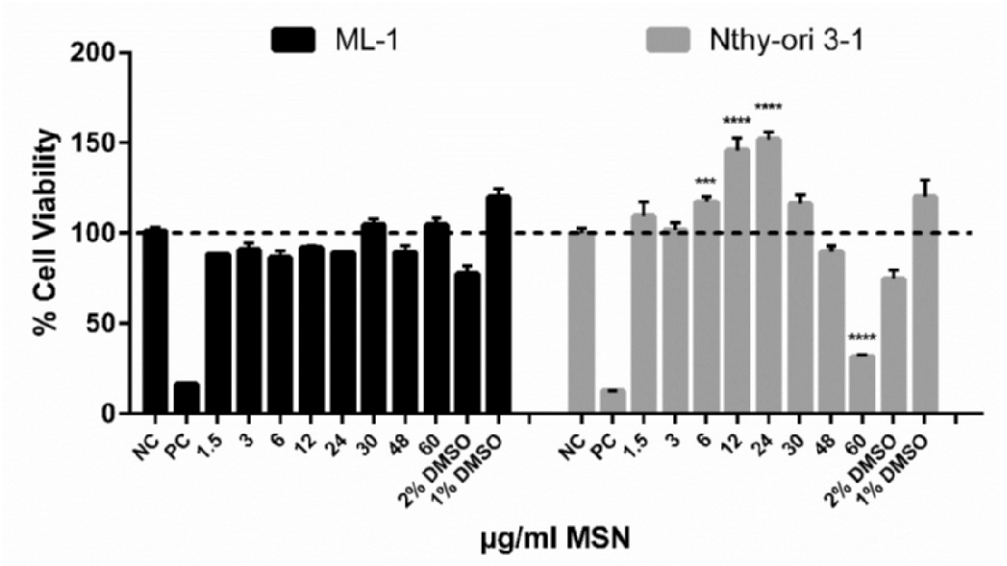

Figure 21. The PEI functionalized MSNs have variable effect on cells metabolic activity after 72 hours incubation. The cancerous ML-1 cells show minor differences in cell viability when administering different concentration of MSNs. The normal thyroid cells (Nthy-ori 3-1) shows high variations in cell viability depending on the administered concentration of particles. All data sets were compared with a negative control (NC) without treatment and a positive control (PC) containing caliculin A as well as solvent controls (DMSO). Statistical difference were calculated using Two-way ANOVA with Tukey's multiple comparisons test. Error bars represent ± SEM (n=3), *** $P \leq 0.001$, **** $P \leq 0.0001$ (supp. file ***III***).

5.9. Particle internalization are time and concentration dependent

Particle internalization could be considered a chemical reaction where increasing the amount of the starting substance X (particles) pushes the reaction towards becoming the final substance Y (internalized; Kayala *et al.* 2011). Then the cell type and thus the amount of receptors available at the surface that can facilitate the reaction influence greatly the time needed for the reaction to take place, a little like an thermal reaction where high heat (high receptor expression) increases the reaction time whereas lower temperatures (low receptor expression) are sub-optimal and therefore the limiting factor. However, by giving prolonged time points it is possible to achieve reactions that are not favorable; and this is holds true also in particle internalization kinetics. In order to exemplify at least some of these assumptions, we studied the internalization kinetics at different particle concentrations as well as different time points. Utilizing cervical cancer cells (HeLa) and cancerous thyroid cells (ML-1) that are known to internalize particles as well as normal thyroid cells (Nthy-ori 3-1) that internalize particles in lower amounts, for simulating a more realistic scenario where some of the healthy cells in the body do express FRs for evaluating possible off-target internalization (Figure 22).

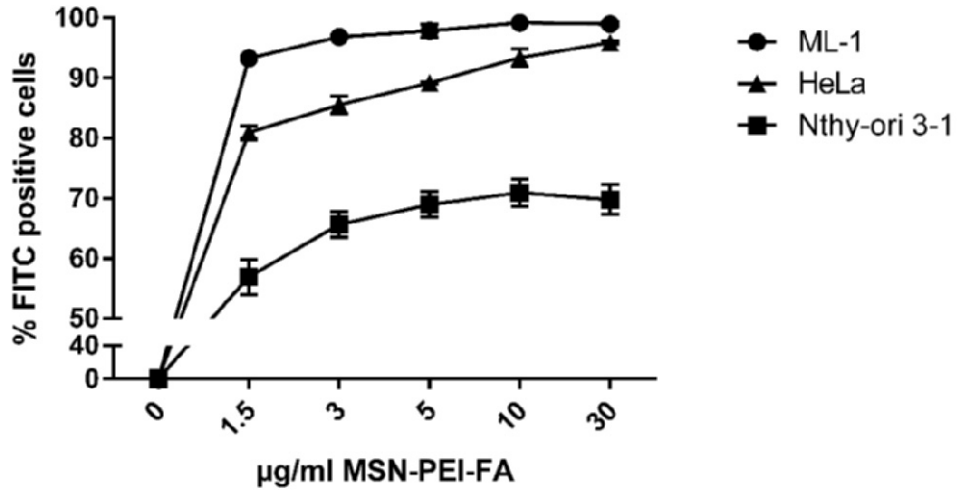

Figure 22. Flow cytometry quantification of concentration dependent internalization kinetics of folate acid conjugated MSNs. Mean % of FITC positive cell population in ML-1, Nthy-ori 3-1 and HeLa cells using 0 - 30 µg/ml of folate conjugated nanoparticles after 4 hours incubation. Error bars represent the standard deviation ± SD of the mean (n=4; unpublished).

The flow cytometry results shows that ML-1 cells has the highest uptake of these three cellines when administering FA conjugated particles, as over 90% of the ML-1 cell population are FITC positive already at low concentrations (1.5 µg/ml). HeLa cells shows a steady increase of internalized particles when the particle amount increases, possible indicating that HeLa cells that has a high expression of FR can handle the high particle load and still efficiently internalize the increased amount of particles (Figure 22). The interesting observation here is that HeLa cells express higher amount of FR compared to ML-1 cells however, the ML-1 cells yields higher FITC positive

population (Figure 22&20). The normal thyroid cells that have low expression of FR do internalize these particles in a less effective manner compared to these two cancerous cell lines that overexpresses the receptor. Even after administering 30 µg/ml of particles, the FITC positive population in the normal thyroid cells is still under 70% from the whole population, indicating that the lower amount of receptors are not able to internalize the increasing amount of particles which the cancerous cells are capable of internalizing (Figure 22&20).

Furthermore, by comparing internalization of passive targeting versus active targeting in a time dependent function by using high amount of administered particles, it is possible to study some of the benefits of active targeting utilizing MSNs (unpublished data). By using high amounts of particles (30 µg/ml) it was possible to minimize the uptake effects caused by the amount of particles available so that the particles themselves would not be the limiting factor in this reaction. As expected, the time dependent experiment shows that by prolonging the incubation time it was possible the increase the internalized particles seen as an increasing FITC positive population in both passive and active targeting. However, by using active targeting it is possible to achieve a higher initial uptake in target cells compered to passive targeting that would be beneficial in personalized drug treatment, where fast uptake of drugs in target tissues would minimize side effects in off-target tissues (data not shown). Taken together, it is clear that functionalized particle uptake is not simply dependent on the expression levels of the target receptor or that the cell of interest will either internalize the particle or not. Considering particle uptake as a living reaction would be a more accurate presumption, where the amount of particles and time given for the reaction together with the amount of available receptors and receptor turnover at the cell membrane all influences the output (Oh & Park 2014). Therefore, doing uptake kinetics with different particle concentrations and different time points using both the target cells and off-target cells would give more realistic information regarding particle internalization kinetics of a living multicellular organism. However, such detailed *in vivo* studies are not always plausible and therefore low concentrations of particles with a few hours of incubation time would be a good starting point for the *in vitro* uptake studies.

5.10. Active targeting with MSNs increase drug efficacy

In order to confirm improved efficacy of the hydrophobic drug celastrol when loaded into MSNs compared to freely administered drug, the apoptotic effect was validated in HeLa cells by propidium iodide staining. The nuclear propidium iodide (PI) staining was selected as viability method that relies on PI binding to fragmented DNA as a marker for cell death (Nicoletti *et al.* 1991). Based on celastrol's ability to destabilize the microtubules that disrupts fast dividing cancer cells, thereby inducing DNA breaks and ultimately cell death (Jo *et al.* 2010). The flow cytometry results shows that an apoptotic effect can be detected already after 24 hours when freely administering celastrol of concentrations around 3-7 µM (Figure 23a). This apoptotic effect is probably due to the mitotic rate of HeLa cells that is around 8-12 hours, therefore 24 hours incubation is sufficient for celastrol to induce mitotic catastrophe leading towards apoptosis (Piras & Piras 1975, Nagase *et al.* 2003). Longer durations and higher dosages did not increase the apoptotic effect, which could be explained by

the fact that prolonged exposure and high concentrations of toxins leads generally to necrosis and fragmentation of cells that are not easily detectable by apoptotic assays such as PI staining (Kroemer *et al.* 2009, Orrenius *et al.* 2011). Therefore, the optimal time point and dosage for inducing apoptosis in HeLa cells was around 5.3 μM of celastrol when incubated for 24 hours. However, the maximal effect in terms of apoptosis by freely administered celastrol was quite low, around 5-10 percentage, which could partially be explained by to poor solubility of the drug in aqueous solution. As there were some variations in the apoptotic effect of free celastrol on cancer cells when comparing different experimental repetitions (Figure 23a&b). HeLa cells were then incubated with celastrol-loaded MSNs with corresponding concentration (5.3 μM) in order to assess the potential gained anti-cancerous efficacy in terms of apoptosis utilizing sugar conjugated nanocarrier systems. All functionalized particles showed significant enhancement of drug efficacy compared to freely administered drug. Intriguingly, the GA_{aq}-PEI-MSN showed lower efficacy compared to the other particles studied (Figure 23b). This particular functionalization was carried out in aqueous conditions and exposure to water is known to affect the silica matrix i.e. also pore structure, which may in turn influence drug loading and drug release (Desai *et al.* 2014).

To confirm the potential beneficial effects of celastrol and celastrol-loaded MSNs, the cytoprotective effect was studied in FR positive HeLa cells and FR negative A549 cells by measuring the heat shock response using western blot analysis. The incubation time was set at 6 hours in order to avoid the toxic effect of celastrol on fast dividing cells; however, giving enough time for detecting changes in expression levels of one of the most important molecular chaperone called Hsp70 (Salminen *et al.* 2010). The western blot analysis shows that HeLa cells are more susceptible to the beneficial effects of freely administered celastrol as low dosage (2.66 μM) increases the Hsp70 expression, however higher dosages (5.33 μM) seems to activate the negative feedback loop and the beneficial effect is diminishing (Figure 23c). The A549 cells that are derived from lung tissue shows different activation kinetics, requiring higher concentrations (around 3.55 μM) for proper activation of the heat shock response (Figure 23d). When comparing the freely administered drug results with the results obtained by drug-loaded MSNs, there is a clear trend where the nanocarrier system prolongs the beneficial effect without the negative feedback loop being turned on. This prolonged efficacy is probably do the steady release kinetics of celastrol from these functionalized nanoparticles (Figure 23e&f). However, the beneficial effect of celastrol-loaded MSNs needs to be further studied in normal healthy cells preferably obtained directly from patients, as immortal cancerous cells have an altered homeostasis and protein expression pattern that can affect the stress response (Elmore 2007, Lee *et al.* 2010a, Hongmei 2012, Gordon *et al.* 2014).

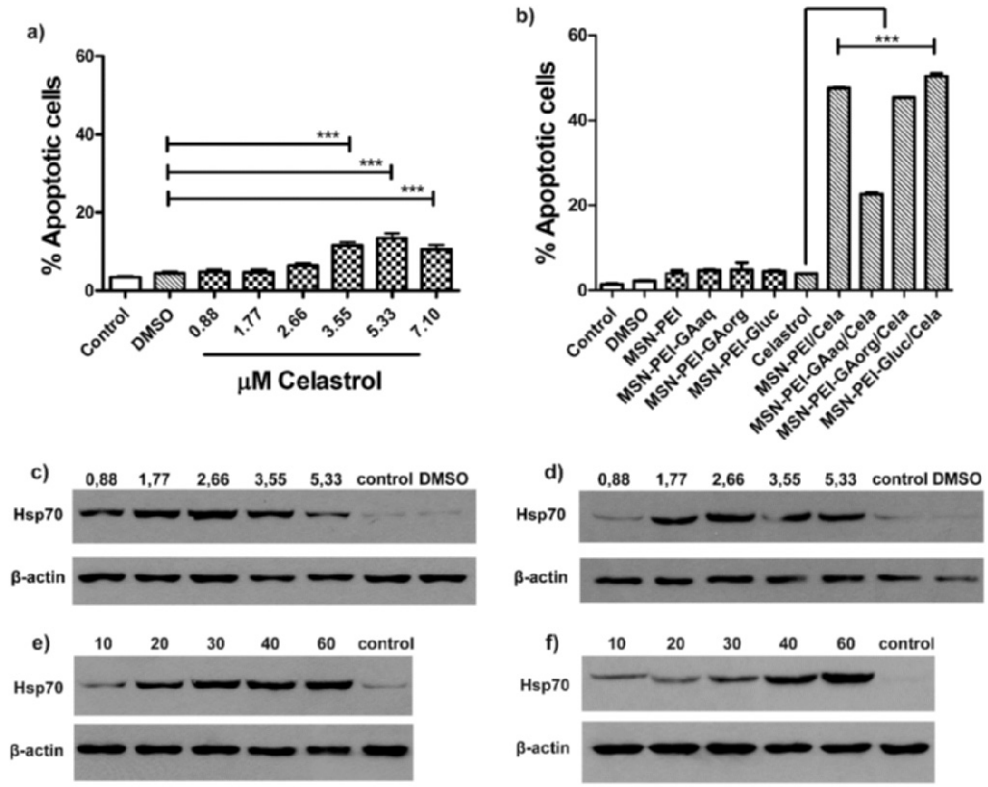

Figure 23. Active targeting increases drug efficasy. a) Flow cytometry quantification of the apoptotic effect of different concentrations of celastrol after 24 hours incubation with HeLa cells using propidium iodide (PI) staining. b) The apoptotic effect of MSNs, celastrol-loaded MSNs and control samples after 24 hours incubation with HeLa cells in concentrations corresponding to 5.3 μM of free celastrol. Error bars represent ± SEM (n≥4), *** P ≤ 0.001 (adapted from ***I***). Celastrol and celastrol-loaded MSNs induces the heat shock response. c) HeLa cells treated with 1.77-3.55 μM celastrol induces the expression of Hsp70. d) A549 cells treated with 2.66-3.55 μM clearly induces the expression of Hsp70. e) HeLa cells treated with increasing concentration (μg/ml) of celastrol-loaded MSNs for 6 hours shows an induction of Hsp70 expression in concentrations over 20 μg/ml. f) A549 cells treated with celastrol-loaded MSNs increases the expression of Hsp70 at higher dosages 40-60 μg/ml (adapted from ***II***).

5.11. Image quantification verifies targeted drug delivery

We utilized image quantification in order to verify successful targeted drug delivery as an end point measurement (***II***). Advanced bioimaging and image analysis has grown to become one of the key methodologies in biomedical research today, where it is possible to acquire both qualitative and quantitative data from the same data set (Nat Methods 2012). However, developing tailor-made image analysis workflows for specific purposes is required in order to transform the vast arrays of image data produced into meaningful quantitative information (Hartig 2013, Eliceiri *et al.* 2012). In this part of the study, we developed an automated imaging workflow based on BioImageXD an open source software package that were utilized to detect targeted cellular responses at the single cell level (Kankaanpää *et al.* 2012). Focusing on the

cellular stress response as the end point measurement; because of its vast importance in stress protection, stress recovery and cellular healing as proteotoxic pathologies are involved in neurodegenerative diseases such as Alzheimer's and Parkinson's (Leak *et al.* 2014, Cascão *et al.* 2017). As visual markers of activated stress response; nuclear stress bodies (nSBs) were detected by laser scanning confocal microscopy as local fluorescence intensity clusters of Heat shock factor 1 (HSF1) inside the cell nucleus. The first step in the study was to evaluate the automated workflow efficacy and reproducibly in identifying single cells that displayed nSBs compared to manually counted nSBs. For this validation we heat shocked HeLa cells at 42°C, which is known to induce the formation of nSBs in human cells when incubated for 15-120 minutes, which served as an activated stress response reference for the experimental setup (Holmberg *et al.* 2000, Biamonti & Vourc'h 2010).

The confocal images of the heat treated samples were first quantified manually by counting the nSBs positive cell form the total population then the same image dataset was then quantified using the image analysis workflow. In short, the steps for the automated workflow were as follows; 1) the cell nucleus was detected from the DAPI channel where the amount of cells can be calculated then 2) the nSBs were measured with dynamic thresholding and 3) object separation from the HSF1 channel. By 4) object-based co-localization it was possible to calculate the percentages of nSBs positive cells from the total population that had one or more stress granule(s) in the nucleus (***II***). The results from the heat shocked HeLa cells show that both methods give similar mean values, as there is no statistical difference between the two quantifications, demonstrating the potential of the automated image analysis (Figure 24). Both quantifications show that there is a temperature and time dependent formation kinetics of nSBs in HeLa cells correlating with previous studies, validating the usefulness of the image quantification workflow in detecting nSBs formation under different conditions (Figure 24; Holmberg *et al.* 2000). Furthermore, utilizing imaging workflows it is possible to obtain information regarding size distribution of object of interest, in this case the size distribution of nSBs from 3D image dataset, which would manually be too laborious and subjective in order to execute precisely (Figure 24c; Nat Methods 2012, Kankaanpää *et al.* 2012, Carpenter *et al.* 2012).

Celastrol has the ability to induce the heat shock response that increases the expression of heat shock proteins, however celastrols effect on the formation of nSBs have remained rather elusive (Salminen *et al.* 2010, Westerheide *et al.* 2004). In this part of the study, we showed that celastrol has indeed the ability to induce the formation of nSBs in HeLa cells in similar manner as heat shock (***II***; Holmberg *et al.* 2000). The results shows that for inducing nSBs by celastrol in HeLa cells the concentration needs to be over 3.55 µM and that the optimal dosage is around 5.33 µM as higher dosages reduces the amount of nSBs positive cells in the population probably due to negative feedback loop or induced toxicity (***II***; Nagase *et al.* 2003). Most importantly there is no significant difference in the quantification methods validating the usefulness of our tailor made image quantification workflow for numerous biological research scenarios. Furthermore, the innate batch processing capability would even enable high throughput imaging applications to be combined with both 2D and 3D image data analysis are useful traits for future personalized diagnostics. Taken together, the

results shows that these celastrol-loaded MSNs could potentially be beneficial for patients with protein aggregate associated diseases by inducing a specific and effective heat shock response in the target cells.

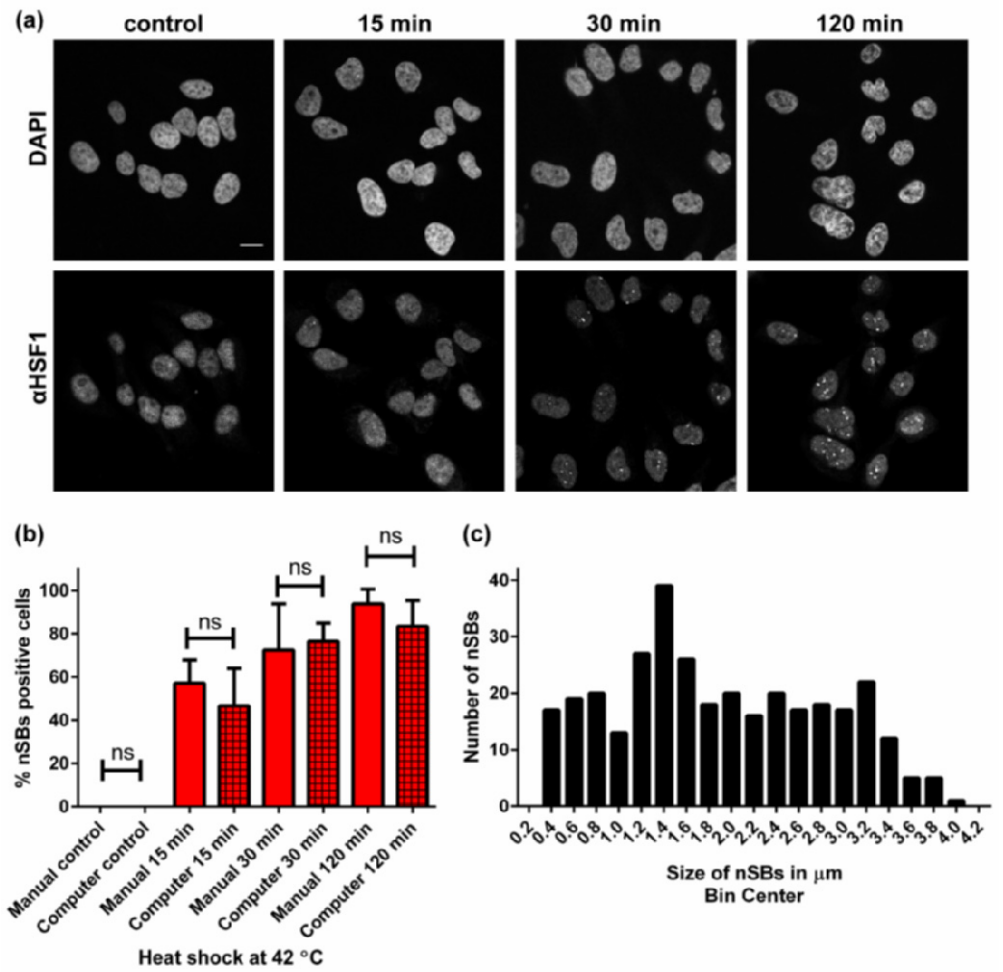

Figure 24. Formation kinetics of nSBs in heat shocked HeLa cells. a) The confocal images shows that cells that have been heat treated for 15 minutes at 42°C only have a few HSF1 accumulations in the nucleus, whereas 30 and 120 minutes of heat shock induces clear formation of nSBs in almost all cells. Control cells that have been cultured in 37°C does not form nSBs, scale bar 15 μm. b) Both quantification methods show similar heat shock induced nSBs kinetics, as there is no significant (ns) difference between the manual and computer based methods. Manually counted cell number (n=338), computer based analyzed cell number (n=357), error bars represent ± SEM. c) Size distribution in μM of nSBs in HeLa cells after 120 minutes of 42°C heat shock, quantified from 3D datasets (n=332; ***II***).

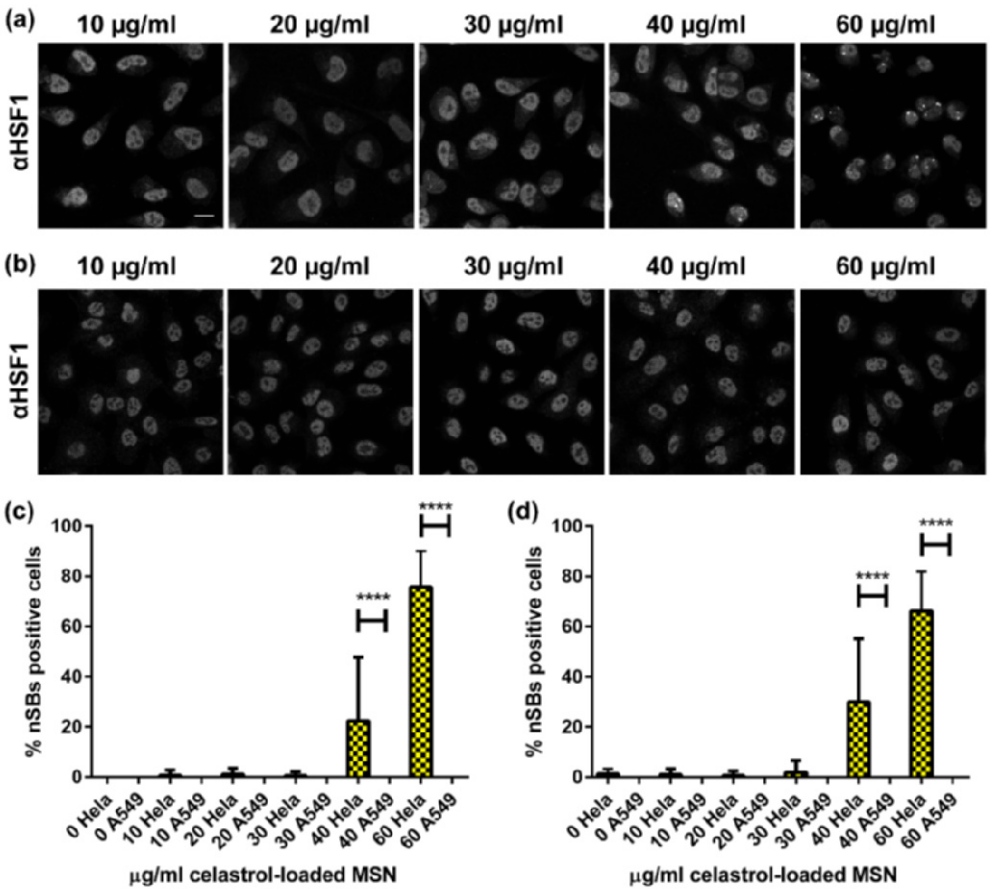

Figure 25. Celastrol-loaded MSNs induce targeted nSBs formation in FR-positive cells. a) HeLa cells treated with celastrol-loaded MSNs shows clear induction of nSBs when administered over 40 µg/ml of drug-loaded MSNs. b) A549 treated cells shows no nSBs formation even the highest dose of 60 µg/ml celastrol-loaded MSNs, scale bar 15 µm. c) Manually counted nSBs positive cells shows that there is a significant difference between cell lines when treating with 40 and 60 µg/ml of drug-loaded MSN. d) Computer based quantification shows similar results where HeLa cells show a significant increase in the percentage of stressed cells compared to A549 cells treated with same concentration. Both quantifications methods show that concentration lower than 40 µg/ml does not induce formation of nSBs in HeLa or A549 cells. Number of cells analyzed in the manually counted quantification (n=2368), and with the computer based quantification (n=2436), error bars represent ± SEM, **** $P \leq 0.0001$ (***II***).

One of the major benefits of targeted drug delivery is the higher drug accumulation at target tissue compared to the off-target tissues, which is important in administering molecules that gives beneficial effects in low dosage but toxic effect in higher dosages (Salminen *et al.* 2010, Jo *et al.* 2010, Muller & Milton 2012). Therefore, we loaded celastrol in FA conjugated MSNs in order to evaluate if these particles could be potential candidates in personalized medicine where activated heat shock response could be beneficial in FR expressing target tissues. HeLa cells were selected as the

FR positive cell line and A549 cells were selected as the FR negative cell line in order to validate the potential targeted effect and unwanted off-target effect. The results shows that when comparing the percentage of nSBs positive cells after 6 hours treatment of celastrol-loaded nanoparticles in both cell lines, a significant induction of nSBs formation in HeLa cells can be detected, whereas no formation of nSBs can be detected in A549 cells (Figure 25). Already at 40 µg/ml of celastrol-loaded nanoparticles (around 3.55 µM celastrol); both the manual and computer based quantifications gives about 20% nSBs positive population of HeLa cells however this concentration give no effect reagarding nSBs formation in A549 cells (Figure 25). When HeLa cells were treated with 60 µg/ml of celastrol-loaded MSNs (~5.33 µM celastrol) there was over 60% of the population showing formation of nSBs in the nucleus whereas the A549 cells did not show any detectable nSBs (Figure 25c&d). The significant differences between HeLa and A549 cell lines in terms of nSBs positive cells validates that celastrol-loaded and FA conjugated nanoparticles can be used as effective targeted therapies towards cells that express FR at their cell membrane for fighting diseases caused by protein aggregation.

5.12. Multidrug-loaded MSNs increases efficacy

Metastatic tumors are the main cause of cancer-related death, as the invasion of cancerous cells towards healthy tissues disrupts organ function that can be fatal for the patient (Riihimäki *et al.* 2013, Anderson *et al.* 2018). Therefore, it is important to create new forms of cancer treatment that are more efficient with fewer side effects on the patient. This is especially true when the cancer has created metastases and multiple surgery is too dangerous for the patient for being a plausible treatment option (Miller *et al.* 2013, Tohme *et al.* 2017). By giving combination chemotherapy it is possible to combat metastatic cancers where one drug blocks the invasiveness of the cancer and another induces apoptosis, however such drug cocktails often has severe adverse effects on the patient (Preissner *et al.* 2012). Therefore, by loading a carrier systems with combination therapy it would be possible for targeted drug delivery towards cancer cells with synergistic effect with significantly less side effects compared to the freely administered drugs (Rosenholm *et al.* 2009, Hu *et al.* 2017). In this part of the study, we created a multidrug-loaded nanoparticle that specifically targets cancer and releases synergistically two different drugs with two different mechanism of action for increasing drug efficacy and minimizing possible negative effects (***III***). The MSNs were loaded with an anti-proliferating molecule fingolimod (FTY720) that works by inhibiting the phosphorylation of sphingosine and thereby blocks the production of the bioactive molecule sphingosine 1-phosphate (S1P), which is an important signaling lipid for cell growth, survival and migration. By blocking the production of S1P by targeted drug delivery, these metastatic cancer cells are immobilized and pushed towards apoptosis (Loveridge *et al.* 2010). As the active ligand, we selected methotrexate (MTX) which is a folate antagonist that has been used for chemotherapy for decades (Huennekens 1994). MTX therapeutic efficacy works by mimicking folate that is essential in the synthesis of thymine and purine nucleotides thereby leading to cell cycle arrest and ultimately cell death in proliferating tumors (Goodsell 1999).

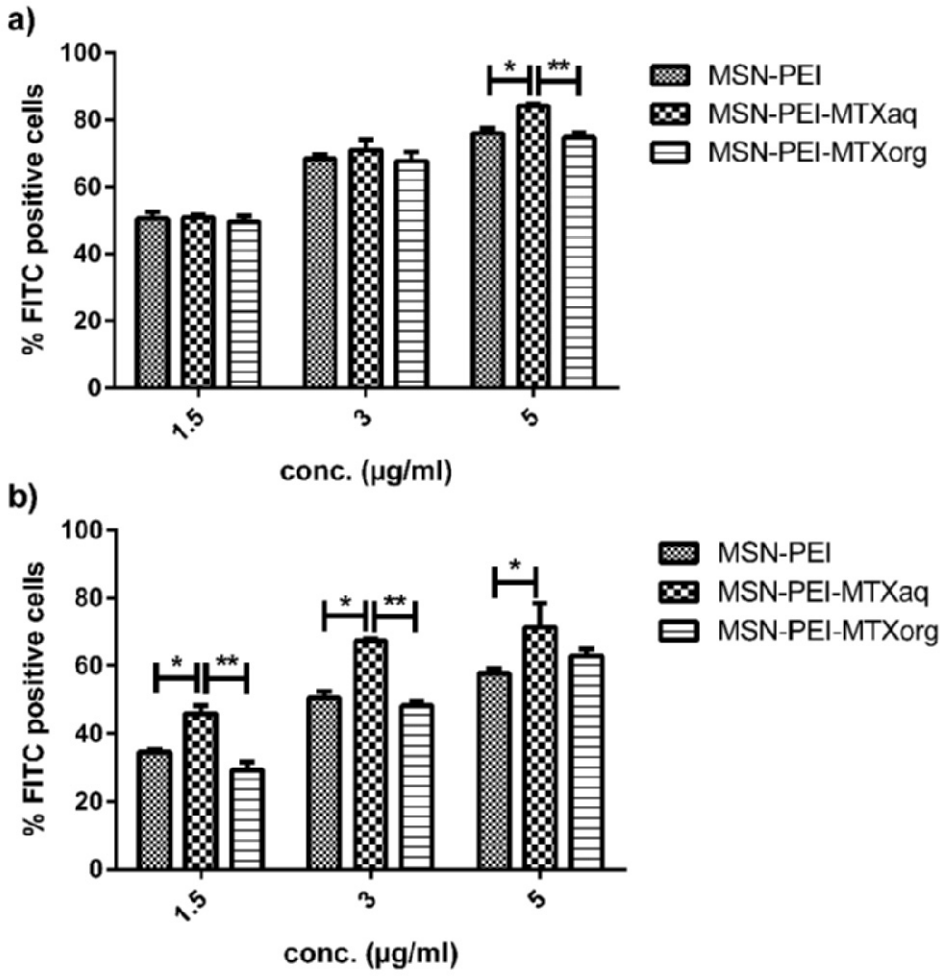

Figure 26. Flow cytometry quantification of the cellular uptake of different functionalized MSN in cancerous thyroid cells and normal thyroid cells after 4 hours incubation. a) % FITC positive ML-1 cells using 1.5 - 5 µg/ml of nanoparticles, showing high internalization of these three different MSNs. b) % FITC positive Nthy-ori 3-1 cells administered 1.5 - 5 µg/ml of nanoparticles gives lower internalization kinetics that the cancerous counterpart. Error bars represent ± SEM (n=3), * $P \leq 0.05$, ** $P \leq 0.01$ (***III***).

First, the two MTX conjugated MSNs versus PEI functionalized MSNs uptake efficacy was measured using flow cytometry (***III***). The cell lines utilized were FR expressing cancerous thyroid cells (ML-1) as well as normal thyroid cells (Nthy-ori 3-1) that express lower amounts of FR. The results shows that after 4 hours incubations the MSN-PEI-MTX_{aq} are internalized in higher efficacy in both cell lines, and was therefore selected as the functionalized particle for further study (Figure 26). Intriguingly the uptake efficacy of MTX conjugated MSNs in the ML-1 cells were significantly lower than the uptake of FA functionalized MSNs using the same

concentration, time point and cell line (Figure 20&26). This difference could possibly be explained by that the drug MTX already starts affecting the cell homeostasis slowing down receptor turnover, or possibly because MTX having lower affinity for the FR than FA and would therefore be less efficiently internalized by FR expressing cells (***III***; Wong & Choi 2015).

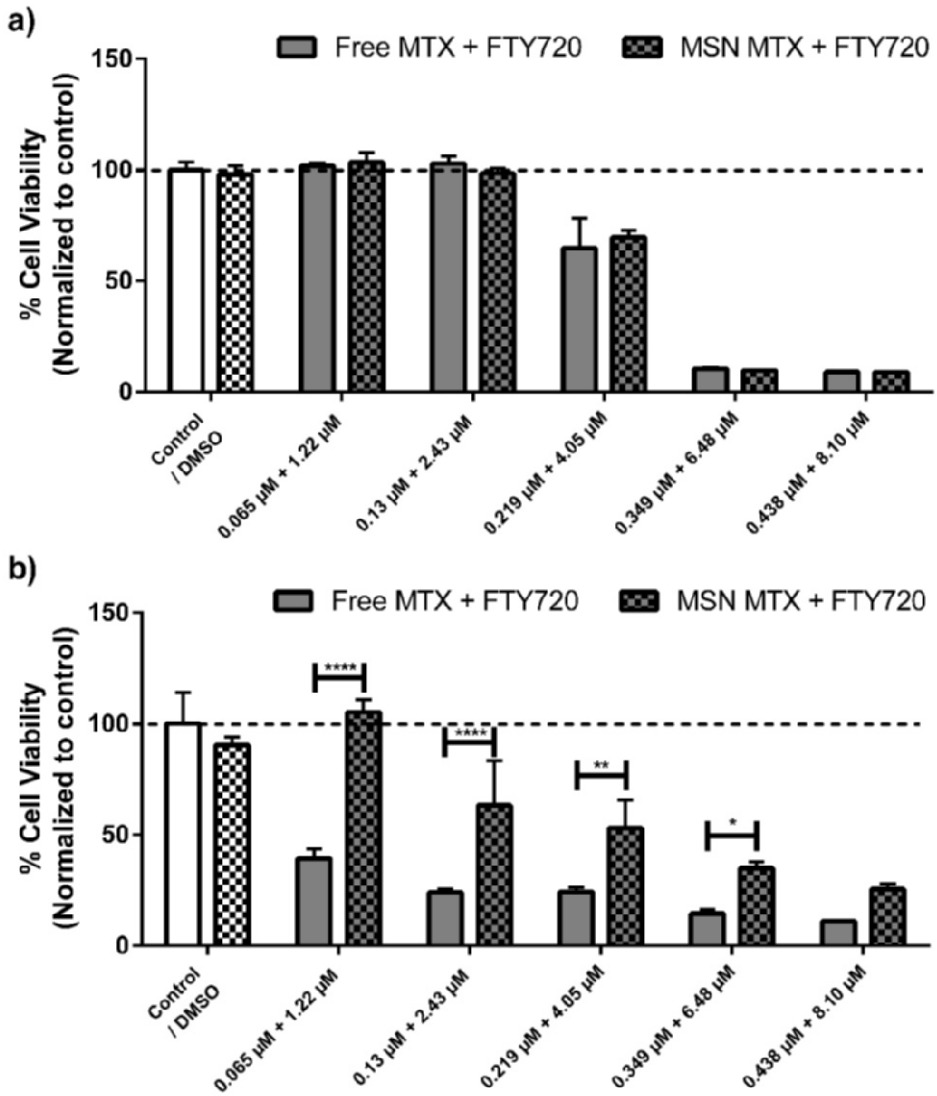

Figure 27. Viability measurement using WST-1 metabolic assay for detecting combination drug efficacy in cancerous thyroid cells and normal thyroid cells after 72 hours incubation. a) The metabolic assay shows similar decreasing viability when increasing drug concentration in the ML-1 cells in using both the free drug combination and the drug-loaded MSNs. b) The Nthy-ori 3-1 cells are sensitive to the free drug cocktail whereas the drug-loaded MSN shows significantly less off-target effects. Values normalized to control (untreated sample) next to 0.2% v/v DMSO (vehicle control). Error bars represent ± SEM (n=3), * $P \leq 0.05$, ** $P \leq 0.01$, **** $P \leq 0.0001$ (***III***).

Then, the selected carrier system (MSN-PEI-MTX_{aq}) was loaded with FT720 in order to estimate the enhanced effect of multidrug-loaded nanoparticles compared to free drug. The concentrations used in both the free drug and the calculated amounts of drugs in the MSNs were as follows: 0.065 µM MTX and 1.22 µM FTY720, 0.13 µM MTX and 2.43 µM FTY720, 0.219 µM MTX and 4.05 µM FTY720, 0.349 µM MTX and 6.48 µM FTY720, 0.438 µM MTX and 8.10 µM FTY720. As the drug combination induces necrosis and cell blebbing resulting in cell fragments that are hard to analyze in flow cytometry and confocal microcopy we utilized a metabolic assay for detecting the cell viability of the drug combination treatment (***III***). The results shows similar efficacy in terms of decreasing metabolic activity in the ML-1 cells when administering similar amount of either free drug combination or drug-loaded MSNs (Figure 27a). More importantly, the results shows that there is significantly less off-target effects in the normal thyroid cells when administering the drug-loaded MSNs compared to the free drug cocktail (Figure 27b). Based on the WST-1 measurements the *in vitro* peak anti-cancerous efficacy in the ML-1 cells without toxicity in the Nthy-ori 3-1 cells would be around 4.05 µM FTY720 and 0.219 µM MTX, and that concentration was selected for further validating the apoptotic efficacy of the drug combination (Figure 27).

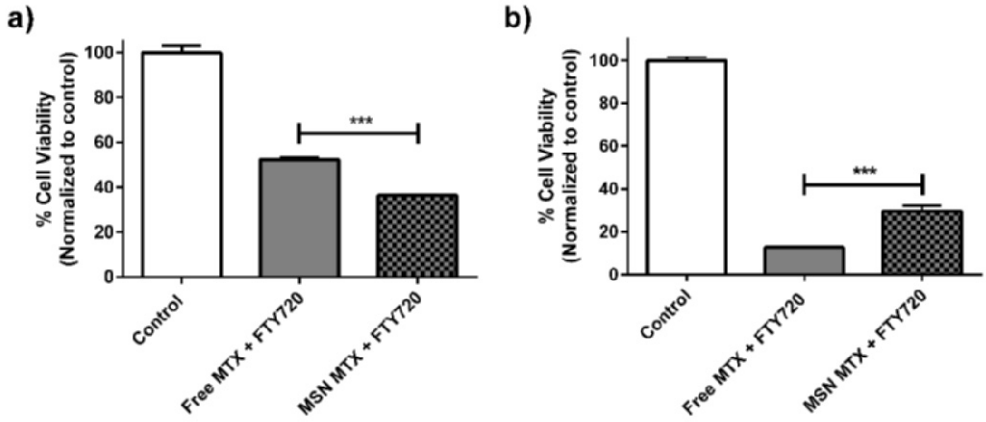

Figure 28. Traditional *in vitro* viability measurements of combination drug efficasy. a) Cell viability in ML-1 cells using crystal violet after 72 hours incubation of free drug cocktail or drug-loaded MSN normalized to control samples shows increased efficacy in terms of anti-cancerous activity in the drug-loaded particles (n=4). b) Cell viability of Nthy-ori 3-1 cells by cell counting after 72 hours of incubation of cells with either free FTY720 and MTX or multi drug-loaded MSNs normalized to control samples (n=3). Drug concentration used: 0.219 µM MTX and 4.05 µM FTY720. Error bars represent ± SEM, ***, $P \leq 0.001$ (supp. file ***III***).

Because of the limited toxicity measurements available for highly fragmenting cells as a result of the drug treatment, we utilized a more traditional approach by cell counting and crystal violet for validating the drug efficacy (Figure 28; Kroemer *et al.* 2009). The cell viability by cell counting shows a significant difference in the toxic effect after 72 hours detected in the normal thyroid cells when administering the free drug cocktail compared to the drug-loaded MSN in similar concentration of drugs (Figure 28b). Validating that these multidrug carrier systems have significant less off-target effects in normal thyroid cells that express low amounts of FR even though

small amounts FA conjugated nanoparticles are internalized in these cells (Figure 20&28). In addition, the drug-loaded MSN showed higher anti-cancerous efficacy in ML-1 cells when using crystal violet as viability assay (Figure 28a). However, shorter time points than 72 hours did not induce apoptosis when administering drug-loaded MSNs which is most likely due to the release kinetics of the anti-cancerous drug MTX being conjugated at the surface of the particle as enzyme driven drug release in target cells takes more time (Popat *et al.* 2012).

In order to validate the results obtained from the traditional viability assays we utilized image analysis performed by external experts using the instrument Phasefocus VL21 that utilizes light for reconstructing an image of the samples refractive properties without labeling and toxic lasers (***III***; Marrison *et al.* 2013). The reconstructed images shows that ML-1 cells administered either the free drug cocktail or the drug-loaded MSNs both showed a more rounded up phenotype compared to the elongated spread out normal phenotype of the control sample (Figure 29a). The results from the image quantification done by the external experts are as follows: *"The volume of the drug treated cells also begins to decrease, resulting in a significant reduction compared to control cells by day 4 of treatment. Indeed, blebbing, which is evident in VL21 images of both drug-treated groups from day 3 onwards, is often accompanied (and followed by) a reduction in cell volume as cells die"*. The statistical analysis verifies that both free drug and drug-loaded MSNs decreases cell volume after 72 hours compared to control, and that sphericity was decreased in the drug-loaded MSNs compared to the free drug treatment (Figure 29b&c). This quantification detecting the decrease in sphericity combined with the VL21 images showing blebbing of cells is an indication that these ML-1 cells exhibit a more apoptotic/necrotic phenotype after administration of nanoparticle loaded with FTY720 and MTX compared to freely administered drug cocktail. Furthermore, the experts concluding statements are as follows: *"The silica nanoparticles potentially enable drug retention during transit to the target cancerous site, preventing off-target killing of non-cancerous tissues, but enable release of the drug in order to effectively kill cells at the target destination"*.

Taking together, our proposed multidrug-loaded MSN could potentially be considered to combat metastatic tumors originated from thyroid cells when the drug efficacy and potential off-target effects are further studied *in vivo* (see next section). As the drug cocktail induced cell death leading towards cell fragmentation there was limited *in vitro* cell viability methods available. Many cancer drugs have high lipophilicity and low water-solubility, which is also true with the selected drugs that makes it hard to administer the drugs to target cells due to limited bio-distribution. In this study, the poorly water soluble drug methotrexate was conjugated at the surface of the particle that increased it bio-distribution as the PEI branching with its positive charge makes the nanoparticle more dispersible in aqueous solution. The second drug fingolimod (FTY720) was loaded inside the pores shielded by the PEI branching functioning as a molecular gate preventing premature release. This means of drug encapsulation and drug conjugation explains the slow release of the drugs from the nanoparticle as 72 hours of incubation time was necessary in order to achieve an effective response in target cells compared to the freely administered drug cocktail that gave a faster non-specific response in both cell lines.

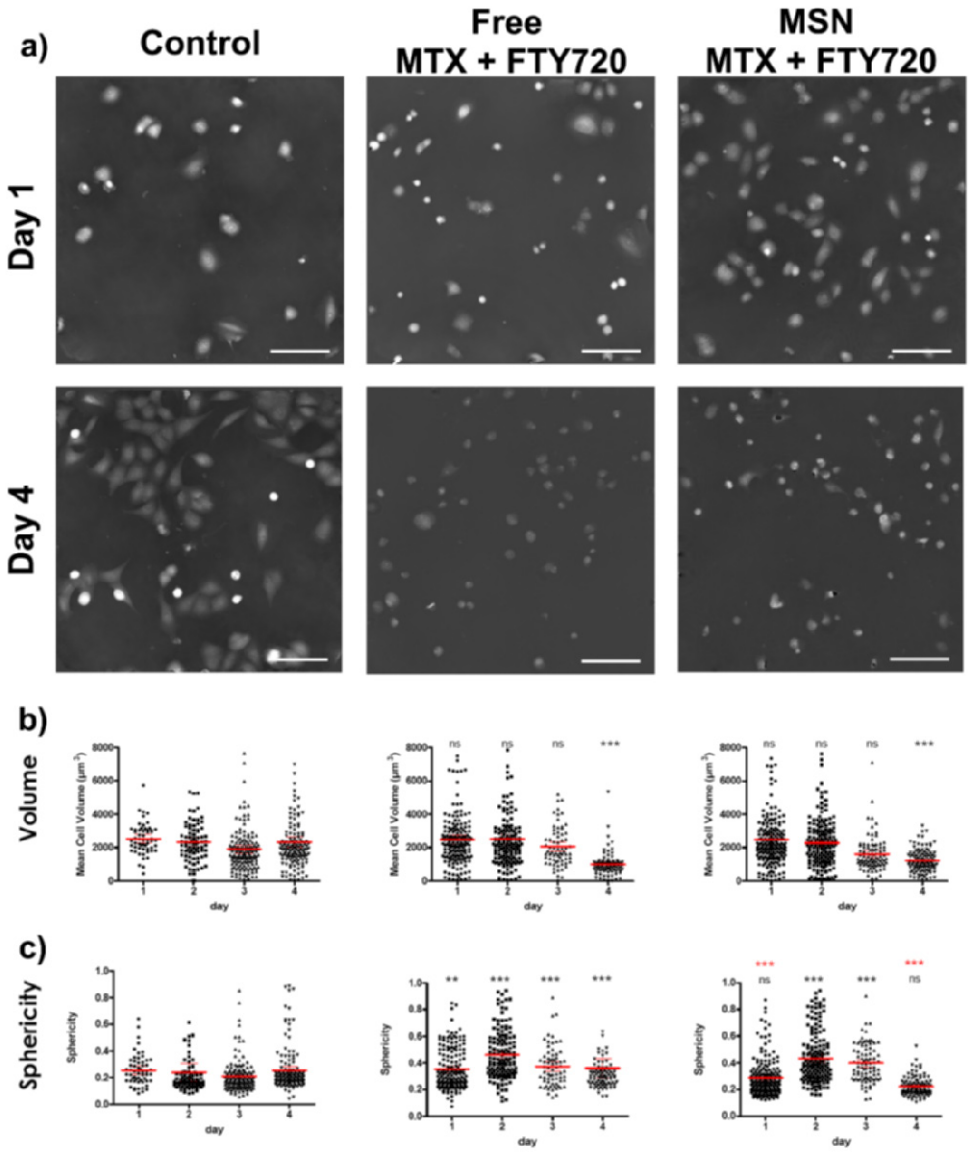

Figure 29. Phasefocus measurments of ML-1 cancer cells treated with MTX and FTY720 or MSN loaded with drug combination. a) The multidrug-loaded MSN treated cells are more necrotic and apoptotic than the cells treated with the free drug cocktail, seen as more condensed cells in the MSN treated, scale bar 150 μm. Image quantification showing the b) volume and c) sphericity of the cell populations in control, free drug and drug-loaded MSN. The image analysis shows that the ML-1 cells administered with drug-loaded MSNs have after 4 days a less spherical phenotype and smaller volume compared to cells treated with free drugs. Statistics in black indicate comparison between control and drug-treated samples. Points of statistical significance between control and treated samples or difference between free drug samples and drug-loaded MSNs indicated by red asterisks. Drug concentration used: 0.219 μM MTX and 4.05 μM FTY720. Number of cells analyzed (n=1524). Error bars represent ± SEM, **, $P \leq 0.01$, ***, $P \leq 0.001$ (***III***).

Furthermore, it is possible that the free drug efficacy was at least partly due to the fact that drug FTY720 is not water insoluble and therefore, partial drug dissolution in the cell medium occurred that induced cell death in the administered cells (data not shown). This drug dissolution could at least partly explain the *in vitro* results that clearly demonstrate that the free drug cocktail has significantly more off-target effect on the normal thyroid cells than the multidrug-loaded MSNs (Figure 27). Another plausible explanation could be that the normal thyroid cells are more sensitive to foreign materials than their cancerous counterparts (Figure 21). These findings regarding efficacy differences were further validated by propidium iodide staining and by the Phasefocus image analysis showing significantly more apoptotic cells quantified as rounding up and blebbing of thyroid cancer cells given the drug-loaded MSNs compared to freely administered drug cocktail (***III***).

5.13. *In vivo* efficacy studies of multidrug-loaded MSNs

After successful *in vitro* studies showing nanoparticle accumulation, retention and specific drug release in target cells; the selected carrier systems were further tested *in vivo* in order to confirm their efficacy in a more clinically relevant setting. In order to keep the cost at a reasonable level the chick chorioallantoic membrane (CAM) assay was utilized for the *in vivo* studies (Zeisser-Labouèbe *et al.* 2004). The CAM is a highly vascularized extraembryonic membrane that is important during embryonic development functioning as a barrier and gas exchange system. The CAM assay has received increased interest in the field of cancer research and drug development during the last decades, as the tumors are easily accessible for experimental manipulation (Nowak-Sliwinska *et al.* 2014). Furthermore, the chick embryo is naturally immunodeficient, supporting the inoculation of both normal and cancerous human cells (Zijlstra *et al.* 2002). Therefore, the avian CAM makes an exceptionally useful model in investigating cancer cell behavior such as tumor growth, invasion, angiogenesis and the remodeling of the surrounding tissue (Zijlstra *et al.* 2002, Zeisser-Labouèbe *et al.* 2004, Kain *et al.* 2013).

The drug efficacy in terms of inhibition of invasiveness of cancer cells was studied on ML-1 derived xenografts by measuring the tumor weight and tumor size by image quantification combined with histology for classifying tumor phenotypes (Ossowski & Reich 1980, Nowak-Sliwinska *et al.* 2014, Lokman *et al.* 2012). In short, the image quantification were done using ImageJ by manually selecting the tumor area of first the pre-treated tumors then comparing that area with the post-treated tumor area of the same tumors giving the difference in tumor size in percentages (Kalhori *et al.* 2016). The drug cocktails were suspended in HEPES buffer before topical administration and the concentration of both free drugs and MSN loaded with drugs was 1 µg MTX and 13 µg FTY720 per used egg. The control tumors (0.5% DMSO and 1.6 mg/ml empty MSN) showed significant reduction in size from pre-treatment on EDD 9 to post-treatment on EDD 12 demonstrating that these ML-1 cells are highly invasive (Figure 30&31). The selected multidrug-loaded carriers systems showed significant retention of the tumor mass on the CAM compared to the freely administered drug combination (Figure 31c). This increased retention effect by drug-loaded MSNs was validated by image analysis quantifying the tumor size combined

with weighing the removed tumor masses after the treatment (Figure 31b&c). The result indicates that these multidrug-loaded MSN has the ability of blocking the invasiveness of these ML-1 derived xenografts (Figure 31). Furthermore, the histology shows that these drug-loaded MSN inhibit the epithelial-mesenchymal transition (EMT) seen as a decrease of EMT marker vimentin as well as a decrease in thyroid transcription factor 1 (TTF-1) which is considered a metastatic marker by pathologists (Figure 32; Sotiriou *et al.* 2017). The hematoxylin and eosin (H&E) staining of whole tumors validates the highly metastatic nature of the ML-1 cells in the both control tumors seen as invading tumor cells at the chick chorioallantoic membrane whereas both drug treated tumors has a non-invasive phenotype (Figure 30). The histology also shows that the tumors treated with the drug-loaded MSNs has an more necrotic/apoptotic phenotype seen as nuclear condensation and cell fragments compared to the other tumor samples (Figure 30&32).

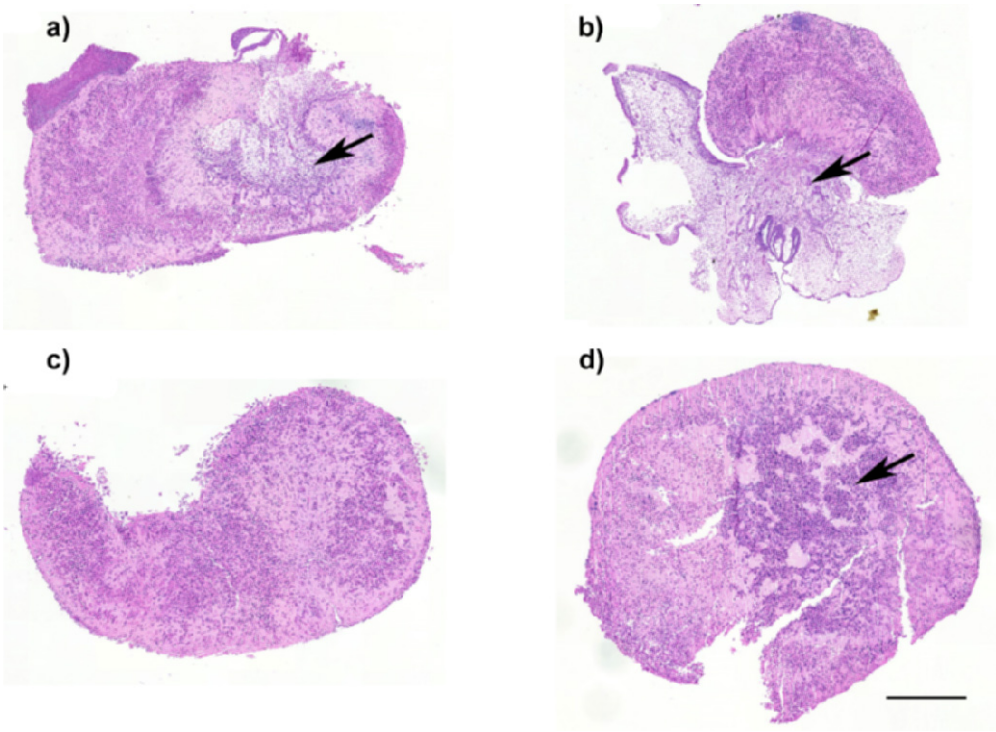

Figure 30. Hematoxylin and eosin (H&E) histological staining of ML-1 xenografts grown on chorioallantoic membrane (CAM). a) Control (0.5% DMSO) tumor showing invasion of the ML-1 cells through the CAM indicated by black arrow. b) Particle control (1.6 mg/ml empty MSN) tumor showing clear invasion of cancer cells to CAM epithelial cell layer indicated by black arrow. c) The free drug treated tumors shows non-invasive behavior of the cancer cells. d) The drug-loaded MSN treatments shows necrotic and apoptotic morphologies indicated by black arrow as well as loss of invasive phenotype. Scale bar 500 µm. (supp. file ***III***).

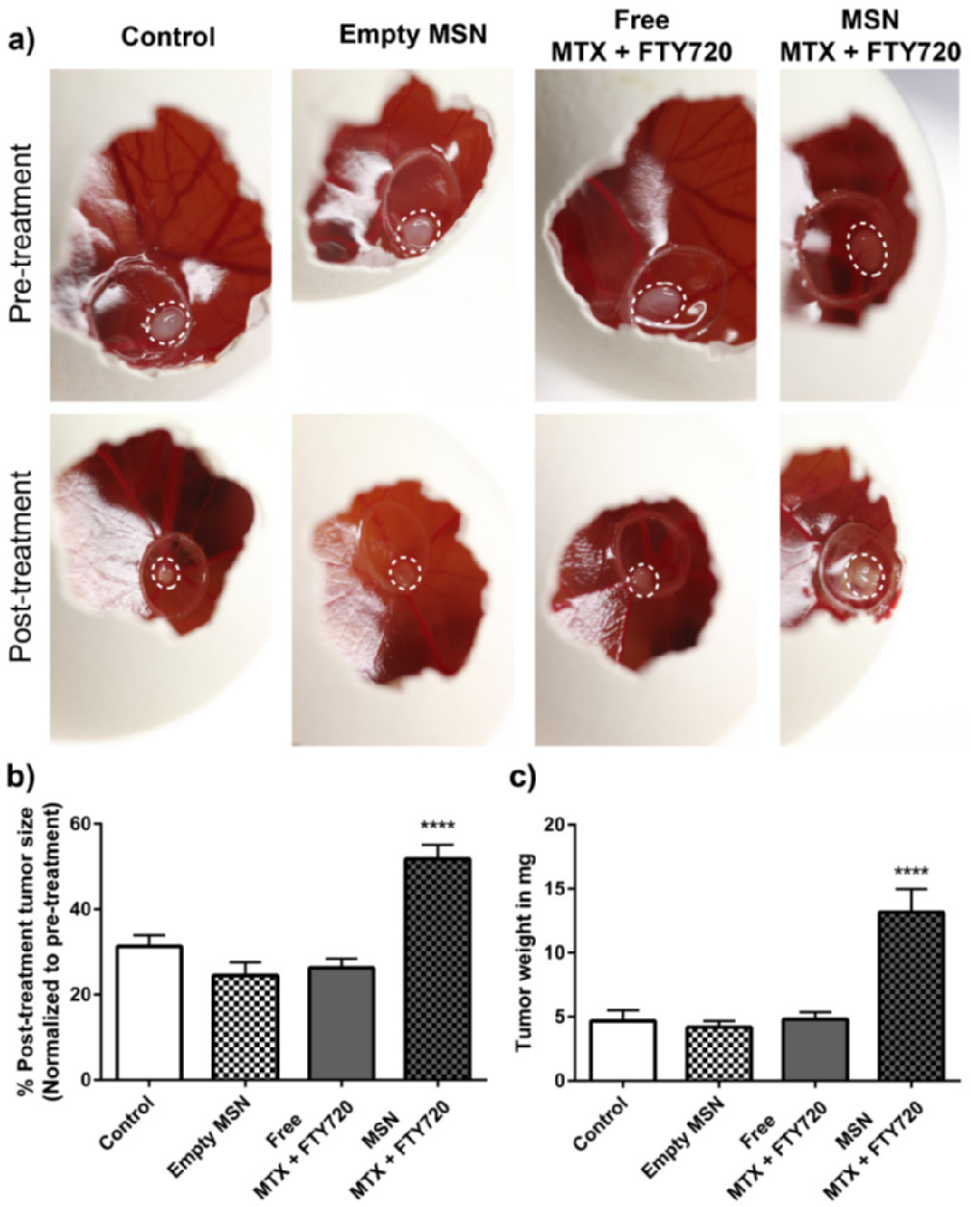

Figure 31. Chick chorioallantoic membrane (CAM) assay for evaluating the *in vivo* drug efficacy. a) Images of pre-treated and post-treated tumors showing decreased tumor size in control (0.5% DMSO), particle control (1.6 mg/ml empty MSN) and free drug treatment (1 µg MTX and 13 µg FTY720). The drug-loaded MSNs (1 µg MTX and 13 µg FTY720) treatment shows clear retention in post-treatment tumor size as well as yellow and white discolorations as signs of inflammation and necrosis. b) Image quantification of mean visible tumor size of post-treated tumors normalized to pre-treated tumors size shows decreased tumor size on all samples except the drug-loaded MSN showing a retention of tumor size c) Post tumor weighing shows significantly larger tumors after the drug-loaded MSN treatment validating the anti-invasive efficacy. Error bars represent ± SEM (n≥4), **** $P \leq 0.0001$ (***III***).

In addition, the necrotic phenotype of the ML-1 xenografts can visually be detected as disrupted morphology and discoloration of the tumor mass seen on the images (Figure 31a; Grey *et al.* 2006). However, the invasiveness of these cancer cells as well as the potential inhibition by drug-loaded MSNs needs to be further studied, preferably by detecting the human genetic content in different organs as a marker of metastasis or histology of the chicken embryo organs using human antibodies for detecting the possible tumor cells (Sotiriou *et al.* 2017, Maacha *et al.* 2018). Unfortunately, such detailed *in vivo* experiments regarding the invasiveness of these tumors were not plausible at that time due to limited resources. Therefore, in the next part of the study, we utilized *in vitro* invasion assay for validating the metastatic potential of these ML-1 cells as well as the inhibitory effect of the combined drug cocktail. Taken together, our nanoparticle containing two active molecules has an advantage in terms of anti-cancerous activity than nanoparticles with only one active agent for inhibition of metastasis and inducing cell death in thyroid cancer cells.

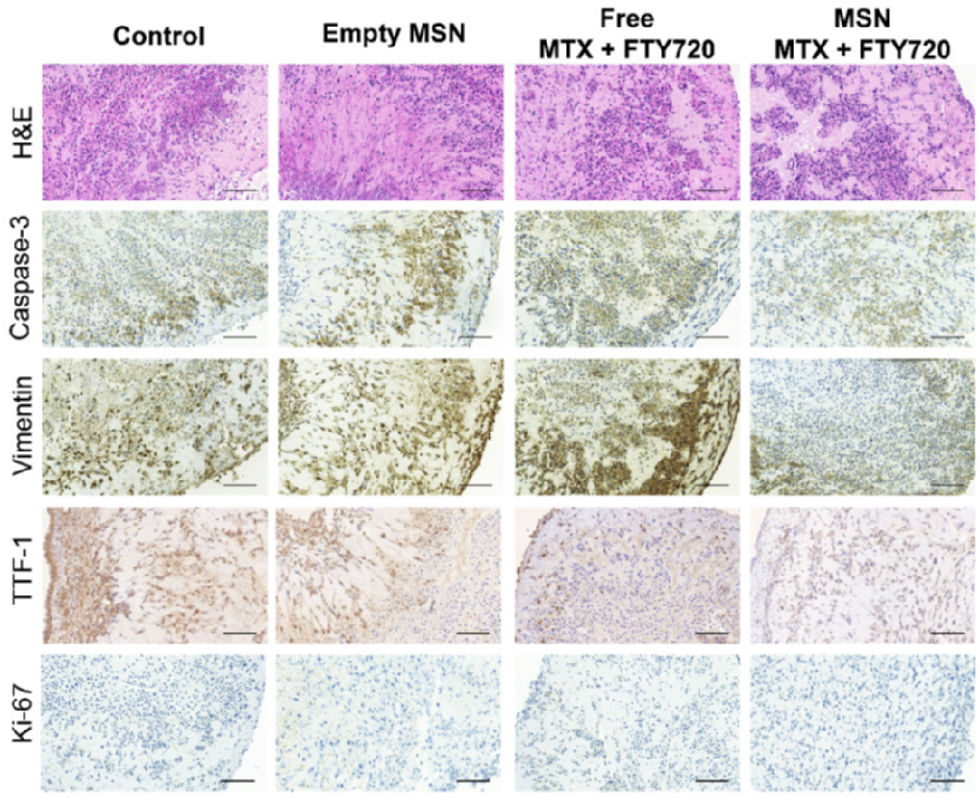

Figure 32. Immunohistochemistry staining of ML-1 xenografts grown on CAM. The H&E staining shows migrating cells in control and empty particle samples whereas the drug treated cells do not display invasive phenotype. High vimentin expression in all samples except the drug-loaded MSN treated samples indication of the drug inhibiting the EMT. The ML-1 xenografts exhibits a low proliferative profile shown as weak Ki-67 staining and some variable basal caspase-3 activity in all samples seen mostly in the center of the tumor. Clear decrease of TTF-1 staining in drug-loaded MSNs treated tumors compared to all other samples indicating a less malignant phenotype. Scale bar 50 μm (adapted from ***III***).

5.14. Invasion assay validates inhibitory effect of the drug cocktail

In order to validate that the drug cocktail inhibits the metastasis of these thyroid cancer cells; invasion assay were utilized using 8 µm pore size inserts with collagen IV coating for mimicking physiological relevant conditions of the extra cellular matrix (ECM; Kramer *et al.* 2013, Justus *et al.* 2014). High concentration (20%) of fecal bovine serum (FBS) was used in the lower well as the chemoattractant in order to steer the direction of the cells through the inserts. The ML-1 cells exhibited rapid invasiveness as the optimal time point for counting the migrated cells were at 7 hours and not 24 hours that is often used for low motility cells (Kramer *et al.* 2013, Justus *et al.* 2014). The drug concentrations of MTX and FTY720 were as followed; the low dosage was 0.13 µM MTX and 2.43 µM FTY720 the high dosage was 0.438 µM MTX and 8.10 µM FTY720. The result shows that the high drug dosage inhibits efficiently the migration of the ML-1 cells seen in the microcopy images from the invasion assay (Figure 33). The quantification obtained from the invasion assay validates that the drug combination treatment does in fact block the invasiveness of these ML-1 cells demonstrating the potential of this combination therapy (Figure 33d).

Intriguingly, the lower dosage significantly increases the cancer cell invasion functioning as an accelerant. This was seen as an increased migration of the ML-1 cells from the upper well towards the lower well when comparing to the untreated condition (Figure 33). However, such opposite effect of the low concentration drug cocktail would need further study in order to validate the underlying mechanism seen in this study. Nevertheless, several other studies have shown that a drug can exhibit a biphasic effect, where the low dosage has a stimulating effect, and the high dose has an inhibitory effect (Bhakta-Guha & Efferth 2015). Furthermore, the same experiment setup was conducted using drug-loaded MSNs instead of freely administered drug (data not shown). The result obtained using the drug-loaded MSNs showed non-significant effect on the invasion of these ML-1 cells, which corresponds to the results from the viability experiments showing that over 24 hours is necessary for the drug to be released in target cells in order to induce an effect. Therefore, an 7 hours experiment where the freely administered compound can immediately give an anti-invasive effect comparing those results with another treatment form where 7 hours is not even enough for the carrier system to release the drug compound is like "comparing apples and oranges". By prolonging the incubation time to 24 hours it could, in principle, be possible to compare the results of the two treatment forms. However, the toxic effect of the freely administered drug would be the governing force seen in the 24 hours viability assay (data not shown), and the "side effect" of the dying ML-1 cells would most likely be lower invasion score and not the actual anti-invasive effect. Taking together, the invasion assay verifies that the MTX and FTY720 drug combination does indeed inhibit the invasiveness of thyroid cancer cells. However, further more clinically relevant *in vivo* studies needs to be executed for validating the anti-invasive potential of these multidrug-loaded MSNs in order to go towards product development.

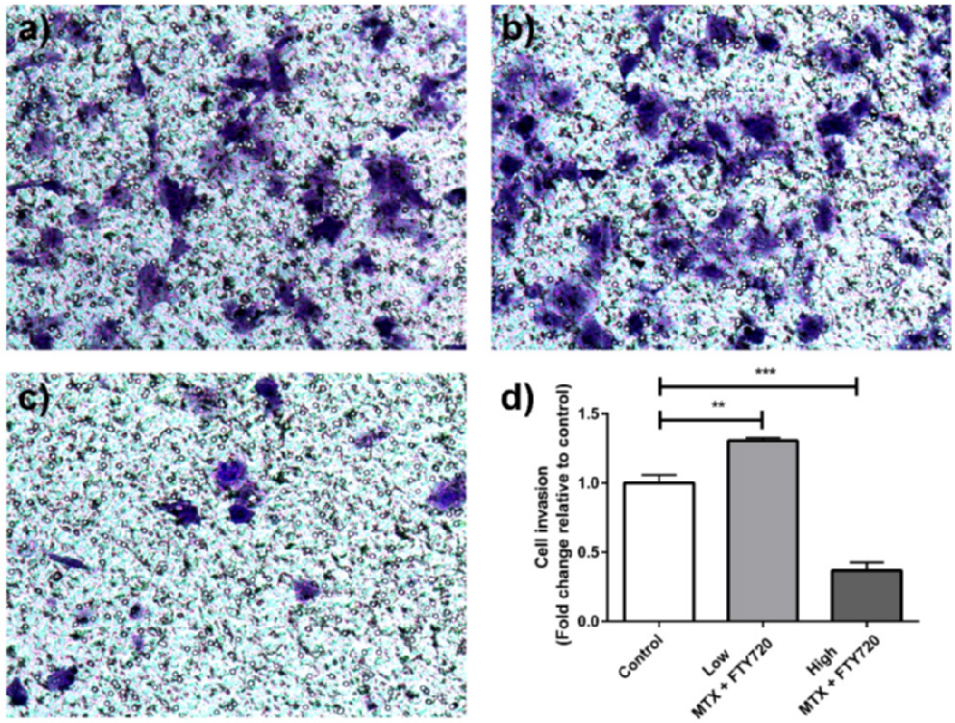

Figure 33. Invasion assay showing crystal violet-stained ML-1 cells after 7 hours. a) In the control sample ML-1 cells are visible on the insert after 7 hours showing that the cells are highly invasive. b) Low dosage of combination treatment (0.13 µM MTX and 2.43 µM FTY720) shows slight increase in the invasive potential of the ML-1 cells compared to control. c) The high dosage (0.438 µM MTX and 8.10 µM FTY720) show less migrating ML-1 cells on the insert and the d) quantification of the invasion assay validates that the high combination treatment block the invasiveness of these ML-1 cells. Error bars represent ± SEM (n=4), ** $P \leq 0.01$, *** $P \leq 0.001$ (***III***).

5.15. Validating the hypothesis of MSNs for targeted drug delivery

In order to validate an academic idea, concept or mechanism; one have to find the appropriate methods for testing the null hypothesis which is an default position where there is no relationship between two measured phenomena or no association among the different groups (Banerjee *et al.* 2009, Pernet 2016). In targeted drug development, that null hypothesis could be that "there is no enhanced targeted drug efficacy when utilizing the carrier system compared to freely administered drug". Subsequently using different relevant methods for testing if the drug carrier has an increased effect on target cells and lower effect on off-target cells. If the data shows a statistically significant difference between the two groups the null hypothesis is rejected and an alternative hypothesis can be accepted in its place. In these academic studies, the alternative hypothesis was that the carrier system functions as an effective targeting strategy that could be employed in the future for minimizing human suffering (***I-III***).

However, when conducting experimental setups with carrier systems versus freely administered drug compounds it is not always an easy and straightforward task as the release mechanism and as a consequence the drug effect of the two administrations can be quite different. Therefore, during the idea phase of the development of targeted drug delivery, it is important to consider the targeting strategy in order to achieve maximal uptake in target cells with minimal off-target internalization together with selecting the relevant methods for testing the null hypothesis. Then the drug of interest need to be carefully considered for appropriate loading so that the drug matches the properties of the carrier system, for example, a water-soluble drug loaded inside the porous structure of an MSN would result in a premature release of the drug in the extracellular space giving potential off-target effect (Desai *et al.* 2014). Or making a particle with pore size of a few nm for drug adsorption and then load the particle with large hydrocarbon molecules that are too big for the porous structures and, as a consequence, the drug would be attached on the surface of the particle creating a leaking particle system instead of targeted drug delivery. The saying that "everything affects everything" holds some truth in the development of nanoparticles for targeted drug delivery; and therefore, a case-by-case evaluation on these man-made materials would be preferred as generalizations will often give a misleading interpretation of both the efficacy and toxicity of nanomaterial based carrier systems (Paaby & Rockman 2012, Desai *et al.* 2014, Pillai 2014, Bobo *et al.* 2016, Bremer-Hoffmann *et al.* 2018).

Therefore, in this thesis, these MSNs were scrutinized by diverse scientific methods and by pushing the experimental setup by using high concentrations of particles, longer incubation times and utilizing different cell lines that made it possible to obtain relivable data showing that the alternative hypothesis holds true that these carrier systems could be used for targeted drug delivery for specific cell types in certain disease conditions originated from disruption in the cellular homeostasis (***I-III***). The null hypothesis was rejected in the first study, as the drug efficacy in terms of apoptosis showed significant (p-value less than 0.001) enhancement when utilizing celastrol-loaded sugar decorated MSNs compared to free drug in cervical cancer cells (Figure 23). In the second study, the null hypothesis was rejected as the efficacy in terms of inducing the stress response using folic acid functionalized celastrol-loaded MSNs showed superior efficacy compared to freely administered drug as the p-value was under 0.0001 (Figure 25). In the third and last study the null hypothesis was rejected as the multidrug-loaded MSNs showed significant (p-value less than 0.0001) retention of tumor size compared to the freely administered drug cocktail combined with significant efficacy (p-value less than 0.001) in terms of cell viability when using MTX and FTY720 loaded nanoparticles (Figure 31&28). However, as empirical science cannot be 'proven' by statistical significances the alternative hypothesis was selected as the most plausible explanation based on the results as a whole (Banerjee *et al.* 2009, Robergs 2017, Amrhein *et al.* 2019).

6. CONCLUSION AND FUTURE PROSPECTS

Cancer is one of the main causes of death in the western world and the numbers are estimated to rise; by the year 2020 there will be over 15 million new cancer cases worldwide. Traditional chemotherapy that arise after the first and second world war with all their potential side effects started the race towards targeted drug development, and the first breast cancer drug, tamoxifen, came out on the market in the 1970s. The advancement in the past decades in the knowledge of oncogenes and tumor suppressor genes together with digitalization and the development of sophisticated instruments has paved the way for personalized medicine. Nanomedicine is an emerging interdisciplinary field that combines nanotechnology with medicine for the development of therapeutics that could be used for personalized drug delivery and diagnostics for increased accumulation and retention of drug molecules in target tissue while minimizing potential off-target effects. Nanoparticles have shown great potential as drug delivery vehicles due to low toxicity, high drug loading capacity together with tailor-made surface functionalization for cell specific internalization, thus increasing the therapeutic index and lowering the possible side-effects of the drug. Inorganic silica based nanoparticles were selected as the drug carrier system, as they can be loaded with hydrophobic molecules and allow ease of functionalization of different targeting motifs combined with being biocompatible and biodegrade, as silica degrades in aqueous environment to silicic acid and ultimately gets excreted via urine. In this thesis, different targeting strategies utilizing mesoporous silica nanoparticles (MSNs) were developed and studied for estimating the targeted delivery and the potentially increased drug efficacy and possible off-target effects of these carrier systems.

In the first part of the study, we investigated the potential use of glucose conjugated MSNs to selectively and efficiently deliver the hydrophobic drug celastrol to sugar craving cancer cells. We evaluated internalization of sugar-derivatized MSNs via eight different surface functionalization regimes by flow cytometry, confocal microscopy, spectrophotometry and image analysis, from which the functionalization that had the highest uptake in cancer cells while keeping the uptake in healthy cells reasonably low, was selected for further drug efficacy studies. The particle design with a hyperbranched, PEI polymeric surface structure together with the selected (GA_{org}) sugar moiety providing an overall net positive surface was then loaded with small amounts of celastrol for evaluating the potentially gained anti-cancerous efficacy. The results show that there was no premature drug release of the selected carrier system under physiological conditions, thereby minimizing possible off-target effects that might give rise by freely administered celastrol. The glucose conjugated particle uptake in target cancerous cells was around five times higher than in the normal cells. Furthermore, the drug efficacy in terms of inducing apoptosis in cancer cells were remarkably enhanced when using the GA_{org} functionalized MSN compared to the same amount of free celastrol. Taken together, our results shows that sugar-decorated MSNs loaded with the poorly water soluble drug celastrol has the ability to efficiently enhance and induce apoptosis in cancer cells with minimal uptake in off-target healthy cells.

In the second study, we investigated the use of a tailor-made BioImageXD-based quantification method for counting and analyzing nuclear stress bodies (nSBs) in folate receptor (FR) positive cells induced by folic acid (FA) functionalized celastrol-loaded nanoparticles. The computerized quantification method was first validated by comparing the nSBs formation kinetics induced by heat shock with manually counting the nSBs positive cells from the whole population. The quantifications showed that there was no significant difference between the two methods; demonstrating that the automated image analysis workflow can be accurate, reliable and versatile for detecting and quantifying nSBs in stressed human cells. The image based quantification validates the specific drug delivery capabilities of these celastrol-loaded MSNs, as demonstrated by highly significant differences between the nSBs activation kinetics when comparing the FR-positive HeLa population with the FR-negative A549 population. Furthermore, the heat shock response was studied by western blot, indicating that the celastrol-loaded MSNs increased the expression of the molecular chaperone Hsp70 in HeLa cells already at low dosages, and that those similar concentrations did not properly induce the stress response in A549 cells. Taken together, the results of this study show that celastrol-loaded MSNs could potentially be beneficial for patients with protein aggregate associated diseases by inducing a specific and effective heat shock response in the target cells. Combining the targeted drug delivery capabilities of these MSNs with our computerized image quantification methods for detecting and characterizing nSBs positive cells could open up possibilities for future automated diagnostics and personalized medicine.

In the third and last project, we created a multidrug-loaded nanoparticle that specifically targets cancer cells by utilizing an active targeting ligand methotrexate (MTX), which is a folate antagonist that has been used as chemotherapy for decades. In this manner, we created a carrier system that has a drug with targeting capability on the surface of the nanoparticle that opens the possibility of loading the particle with a second drug, in this case a Sphingosine Kinase 1 Inhibitor named fingolimod (FTY720). The drug FTY720 works by inhibiting the phosphorylation of sphingosine and thereby blocks the production of the bioactive molecule sphingosine 1-phosphate (S1P), which is important for cell growth, survival and migration. As a consequence of blocking the production of S1P by the drug FTY720; migrating cells are halted and pushed towards apoptosis. The active ligand MTX on the other hand blocks the synthesis of thymine and purine nucleotides leading to replication errors and cell death of the fast dividing cancer cells. The results shows that the multidrug-loaded MSNs has significantly lower off-target effects on healthy cells compared to freely administered drugs, and that the drug-loaded particles efficiently induces cell death in target cells. The drug cocktail induced necrosis and cell fragmentation that implemented some difficulty in selecting appropriate *in vitro* methods for evaluating the apoptotic efficacy. However, by using traditional cell viability assays such as cell counting and crystal violet it was possible to distinguish live and dead cells from the population showing enhanced drug efficacy in the drug-loaded MSNs compared to freely administered drugs. The drug efficacy was further validated by external expert using an advanced microscopy technique combined with image analysis showing that the drug-loaded MSNs induced enhanced apoptosis in target thyroid cancer cells compared to freely administered drug cocktail detected as increased blebbing,

fragmentation and rounding up of dying cancer cells. Furthermore, the drug cocktail efficiently blocked the thyroid cancer cells migration *in vitro* using an invasion assay and the *in vivo* studies done on chick chorioallantoic membrane (CAM) assay showed that the drug-loaded MSNs retained the tumor size thus blocking the cancer cell invasion towards the chicken embryo. The histology done on the *in vivo* tumors shows that the drug-loaded MSNs also blocks the epithelial-mesenchymal transition (EMT) that is necessary for proper invasiveness of tumor cells. Taken together, our nanoparticle containing two active molecules has an advantage in terms of anti-cancerous activity than nanoparticles with only one active agent for inducing selective and efficient apoptosis and inhibition of metastasis in cancer cells expressing folate receptors.

Developing targeted drug delivery is not a simple task, going from idea towards reality, where material composition and functionalization needs to be carefully considered for successful drug loading and maximizing targeted drug delivery for each specific cell type. The drug carrier itself needs to be biodegradable and non-toxic in the administered dosages in order to minimize possible side effects in patients. However, in order to advance to clinical trials, massive *in vitro* and *in vivo* studies need to be executed and passed with excellence. Combined with the monetary challenges of today's research with the potential pitfalls of protecting the intellectual property rights of nanomaterials, the task can be daunting. However, there are some Food and Drug Administration (FDA) approved nanomedicines in the market showing that the efforts are not futile in the pursuit of targeted medicine. For example, our sugar decorated celastrol-loaded MSN could be used as a first line of defense against cancers, as most of the human tumors have an increased metabolic rate compared to healthy tissues and would therefore specifically internalize our proposed particles in higher amounts gaining enhanced drug efficacy. Also, by integrating targeted drug delivery with image analysis, it would be possible in the future for personalized disease treatment and diagnostics that could yield in quicker identification of target cells, and therefore minimize possible off-target effects. Furthermore, by combining two different drug molecules in one drug carrier it would be possible to reduce the administered dosage for the patient and enhance the synergistic effect of the drug cocktail by specific drug uptake in target cells, yielding enhanced efficacy with less side effects. Taken together, the findings in this thesis function as an academic proof of concept demonstrating that it is possible for targeted drug delivery and enhanced drug efficacy utilizing functionalized mesoporous silica nanoparticles. However, in order to achieve the ultimate goal of creating a new form of cancer treatment, significant input of research and resources from both academia and industry would be necessary as the accumulative cost of drug development goes up to millions of dollars.

7. ACKNOWLEDGEMENT

This work was carried out at the Faculty of Science and Engineering, Cell Biology, Åbo Akademi University and at the Turku Bioscience Centre, University of Turku and Åbo Akademi University and the thesis was written in our garage at home in Helsinki.

First and foremost I would like to thank my supervisors John Eriksson and Jessica Rosenholm for giving me the opportunity and support to be able to work together with two different and dynamic research groups in this highly interdisciplinary field of nanomaterials. I was only a freshman year undergraduate student when John inspired me by his legendary seminar about how the cell functions and after that I knew that I wanted to work in his group. Because of with my naive hope of curing cancer I wanted to collaborate with the nanoparticle guru Jessica who loves "Hello Kitty" and the color of pink in any format. Combining John's cell signaling knowledge with Jessica's "can-do" attitude I found the perfect match for developing targeted drug delivery systems. Also the friendship with Pasi Kanakaanpää formed from the long hours at Biocity basement using expensive microscopes and image analysis has had a profound impact on how I think as a scientists. Jouko Peltonen and Ronald Östbacka - even though the research done in your groups is not directly linked to my thesis our collaborations during the years has most certainly broaden my horizon and opened new possibilities in the field of material development.

I am grateful for Diana Toivola and Annika Meinander for supporting my research and writing process by giving positive feedback and because they always believed in my sometimes rather non-canonical ideas. I would also like to thank the professors Kid Törnqvist, Cecilia Sahlgren, Niklas Sandler, Jouko Peltonen, Ronald Östbacka and Lea Sistonen for an open and enthusiastic scientific atmosphere combined with state of the art equipment's at the Faculty of Science and Engineering. Furthermore, the help given by Thomas Bymark, Jouko Sandholm, Markku Saari and Ketlin Adel has been instrumental for keeping things rolling during my PhD journey.

A big thank you to goes to Hélder Santos and Gøril Flaten for reviewing my thesis and for giving their positive comments and suggestions as they strengthen my confidence in academic writing. Also thank you Róisín Owens for being my opponent! I'm certain the discussions will be fruitful during the defense.

I would like to express my gratitude to all of my friend and colleagues: Daniel, Jonas, Puusti, Rasmus, Sebi, Marco, Johan, Heidi, Josef, Julia, Alexandra, Elina, Preethy, Senthil, Rose, Terhi, Joel, Calle, Arun, Puonno, Alia, Hend, Ezgi, Jenny, Kati, Anna, Aravind and Jordan for the support and optimism – all of you made my years as an undergraduate student awesome. Especially thankful to Puusti, Daniel and Rasmus for being such good friends of mine - always helping out with anything e.g. abstract writing, protocol optimization, debating over the meaning of life or finding a nice restaurant to eat at. Jonas – you are like an extension of our family and always ready to be of assistance; either in building IKEA furniture's late at night or giving us refugee in our home while we were renovating our own apartment. Also thankful for all the group members from Rosenholm's, Eriksson's, Meinander's, Sistonen's,

Törnqvist's, Sandler's and Östbacka's labs we have an amazing community. I would also like to thank our study group during our undergraduate time: Atte, Vimi, Dada, Nina, Malin, Classe, Miche and Mickan. You guys made my study time fun and full of adventures and for that I will always be thankful for.

There are two colleagues and good friends of mine I want to especially acknowledge; they are Diti and Emil. Without your support I would not have made it through the PhD jungle. Alone one cannot succeed in interdisciplinary research and this was true working on either nanoparticles or polymer development. Diti who was my partner-in crime she was the brain behind the synthesis of the different nanoparticles and Emil my intellectual brother from another mother was the one who created the polymers that could control cell growth. The collaboration with the two of you made my research so much more intriguing and inspiring not to mention publishable and for that I will always be grateful.

Lauri and Camilla the innovation agents that actually believed in our ideas that made it possible to patent our inventions which in turn has given me the courage to believe in myself. Maria and Emine thank you for the support you gave during the years; either by correcting my manuscripts or teaching the importance of networking and pitching. Stuart – I was still a blue-eyed student when I first met you and by shattering my bubble I started to see things more clearly and that's when I realized that the truth is out there in the real world and not in the never ending pipetting.

My relatives – Gudrun, Gunnar, Pasi, Enni, Micke, Gretel, Jonas, Helena, Reko, Satu, Auli, Pekka, Saila and Thomas you all made by childhood great with all the adventures we had and supported me in deciding what I wanted to study. Tuomo, Hanna, Oona, Jontte, Anneli, Pauli, Sauli, Kirsi, Jouni, Irene, Teuvo, Sanna, Maija, Heikki, Erkki, and the whole Lähdeniemi and Paavola clan – you accepted me with open arms to your family with all of my flaws and virtues and for that I am forever grateful. Jani - thanks to your invaluable comments as an investment banker they help me realize how investors and business angels thinks about academic innovations. Paavo and Sanna thank you for you support during the years they ment a lot to me as we could relax at your place and enjoy the food, the outdoors and your company. Lasse and Martta thank you for being such nice neighbors always helping out, making amazing food and most of all giving your support. My childhood friends – Basse, Nikke, Dankku, Jonatan, Emil, Jörre, Axel and Jocki you guys took this strange boy under you wings and supported me in during my school years by either help me write an essay or to do my math homework or lift me up when I was down and for that I will always be grateful fore.

My dearest brothers - Max, Anton and Mixu, life hasn't been the easier for the Niemelä brothers but here we are still standing strong and united. After our mother passed away in 2006 my older brother Max took the responsibility of the funeral arrangements as well as contacted a lawyer for dividing the estate. Your support as an older brother has guided me through my life and it was based on your recommendation that I applied to Åbo Akademi University that opened many doors for me both career-wise and personally. Anton my younger brother you are my original collaborator and

innovator, together we saw in to the future what can be possible and you are one of the few persons who truly knows me. Mixu you are the newest edition of the band of brothers and with your communication skills and multi-cultural understanding you will without a doubt be successful one day on whatever you want to be. Without my brothers combined strength I would not have made it this far in life and for that I will always be grateful. I hope somewhere over the rainbow our mother can see us and be proud of us and what we are doing as we are following your guidance by listening to our hearts.

Rauno – my father, you are my hero. You are simultaneously strong and kind, your support through our lives has been the driving force behind the scenes. You are always there for us regardless of the situation, unselfishly helping us out even at your own expense. Your sales-personality was sometimes embarrassing to us as teenager, but now I understand what you meant by "everything is negotiable" which has been a powerful mindset in my career when supposable all options were exhausted. I hope that one day we can repay the input you have given us and this thesis functions as a good example of how your support has help us to excel ourselves.

Last but not least, Iris, love of my life, my true opponent and best friend. We met over 10 years ago and you turned my life up-side down. Already during the first night out with our study-buddies you dared to challenge me and so you caught my everlasting attention. You polished this rebel without a cause to the man I have now become and for that I am forever grateful. Without your "tough love" my master thesis would have failed, but with your input and support I managed to graduate in time that enabled the start of my PhD journey. You thought me to live again after the tragedy that happened to my mother when I was a teenager. Iris you gave me the best gift one can get by giving birth to two healthy children Elli and Edvin. You give me purpose in life and your undying support makes me want to strive further and to become an even better person, husband and father. Now when I have graduated (one year later than you) it is time for our children to grow up, graduate and become to the persons they want to be and do what they to do. Thank you Iris for everything, we made, it both of us! Let's continue this journey of life together and see how far we will go!

This work was financially supported by the Sigrid Jusélius Foundation, Otto A. Malm Foundation, Swedish Cultural Foundation, Waldemar von Frenckell Foundation, K. Albin Johanssons Foundation, Paulo Foundation, Finnish Cultural Foundation, Cancer Society of Finland, Jane and Aatos Erkko Foundation, Academy of Finland, the Foundation of the Åbo Akademi University, and the Turku Doctoral Network in Molecular Biosciences and by my father by buying exam books and other necessities.

Words cannot describe the gratitude for having so many great friends, colleagues and family members.

Erik Niemelä

Helsinki, 08.08.2019

8. REFERENCE

Abbott A, Cyranoski D, Jones N, Maher B, Schiermeier Q, Van Noorden R. (2010). Metrics: Do metrics matter? Nature 465(7300): 860-2. doi: 10.1038/465860a.

Adachi H, Katsuno M, Waza M, Minamiyama M, Tanaka F, Sobue G. (2009). Heat shock proteins in neurodegenerative diseases: pathogenic roles and therapeutic implications. Int J Hyperthermia 25(8):647-54. doi: 10.3109/02656730903315823.

Adamo JE, Bauer G, Berro M, Burnett BK, Hartman KA, Masiello LM, Moorman-White D, Rubinstein EP, Schuff KG. (2012). A roadmap for academic health centers to establish good laboratory practice-compliant infrastructure. Acad Med. 87(3):279-84. doi: 10.1097/ACM.0b013e318244838a.

Aggarwal BB. (2003). Signalling pathways of the TNF superfamily: A double-edged sword. Nat Rev Immunol. 3: 745-756. doi: 10.1038/nri1184.

Albanese A, Tang PS, Chan WC. (2012). The effect of nanoparticle size, shape, and surface chemistry on biological systems. Annu Rev Biomed Eng. 14:1-16. doi: 10.1146/annurev-bioeng-071811-150124.

Allan JM, Travis LB. (2005). Mechanisms of therapy-related carcinogenesis. Nat Rev Cancer. 5: 943-955. doi: 10.1038/nrc1749.

Amidon GL, Lennernäs H, Shah VP, Crison JR. (1995). A theoretical basis for a biopharmaceutic drug classification: the correlation of in vitro drug product dissolution and in vivo bioavailability. Pharm Res. 12(3):413-20. doi: 10.1023/a:1016212804288.

Varkouhi AK, Scholte M, Storm G, Haisma HJ. (2011). Endosomal Escape Pathways for Delivery of Biologicals. J Control Release. 151(3):220-8. doi: 10.1016/j.jconrel.2010.11.004.

Amrhein V, Greenland S, McShane B. (2019). Scientists rise up against statistical significance. Nat Comments. 567:305. doi: 10.1038/d41586-019-00857-9.

Anand P, Kunnumakkara AB, Sundaram C, Harikumar KB, Tharakan ST, Lai OS, Sung B, Aggarwal BB. (2008). Cancer is a preventable disease that requires major lifestyle changes. Pharm Res.25(9):2097-116. doi: 10.1007/s11095-008-9661-9.

Anderson RL, Balasas T, Callaghan J, Coombes RC, Evans J, Hall JA, Kinrade S, Jones D, Jones PS, Jones R, Marshall JF, Panico MB, Shaw JA, Steeg PS, Sullivan M, Tong W, Westwell AD, Ritchie JWA; Cancer Research UK and Cancer Therapeutics CRC Australia Metastasis Working Group. (2018). A framework for the development of effective anti-metastatic agents. Nat Rev Clin Oncol. doi: 10.1038/s41571-018-0134-8.

Andersson J, Rosenholm J, Areva S, Lindén M. (2004). Influences of Material Characteristics on Ibuprofen Drug Loading and Release Profiles from Ordered Micro- and Mesoporous Silica Matrices. Chemistry of Materials 16(21): 4160–67. doi: 16. 10.1021/cm0401490.

Arruebo M, Vilaboa N, Sáez-Gutierrez B, Lambea J, Tres A, Valladares M, González-Fernández Á. (2011). Assessment of the Evolution of Cancer Treatment Therapies. Cancers (Basel). 3(3): 3279–3330. doi: 10.3390/cancers3033279.

Atanasov AG, Waltenberger B, Pferschy-Wenzig EM, Linder T, Wawrosch C, Uhrin P, Temml V, Wang L, Schwaiger S, Heiss EH, Rollinger JM, Schuster D, Breuss JM,

Bochkov V, Mihovilovic MD, Kopp B, Bauer R, Dirsch VM, Stuppner H. (2015). Discovery and resupply of pharmacologically active plant-derived natural products: A review. Biotechnol Adv. 33(8):1582-1614. doi: 10.1016/j.biotechadv.2015.08.001.

Attarwala H. (2010). Role of antibodies in cancer targeting. J Nat Sci Biol Med. 1(1): 53–56. doi: 10.4103/0976-9668.71675.

Bae YH, Park K. (2011). Targeted drug delivery to tumors: Myths, reality and possibility. J Control Release. 153(3): 198–205. doi: 10.1016/j.jconrel.2011.06.001.

Baer DR. (2018). The Chameleon Effect: Characterization Challenges Due to the Variability of Nanoparticles and Their Surfaces. Front Chem. 6: 145. doi: 10.3389/fchem.2018.00145.

Bagnoli M, Canevari S, Mezzanzanica D. (2010). Cellular FLICE-inhibitory protein (c-FLIP) signalling: a key regulator of receptor-mediated apoptosis in physiologic context and in cancer. Int J Biochem Cell Biol. 42(2):210-3. doi: 10.1016/j.biocel.2009.11.015.

Bali A, Bali D, Sharma A. (2013). An overview of gene therapy in head and neck cancer. Indian J Hum Genet. 19(3):282-90. doi: 10.4103/0971-6866.120811.

Ballabh P, Braun A, Nedergaard M. (2004). The Blood-Brain Barrier: An Overview: Structure, Regulation, and Clinical Implications. Neurobiol Dis. 16(1):1-13. doi: 10.1016/j.nbd.2003.12.016.

Baltazar GC, Guha S, Lu W, Lim J, Boesze-Battaglia K, Laties AM, Tyagi P, Kompella UB, Mitchell CH. (2012). Acidic nanoparticles are trafficked to lysosomes and restore an acidic lysosomal pH and degradative function to compromised ARPE-19 cells. PLoS One. 7(12):e49635. doi: 10.1371/journal.pone.0049635.

Banerjee A, Chitnis UB, Jadhav SL, Bhawalkar JS, Chaudhury S. (2009). Hypothesis testing, type I and type II errors. Ind Psychiatry J. 18(2):127-31. doi: 10.4103/0972-6748.62274.

Bartrip P. (2004). History of asbestos related disease. Postgrad Med J. 80(940): 72–76. doi: 10.1136/pmj.2003.012526.

Barua S, Mitragotri S. (2014). Challenges associated with Penetration of Nanoparticles across Cell and Tissue Barriers: A Review of Current Status and Future Prospects. Nano Today. 9(2):223-243. doi: 10.1016/j.nantod.2014.04.008.

Bazak R, Houri M, Achy SE, Hussein W, Refaat T. (2014). Passive targeting of nanoparticles to cancer: A comprehensive review of the literature. Mol Clin Oncol. 2(6):904-908. doi: 10.3892/mco.2014.356.

Beck JS, Vartuli JC, Roth WJ, Leonowicz ME, Kresge CT, Schmitt KD, Chu CT, Olson DH, Sheppard EW, McCullen SB, Higgins JB, Schlenker JL. (1992). A new family of mesoporous molecular sieves prepared with liquid crystal templates. J Am Chem Soc. 114: 10834–43. doi: 10.1021/ja00053a020.

Benet LZ. (2013). The role of BCS (biopharmaceutics classification system) and BDDCS (biopharmaceutics drug disposition classification system) in drug development. J Pharm Sci. 102(1):34-42. doi: 10.1002/jps.23359.

Beutler JA. (2009). Natural Products as a Foundation for Drug Discovery. Curr Protoc Pharmacol. 46:9.11.1-9.11.21. doi: 10.1002/0471141755.ph0911s46.

Bhakta-Guha D, Efferth T. (2015). Hormesis: Decoding Two Sides of the Same Coin. Pharmaceuticals (Basel). 8(4):865-83. doi: 10.3390/ph8040865.

Bharti C, Nagaich U, Pal AK, Gulati N. (2015). Mesoporous silica nanoparticles in target drug delivery system: A review. Int J Pharm Investig. 5(3):124-33. doi: 10.4103/2230-973X.160844.

Biamonti G, Vourc'h C. (2010). Nuclear stress bodies. Cold Spring Harb Perspect Biol. 2(6):a000695. doi: 10.1101/cshperspect.a000695.

Blumenfeld Z. (2012). Chemotherapy and fertility. Best Pract Res Clin Obstet Gynaecol. 26(3):379-90. doi: 10.1016/j.bpobgyn.2011.11.008.

Boatright KM, Renatus M, Scott FL, Sperandio S, Shin H, Pedersen IM, Ricci JE, Edris WA, Sutherlin DP, Green DR, Salvesen GS. (2003). A unified model for apical caspase activation. Mol Cell 11(2): 529-541. doi: 10.1016/s1097-2765(03)00051-0.

Bobo D, Robinson KJ, Islam J, Thurecht KJ, Corrie SR. (2016). Nanoparticle-Based Medicines: A Review of FDA-Approved Materials and Clinical Trials to Date.Pharm Res. 33(10):2373-87. doi: 10.1007/s11095-016-1958-5.

Bondarenko O, Juganson K, Ivask A, Kasemets K, Mortimer M, Kahru A. (2013). Toxicity of Ag, CuO and ZnO nanoparticles to selected environmentally relevant test organisms and mammalian cells in vitro: a critical review. Arch Toxicol. 87(7):1181-200. doi: 10.1007/s00204-013-1079-4.

Brar SK, Verma M, Tyagi RD, Surampalli RY. (2010). Engineered nanoparticles in wastewater and wastewater sludge--evidence and impacts. Waste Manag. 30(3):504-20. doi: 10.1016/j.wasman.2009.10.012.

Bremer-Hoffmann S, Halamoda-Kenzaoui B, Borgos SE. (2018) Identification of regulatory needs for nanomedicines. J Interdiscip Nanomed. 3(1), 4–15. doi: 10.1002/jin2.34.

Brevet D, Gary-Bobo M, Raehm L, Richeter S, Hocine O, Amro K, Loock B, Couleaud P, Frochot C, Morère A, Maillard P, Garcia M, Durand JO. (2009). Mannose-targeted mesoporous silica nanoparticles for photodynamic therapy. Chem Commun (Camb). (12):1475-7. doi: 10.1039/b900427k.

Brinker J, Scherer GW. (1990). Sol-Gel Science: The Physics and Chemistry of Sol-Gel Processing, 1 edition (Boston: Academic Press). doi: 10.1016/b978-0-08-057103-4.50001-5.

Broxmeyer L. (2004). Is cancer just an incurable infectious disease? Med Hypotheses. 63(6):986-96. doi: 10.1016/j.mehy.2004.05.008.

Butterfield LH. (2015). Cancer vaccines. BMJ. 350:h988. doi: 10.1136/bmj.h988.

Carmeliet P (2005). VEGF as a key mediator of angiogenesis in cancer. Oncology. 69 Suppl 3:4-10. doi: 10.1159/000088478.

Carpenter AE, Kamentsky L, Eliceiri KW. (2012). A call for bioimaging software usability. Nat Methods. 9(7):666-70. doi: 10.1038/nmeth.2073.

Carrillo-Conde B, Song EH, Chavez-Santoscoy, Phanse Y, Ramer-Tait AE, Pohl NL, Wannemuehler MJ, Bellaire BH, Narasimhan B. (2011). Mannose-functionalized "pathogen-like" polyanhydride nanoparticles target C-type lectin receptors on dendritic cells. Mol Pharm. 8(5):1877-86. doi: 10.1021/mp200213r.

Cascão R, Fonseca JE, Moita LF. (2017). Celastrol: A Spectrum of Treatment Opportunities in Chronic Diseases. Front Med (Lausanne). 4:69. doi: 10.3389/fmed.2017.00069.

Castedo M, Perfettini JL, Roumier T, Andreau K, Medema R, Kroemer G. (2004). Cell death by mitotic catastrophe: A molecular definition. Oncogene. 23(16):2825-37. doi: 10.1038/sj.onc.1207528.

Chambers AF, Groom AC, MacDonald IC. (2002). Dissemination and growth of cancer cells in metastatic sites. Nat Rev Cancer. 2(8):563-72. doi: 10.1038/nrc865.

Chen HW, Su SH, Chien CT, Lin WH, Yu SL, Chou CC, Chen J.J.W, Yang PC. (2006). Titanium dioxide nanoparticles induce emphysema-like lung injury in mice. The Faseb Journal. 20:2393-2395. doi: 10.1096/fj.06-6485fje.

Chen Z, Meng H, Xing G, Chen C, Zhao Y, Jia G, Wang T, Yuan H, Ye C, Zhao F, Chai Z, Zhu C, Fang X, Ma B, Wan L. (2005). Acute toxicological effects of copper nanoparticles in vivo. Toxicol Lett. 163(2):109-20. doi: 10.1016/j.toxlet.2005.10.003.

Chow AM, Brown IR. (2007). Induction of heat shock proteins in differentiated human and rodent neurons by celastrol. Cell Stress Chaperones. 12(3):237-44. doi: 10.1379/csc-269.1.

Chung TH, Wu SH, Yao M, Lu CW, Lin YS, Hung Y, Mou CY, Chen YC, Huang DM. (2007). The effect of surface charge on the uptake and biological function of mesoporous silica nanoparticles in 3T3-L1 cells and human mesenchymal stem cells. Biomaterials. 28(19):2959-66. doi: 10.1016/j.biomaterials.2007.03.006.

Clark OH, Levin K, Zeng QH, Greenspan FS, Siperstein A. (1988). Thyroid cancer: the case for total thyroidectomy. Eur J Cancer Clin Oncol. 24(2):305-13. doi: 10.1016/0277-5379(88)90273-8.

Cooper GM. (2000). The Cell: A Molecular Approach. 2nd edition. Sunderland (MA): Sinauer Associates; 2000. The Development and Causes of Cancer. Available from: https://www.ncbi.nlm.nih.gov/books/NBK9963/

Copple IM, Shelton LM, Walsh J, Kratschmar DV, Lister A, Odermatt A, Goldring CE, Dinkova-Kostova AT, Honda T, Park BK. (2014). Chemical tuning enhances both potency toward nrf2 and in vitro therapeutic index of triterpenoids. Toxicol Sci. 140(2):462-9. doi: 10.1093/toxsci/kfu080.

Costa P, Sousa Lobo JM. (2001). Modeling and comparison of dissolution profiles. Eur J Pharm Sci. 13(2):123-33. doi: 10.1016/s0928-0987(01)00095-1.

Crookes-Goodson WJ, Slocik JM, Naik RR. (2008). Bio-directed synthesis and assembly of nanomaterials. Chem Soc Rev. 37(11):2403-12. doi: 10.1039/b702825n.

Del Agua I, Marina S, Pitsalidis C, Mantione D, Ferro M, Iandolo D, Sanchez-Sanchez A, Malliaras GG, Owens RM, Mecerreyes D. (2018). Conducting Polymer Scaffolds Based on Poly(3,4-ethylenedioxythiophene) and Xanthan Gum for Live-Cell Monitoring. ACS Omega. 3(7):7424-7431. doi: 10.1021/acsomega.8b00458.

Desai D, Sen Karaman D, Prabhakar N, Tadayon S, Duchanoy A, Toivola D, Rajput S, Näreoja T, Rosenholm J. (2014). Design considerations for mesoporous silica nanoparticulate systems in facilitating biomedical applications. Mesoporous Biomater. 1:16–43. doi: 10.2478/mesbi-2014-0001.

Desai N. (2012). Challenges in development of nanoparticle-based therapeutics. AAPS J. 14(2):282-95. doi: 10.1208/s12248-012-9339-4.

Denisenko TV, Sorokina IV, Gogvadze V, Zhivotovsky B. (2016). Mitotic catastrophe and cancer drug resistance: A link that must to be broken. Drug Resist Updat.24:1-12. doi: 10.1016/j.drup.2015.11.002.

Donald R. Baer, Prabhakaran Munusamy, Brian D. Thrall. (2016). Provenance information as a tool for addressing engineered nanoparticle reproducibility challenges. Biointerphases. 11(4): 04B401. doi: 10.1116/1.4964867.

Dubey A, Prajapati KS, Swamy M, Pachauri V. (2015). Heat shock proteins: a therapeutic target worth to consider. Vet World. 8(1):46-51. doi: 10.14202/vetworld.2015.46-51.

Dubrez L, Berthelet J, Glorian V. (2013). IAP proteins as targets for drug development in oncology. Onco Targets Ther. 9:1285-304. doi: 10.2147/OTT.S33375.

Ducheyne P, Healy K, Hutmacher DE, Grainger DW, Kirkpatrick CJ. (2015). Comprehensive Biomaterials II. Newnes, Boston. doi: 10.1016/b978-0-12-803581-8.10237-1.

Eckelman BP, Salvesen GS. (2006). The human anti-apoptotic proteins cIAP1 and cIAP2 bind but do not inhibit caspases. J Biol Chem. 281(6):3254-60. doi: 10.1074/jbc.M510863200.

Edwards MA, Roy S. (2017). Academic Research in the 21st Century: Maintaining Scientific Integrity in a Climate of Perverse Incentives and Hypercompetition. Environ Eng Sci. 34(1):51-61. doi: 10.1089/ees.2016.0223.

Eliceiri KW, Berthold MR, Goldberg IG, Ibáñez L, Manjunath BS, Martone ME, Murphy RF, Peng H, Plant AL, Roysam B, Stuurman N, Swedlow JR, Tomancak P, Carpenter AE. (2012). Biological imaging software tools. Nat Methods. 28;9(7):697-710. doi: 10.1038/nmeth.2084.

Elmore S. (2007). Apoptosis: a review of programmed cell death. Toxicol Pathol. 35(4):495-516. doi: 10.1080/01926230701320337.

Eshbach ML, Weisz OA. (2017). Receptor-Mediated Endocytosis in the Proximal Tubule. Annu Rev Physiol. 79:425-448. doi: 10.1146/annurev-physiol-022516-034234.

Esposito S, Tenconi R, Preti V, Groppali E, Principi N. (2016). Chemotherapy against cancer during pregnancy: A systematic review on neonatal outcomes. Medicine (Baltimore). 95(38):e4899. doi: 10.1097/MD.0000000000004899.

Farokhzad OC, Langer R. (2009). Impact of nanotechnology on drug delivery. ACS Nano 3: 16-20. doi: 10.1021/nn900002m.

Finnish Cancer Registry. (2016). Cancer statistics, http://syoparekisteri.fi/tilastot/tautitilastot accessed 14.06.2019.

Fosgerau K, Hoffmann T. (2015). Peptide therapeutics: current status and future directions. Drug Discov Today. 20(1):122-8. doi: 10.1016/j.drudis.2014.10.003.

Franchi L, Eigenbrod T, Muñoz-Planillo R, Nuñez G. (2009). The inflammasome: a caspase-1-activation platform that regulates immune responses and disease pathogenesis. Nat Immunol. 10(3):241-7. doi: 10.1038/ni.1703.

Franco A, Hansen SF, Olsen SI, Butti L. (2007). Limits and prospects of the "incremental approach" and the European legislation on the management of risks related to nanomaterials. Regul Toxicol Pharmacol. 48(2):171-83. doi: 10.1016/j.yrtph.2007.03.007.

Fröhlich E. (2012). The role of surface charge in cellular uptake and cytotoxicity of medical nanoparticles. Int J Nanomedicine. 7: 5577–5591.doi: 10.2147/IJN.S36111.

Fu C, Liu T, Li L, Liu H, Chen D, Tang F. (2012). The absorption, distribution, excretion and toxicity of mesoporous silica nanoparticles in mice following different exposure routes. Biomaterials. 34(10):2565-75. doi: 10.1016/j.biomaterials.2012.12.043.

Fuentes-Prior P, Salvesen GS. (2004). The protein structures that shape caspase activity, specificity, activation and inhibition. Biochem J. 384(Pt 2):201-32. doi: 10.1042/BJ20041142.

Fujiwara A, Hoshino T, Westley JW. (1985). Anthracycline Antibiotics. Critical Reviews in Biotechnology. 3(2): 133. doi:10.3109/07388558509150782.

Galluzzi L, Kepp O, Trojel-Hansen C, Kroemer G. (2012). Non-apoptotic functions of apoptosis-regulatory proteins. EMBO Rep. 13(4):322-30. doi: 10.1038/embor.2012.19.

Galm U, Hager MH, Van Lanen SG, Ju J, Thorson JS, Shen B. (2005). Antitumor antibiotics: bleomycin, enediynes, and mitomycin. Chem Rev. 105(2):739-58. doi: 10.1021/cr030117g.

Gary-Bobo M, Hocine O, Brevet D, Maynadier M, Raehm L, Richeter S, Charasson V, Loock B, Morère A, Maillard P, Garcia M, Durand JO. (2012). Cancer therapy improvement with mesoporous silica nanoparticles combining targeting, drug delivery and PDT. Int J Pharm. ;423(2):509-15. doi: 10.1016/j.ijpharm.2011.11.045.

Gerlowski LE, Jain RK. (1986). Microvascular permeability of normal and neoplastic tissues. Microvasc Res. 31(3):288-305. doi: 10.1016/0026-2862(86)90018-x.

Gialeli C, Theocharis AD, Karamanos NK. (2010). Roles of matrix metalloproteinases in cancer progression and their pharmacological targeting. FEBS J. 278(1):16-27. doi: 10.1111/j.1742-4658.2010.07919.x.

Giang I, Boland EL, Poon GM. (2014). Prodrug applications for targeted cancer therapy. AAPS J. 16(5):899-913. doi: 10.1208/s12248-014-9638-z.

Godbey WT, Wu KK, Mikos AG. (1999). Size Matters: Molecular Weight Affects the Efficiency of Poly(ethylenimine) as a Gene Delivery Vehicle. J Biomed Mater Res. 45(3):268-75. doi:10.1002/(SICI)1097-4636(19990605)45:3<268::AID-JBM15>3.0.CO;2-Q.

Goel HL, Mercurio AM. (2013).VEGF targets the tumour cell. Nat Rev Cancer. 13(12): 871–882. doi: 10.1038/nrc3627.

Golstein P, Kroemer G. (2007). Cell death by necrosis: towards a molecular definition. Trends Biochem Sci. 32(1):37-43. doi: 10.1016/j.tibs.2006.11.001.

Gonzalez-Rodriguez D, Barakat AI. (2015). Dynamics of receptor-mediated nanoparticle internalization into endothelial cells. PLoS One. 10(4):e0122097. doi: 10.1371/journal.pone.0122097.

Goñi FM. (2014). The basic structure and dynamics of cell membranes: An update of the Singer–Nicolson model. Biochim Biophys Acta. 1838(6):1467-76. doi: 10.1016/j.bbamem.2014.01.006.

Goodsell DS. (1999). The molecular perspective: methotrexate. Stem Cells. 17(5):314-5. doi: 10.1002/stem.170314.

Gordon K, Clouaire T, Bao XX, Kemp SE, Xenophontos M, de Las Heras JI, Stancheva I. (2014). Immortality, but not oncogenic transformation, of primary human cells leads to epigenetic reprogramming of DNA methylation and gene expression. Nucleic Acids Res. 42(6):3529-41. doi: 10.1093/nar/gkt1351.

Gottesman MM, Fojo T, Bates SE. (2002). Multidrug resistance in cancer: Role of ATP-dependent transporters. Nat Rev Cancer 2: 48-58. doi: 10.1038/nrc706.

Gouveia BG, Rijo P, Gonçalo TS, Reis CP. (2015). Good manufacturing practices for medicinal products for human use. J Pharm Bioallied Sci. 7(2): 87–96. doi: 10.4103/0975-7406.154424.

Grey JE, Enoch S, Harding KG. (2006). Wound assessment. BMJ. 332(7536):285-8. doi:10.1136/bmj.332.7536.285.

Guertler A, Kraemer A, Roessler U, Hornhardt S, Kulka U, Moertl S, Friedl AA, Illig T, Wichmann E, Gomolka M. (2011). The WST survival assay: an easy and reliable method to screen radiation-sensitive individuals. Radiat Prot Dosimetry. 143(2-4):487-90. doi: 10.1093/rpd/ncq515.

Guo Z, Tan L. (2009). Fundamentals and Applications of Nanomaterials. Norwood: Artech House Publishers. ISBN 978-3-319-64717-3.

Gyrd-Hansen M, Meier P. (2010). IAPs: from caspase inhibitors to modulators of NF-kappaB, inflammation and cancer. Nat Rev Cancer. 10(8):561-74. doi: 10.1038/nrc2889.

Ha SK. (2014). Dietary salt intake and hypertension. Electrolyte Blood Press. 12(1):7-18. doi: 10.5049/EBP.2014.12.1.7.

Hammerstedt RH, Blach EL. (2008). Commercialization of basic research from within the university and return of value to the public. Anim Reprod Sci. 105(1-2): 158–178. doi: 10.1016/j.anireprosci.2007.11.014.

Hanahan D, Weinberg RA. (2000). The hallmarks of cancer. Cell. 100(1):57-70. doi: 10.1016/s0092-8674(00)81683-9.

Handy RD, Owen R, Valsami-Jones E. (2008). The ecotoxicology of nanoparticles and nanomaterials: current status, knowledge gaps, challenges, and future needs. Ecotoxicology. 17(5):315-25. doi: 10.1007/s10646-008-0206-0.

Hao N, Huiyu L, Li L, Dong C, Li L, Tang F. (2012). In Vitro Degradation Behavior of Silica Nanoparticles Under Physiological Conditions. J Nanosci Nanotechnol. 12(8):6346-54. doi: 10.1166/jnn.2012.6199.

Harrison E. (2009). Generally Recognized as Safe Determination for Silicon Dioxide When Added Directly and/or Indirectly to Human Food. Lewis & Harrison, Washington, D. C. 1-77

Hartig SM. (2013). Basic image analysis and manipulation in ImageJ. Curr Protoc Mol Biol. Chapter 14:Unit14.15. doi: 10.1002/0471142727.mb1415s102.

He Q, Zhang Z, Gao F, Li Y, Shi J. (2011). In vivo biodistribution and urinary excretion of mesoporous silica nanoparticles: effects of particle size and PEGylation. Small. 7(2):271-80. doi: 10.1002/smll.201001459.

Heus JJ, de Pauw ES, Leloux M, Morpurgo M, Hamblin MR, Heger M. (2017). Importance of intellectual property generated by biomedical research at universities and academic hospitals. J Clin Transl Res. 3(2). pii: 5. doi: 10.18053/jctres.03.201702.005.

Hilgendorf KI, Leshchiner ES, Nedelcu S, Maynard MA, Calo E, Ianari A, Walensky LD, Lees JA. (2013). The retinoblastoma protein induces apoptosis directly at the mitochondria. Genes Dev. 27(9):1003-15. doi: 10.1101/gad.211326.112.

Hillaireau H, Couvreur P. (2009). Nanocarriers' entry into the cell: Relevance to drug delivery. Cell Mol Life Sci 66: 2873-2896. doi: 10.1007/s00018-009-0053-z.

Hoffmann F, Cornelius M, Morell J, Fröba M. (2006). Silica-based mesoporous organic-inorganic hybrid materials. Angew Chem Int Ed Engl. 45(20):3216-51. doi: 10.1002/anie.200503075.

Holmberg CI, Illman SA, Kallio M, Mikhailov A, Sistonen L. (2000). Formation of nuclear HSF1 granules varies depending on stress stimuli. Cell Stress. 5(3): 219–228. doi: 10.1379/1466-1268(2000)005<0219:fonhgv>2.0.co;2

Homer-Vanniasinkam S, Tsui J. (2012). The continuing challenges of translational research: clinician-scientists' perspective. Cardiol Res Pract. 2012:246710. doi: 10.1155/2012/246710.

Hongmei Z. (2012). Extrinsic and Intrinsic Apoptosis Signal Pathway Review. In Apoptosis and Medicine; InTech: London, UK. 3-22. doi: 10.5772/50129.

Hortobagyi GN. (2001). Overview of treatment results with trastuzumab (Herceptin) in metastatic breast cancer. Semin Oncol. 28(6 Suppl 18):43-7. doi:10.1016/S0093-7754(01)90108-3.

Housman G, Byler S, Heerboth S, Lapinska K, Longacre M, Snyder N, Sarkar S. (2014). Drug resistance in cancer: an overview. Cancers (Basel). 6(3):1769-92. doi: 10.3390/cancers6031769.

Hu Q, Sun W, Wang C, Gu Z. (2016). Recent advances of cocktail chemotherapy by combination drug delivery systems. Adv Drug Deliv Rev. 98:19-34. doi: 10.1016/j.addr.2015.10.022.

Huang X, Zhuang J, Teng X, Li L, Chen D, Yan X, Tang F. (2010). The promotion of human malignant melanoma growth by mesoporous silica nanoparticles through decreased reactive oxygen species. Biomaterials. 31(24):6142-53. doi: 10.1016/j.biomaterials.2010.04.055.

Huang XJ. (2008). Nanotechnology Research: New Nanostructures, Nanotubes and Nanofibers (Nova Publishers). ISBN 978-1600219023.

Huang YW, Cambre M, Lee HJ. (2017). The Toxicity of Nanoparticles Depends on Multiple Molecular and Physicochemical Mechanisms. Int J Mol Sci. 18(12): 2702. doi: 10.3390/ijms18122702.

Huennekens FM. (1994). The methotrexate story: a paradigm for development of cancer chemotherapeutic agents. Adv Enzyme Regul. 34:397-419. doi: 10.1016/0065-2571(94)90025-6.

Ikuma K, Decho AW, Lau BL. (2015). When nanoparticles meet biofilms-interactions guiding the environmental fate and accumulation of nanoparticles. Front Microbiol. 6:591. doi: 10.3389/fmicb.2015.00591.

Irmler M, Thome M, Hahne M, Schneider P, Hofmann K, Steiner V, Bodmer JL, Schröter M, Burns K, Mattmann C, Rimoldi D, French LE, Tschopp J. (1997). Inhibition of death receptor signals by cellular FLIP. Nature 388: 190-195. doi: 10.1038/40657.

Izquierdo MA, Neefjes JJ, Mathari AE, Flens MJ, Scheffer GL, Scheper RJ. (1996). Overexpression of the ABC transporter TAP in multidrug-resistant human cancer cell lines. Br J Cancer. 74(12):1961-7. doi: 10.1038/bjc.1996.660.

Jacob BA, Lefgren L. (2011). The Impact of Research Grant Funding on Scientific Productivity. J Public Econ. 95(9-10): 1168–1177. doi: 10.1016/j.jpubeco.2011.05.005.

Jafri MA, Ansari SA, Alqahtani MH, Shay JW. (2016). Roles of telomeres and telomerase in cancer, and advances in telomerase-targeted therapies. Genome Med. 8(1):69. doi: 10.1186/s13073-016-0324-x.

Jain KK. (2012). The Handbook of Nanomedicine. ISBN 978-1-60327-319-0.

Jain RK. (1999). Understanding Barriers to Drug Delivery: High Resolution in Vivo Imaging Is Key. Clin Cancer Res. 5: 1605–6.

Jiang W, Mashayekhi H, Xing B. (2009). Bacterial toxicity comparison between nano- and micro-scaled oxide particles. Environ Pollut. 157(5):1619-25. doi: 10.1016/j.envpol.2008.12.025.

Jo H, Loison F, Hattori H, Silberstein LE, Yu H, Luo HR. (2010). Natural product celastrol destabilizes tubulin heterodimer and facilitates mitotic cell death triggered by microtubule-targeting anti-cancer drugs. PLoS One. 5(4):e10318. doi: 10.1371/journal.pone.0010318.

Justus CR, Leffler N, Ruiz-Echevarria M, Yang LV. (2014). In vitro cell migration and invasion assays. J Vis Exp. (88). doi: 10.3791/51046.

Kain KH, Miller JW, Jones-Paris CR, Thomason RT, Lewis JD, Bader DM, Barnett JV, Zijlstra A. (2014). The chick embryo as an expanding experimental model for cancer and cardiovascular research. Dev Dyn. 243(2):216-28. doi: 10.1002/dvdy.24093.

Kalepua S, Nekkanti V. (2015). Insoluble drug delivery strategies: review of recent advances and business prospects. Acta Pharm Sin B. 5(5): 442–453. doi: 10.1016/j.apsb.2015.07.003.

Kalhori V, Magnusson M, Asghar MY, Pulli I, Törnquist K. (2016). FTY720 (Fingolimod) attenuates basal and sphingosine-1-phosphate-evoked thyroid cancer cell invasion. Endocr Relat Cancer. 23(5):457-68. doi: 10.1530/ERC-16-0050.

Kalluri R, Weinberg RA. (2009). The basics of epithelial-mesenchymal transition. J Clin Invest. 119(6):1420-8. doi: 10.1172/JCI39104.

Kankaanpää P, Paavolainen L, Tiitta S, Karjalainen M, Päivärinne J, Nieminen J, Marjomäki V, Heino J, White DJ. (2012). BioImageXD: an open, general-purpose and high-throughput image-processing platform. Nat Methods. 9(7):683-9. doi: 10.1038/nmeth.2047.

Karjalainen M, Kakkonen E, Upla P, Paloranta H, Kankaanpää P, Liberali P, Renkema GH, Hyypiä T, Heino J, Marjomäki V. (2008). A Raft-derived, Pak1-regulated entry participates in alpha2beta1 integrin-dependent sorting to caveosomes. Mol Biol Cell. 19(7):2857-69. doi: 10.1091/mbc.E07-10-1094.

Karlsson HL, Cronholm P, Gustafsson J, Möller L. (2008). Copper oxide nanoparticles are highly toxic: a comparison between metal oxide nanoparticles and carbon nanotubes. Chem Res Toxicol. 21(9):1726-32. doi: 10.1021/tx800064j.

Karlsson HL, Gustafsson J, Cronholm P, Möller L. (2009). Size-dependent toxicity of metal oxide particles--a comparison between nano- and micrometer size. Toxicol Lett. 188(2):112-8. doi: 10.1016/j.toxlet.2009.03.014.

Kayala MA, Azencott CA, Chen JH, Baldi P. (2011). Learning to predict chemical reactions. J Chem Inf Model. 51(9):2209-22. doi: 10.1021/ci200207y.

Kermi C, Lo Furno E, Maiorano D. (2017). Regulation of DNA Replication in Early Embryonic Cleavages. Genes (Basel). 8(1). pii: E42. doi: 10.3390/genes8010042.

Kerr JF, Wyllie AH, Currie AR. (1972). Apoptosis: a basic biological phenomenon with wide-ranging implications in tissue kinetics. Br J Cancer. 26(4):239-57. doi: 10.1038/bjc.1972.33.

Kettiger H, Sen Karaman D, Schiesser L, Rosenholm JM, Huwyler J. (2015). Comparative safety evaluation of silica-based particles. Toxicol In Vitro. 30(1 Pt B):355-63. doi: 10.1016/j.tiv.2015.09.030.

Kim TY, Son J, Kim KG. (2011). The Recent Progress in Quantitative Medical Image Analysis for Computer Aided Diagnosis Systems. Healthc Inform Res. 17(3): 143–149. doi: 10.4258/hir.2011.17.3.143.

Kimbrell GA. (2009). Governance of nanotechnology and nanomaterials: principles, regulation, and renegotiating the social contract. J Law Med Ethics. 37(4):706-23. doi: 10.1111/j.1748-720X.2009.00442.x.

Kluenker M, Kurch S, Tahir MN, Tremel W. (2018). Bio-nano: Theranostic at Cellular Level. In: Merkus H, Meesters G, Oostra W. (eds) Particles and Nanoparticles in Pharmaceutical Products. AAPS Advances in the Pharmaceutical Sciences Series. 29: 85-170. doi: 10.1007/978-3-319-94174-5_3.

Kou L, Sun J, Zhai Y, He Z. (2013). The endocytosis and intracellular fate of nanomedicines: Implication for rational design. Asian Journal of Pharmaceutical Sciences. 8:1-10. doi: 10.1016/j.ajps.2013.07.001.

Krakowiak J, Zheng X, Patel N, Feder ZA, Anandhakumar J, Valerius K, Gross DS, Khalil AS, Pincus D. (2018). Hsf1 and Hsp70 constitute a two-component feedback loop that regulates the yeast heat shock response. Elife. 7. pii: e31668. doi: 10.7554/eLife.31668.

Kramer N, Walzl A, Unger C, Rosner M, Krupitza G, Hengstschläger M, Dolznig H. (2013). In vitro cell migration and invasion assays. Mutat Res. 752(1):10-24. doi: 10.1016/j.mrrev.2012.08.001.

Kresge CT, Leonowicz ME, Roth WJ, Vartuli JC, Beck JS. (1992). Ordered mesoporous molecular sieves synthesized by a liquid-crystal template mechanism. Nature. 359:710-2. doi: 10.1038/359710a0.

Kroemer G, Galluzzi L, Vandenabeele P, Abrams J, Alnemri ES, Baehrecke EH, Blagosklonny MV, El-Deiry WS, Golstein P, Green DR, Hengartner M, Knight RA, Kumar S, Lipton SA, Malorni W, Nuñez G, Peter ME, Tschopp J, Yuan J, Piacentini M, Zhivotovsky B, Melino G; Nomenclature Committee on Cell Death 2009. (2009). Classification of cell death: recommendations of the Nomenclature Committee on Cell Death 2009. Cell Death Differ. 16(1):3-11. doi: 10.1038/cdd.2008.150.

Kroll A, Pillukat MH, Hahn D, Schnekenburger J. (2009). Current in vitro methods in nanoparticle risk assessment: limitations and challenges. Eur J Pharm Biopharm. 72(2):370-7. doi: 10.1016/j.ejpb.2008.08.009.

Kroll A, Dierker C, Rommel C, Hahn D, Wohlleben W, Schulze-Isfort C, Göbbert C, Voetz M, Hardinghaus F, Schnekenburger J. (2011). Cytotoxicity screening of 23 engineered nanomaterials using a test matrix of ten cell lines and three different assays. Part Fibre Toxicol. 8:9. doi: 10.1186/1743-8977-8-9.

Kue CS, Kamkaew A, Burgess K, Kiew LV, Chung LY, Lee HB. (2016). Small Molecules for Active Targeting in Cancer. Med Res Rev. 36(3):494-575. doi: 10.1002/med.21387.

Kwon S, Singh RK, Perez RA, Abou Neel EA, Kim HW, Chrzanowski W. (2013). Silica-based mesoporous nanoparticles for controlled drug delivery. J Tissue Eng. 4:2041731413503357. doi: 10.1177/2041731413503357.

Landry BD, Leete T, Richards R, Cruz-Gordillo P, Schwartz HR, Honeywell ME, Ren G, Schwartz AD, Peyton SR, Lee MJ. (2018). Tumor-stroma interactions differentially alter drug sensitivity based on the origin of stromal cells. Mol Syst Biol. 14(8):e8322. doi: 10.15252/msb.20188322.

Lane N. (2015). The unseen world: reflections on Leeuwenhoek (1677) 'Concerning little animals'. Phil. Trans. R. Soc. B. doi: 10.1098/rstb.2014.0344.

Leak RK. (2014). Heat shock proteins in neurodegenerative disorders and aging. J Cell Commun Signal. 8(4):293-310. doi: 10.1007/s12079-014-0243-9.

Leamon CP, Low PS. (2001). Folate-mediated targeting: from diagnostics to drug and gene delivery. Drug Discov. Today. 6(1):44-51. doi: 10.1016/S1359-6446(00)01594-4.

Leamon CP, Reddy JA. (2004). Folate-targeted chemotherapy. Adv Drug Deliv Rev. 56(8):1127-41. doi: 10.1016/j.addr.2004.01.008.

Lee EYHP, Muller WJ. (2010a). Oncogenes and Tumor Suppressor Genes. Cold Spring Harb Perspect Biol. 2(10): a003236. doi: 10.1101/cshperspect.a003236

Lee JE, Lee N, Kim H, Kim J, Choi SH, Kim JH, Kim T, Song IC, Park SP, Moon WK, Hyeon T. (2010b). Uniform mesoporous dye-doped silica nanoparticles decorated with multiple magnetite nanocrystals for simultaneous enhanced magnetic resonance imaging, fluorescence imaging, and drug delivery. J Am Chem Soc. 132(2):552-7. doi: 10.1021/ja905793q.

Li J, Ma FK, Dang QF, Liang XG, Chen XG. (2014). Glucose-Conjugated Chitosan Nanoparticles for Targeted Drug Delivery and Their Specific Interaction with Tumor Cells. Front Mater Sci. 8: 363–72. doi: 10.1007/s11706-014-0262-8.

Li Z, Wu X, Li J, Yao L, Sun L, Shi Y, Zhang W, Lin J, Liang D, Li Y. (2012). Antitumor activity of celastrol nanoparticles in a xenograft retinoblastoma tumor model. Int J Nanomedicine. 7:2389-98. doi: 10.2147/IJN.S29945.

Liberti MV, Locasale JW. (2016). The Warburg Effect: How Does it Benefit Cancer Cells? Trends Biochem Sci. 41(3):211-218. doi: 10.1016/j.tibs.2015.12.001.

Lidén G. (2011). The European commission tries to define nanomaterials. Ann Occup Hyg. 55(1):1-5. doi: 10.1093/annhyg/meq092.

Liong M, Lu J, Kovochich M, Xia T, Ruehm SG, Nel AE, Tamanoi F, Zink JI. (2008). Multifunctional inorganic nanoparticles for imaging, targeting, and drug delivery. ACS Nano. 2(5):889-96. doi: 10.1021/nn800072t.

Liu J, Yu M, Zhou C, Zheng J. (2013). Renal clearable inorganic nanoparticles: a new frontier of bionanotechnology. Mater Today. 16(12):477-86. doi: 10.1016/j.mattod.2013.11.003.

Liu Q, Sun Z, Dou Y, Kim JH, Dou SX. (2015). Two-Step Self-Assembly of Hierarchically-Ordered Nanostructures. J Mater Chem. A. 3: 11688–99. doi: 10.1039/c5ta01162k.

Lokman NA, Elder AS, Ricciardelli C, Oehler MK. (2012). Chick chorioallantoic membrane (CAM) assay as an in vivo model to study the effect of newly identified molecules on ovarian cancer invasion and metastasis. Int J Mol Sci. 13(8):9959-70. doi: 10.3390/ijms13089959.

Loveridge C, Tonelli F, Leclercq T, Lim KG, Long JS, Berdyshev E, Tate RJ, Natarajan V, Pitson SM, Pyne NJ, Pyne S. (2010). The sphingosine kinase 1 inhibitor 2-(p-hydroxyanilino)-4-(p-chlorophenyl)thiazole induces proteasomal degradation of sphingosine kinase 1 in mammalian cells. J Biol Chem. 285(50):38841-52. doi: 10.1074/jbc.M110.127993.

Lu F, Wu SH, Hung Y, Mou CY. (2009). Size Effect on Cell Uptake in Well-Suspended, Uniform Mesoporous Silica Nanoparticles. Small. 5(12):1408-13. doi: 10.1002/smll.200900005.

Lunenfeld B, Stratton P. (2013). The clinical consequences of an ageing world and preventive strategies. Best Pract Res Clin Obstet Gynaecol. 27(5):643-59. doi: 10.1016/j.bpobgyn.2013.02.005.

Maacha S, Saule S. (2018). Evaluation of Tumor Cell Invasiveness In Vivo: The Chick Chorioallantoic Membrane Assay. Methods Mol Biol. 1749:71-77. doi: 10.1007/978-1-4939-7701-7_8.

Maghsoodi M. (2015). Role of Solvents in Improvement of Dissolution Rate of Drugs: Crystal Habit and Crystal Agglomeration. Adv Pharm Bull. 5(1): 13–18. doi: 10.5681/apb.2015.002

Mainzer K. (2011). Interdisciplinarity and innovation dynamics. On convergence of research, technology, economy, and society. Poiesis Prax. 7(4): 275–289. doi: 10.1007/s10202-011-0088-8.

Malhotra V, Perry MC. (2003). Classical chemotherapy: mechanisms, toxicities and the therapeutic window. Cancer Biol Ther. 2(4 Suppl 1):S2-4. doi: 10.4161/cbt.199.

Mamaeva V, Niemi R, Beck M, Özliseli E, Desai D, Landor S, Gronroos T, Kronqvist P, Pettersen IK, McCormack E, Rosenholm JM, Lindén M, Sahlgren C. (2016). Inhibiting Notch Activity in Breast Cancer Stem Cells by Glucose Functionalized Nanoparticles Carrying γ-secretase Inhibitors. Mol Ther. 24(5):926-36. doi: 10.1038/mt.2016.42.

Marrison J, Räty L, Marriott P, O'Toole P. (2013). Ptychography--a label free, high-contrast imaging technique for live cells using quantitative phase information. Sci Rep. 3:2369. doi: 10.1038/srep02369.

Matsumura Y, Maeda H. (1986). A new concept for macromolecular therapeutics in cancer chemotherapy: mechanism of tumoritropic accumulation of proteins and the antitumor agent smancs. Cancer Res. 46(12 Pt 1):6387-92.

Mayer MP, Bukau B. (2005). Hsp70 chaperones: cellular functions and molecular mechanism. Cell Mol Life Sci. 62(6):670-84. doi: 10.1007/s00018-004-4464-6.

Maynard AD. (2011). Don't define nanomaterials. Nature. 475(7354):31. doi: 10.1038/475031a.

Meijerman I, Beijnen JH, Schellens JH. (2008). Combined action and regulation of phase II enzymes and multidrug resistance proteins in multidrug resistance in cancer. Cancer Treat Rev 34: 505-520. doi: 10.1016/j.ctrv.2008.03.002.

Micheau O, Lens S, Gaide O, Alevizopoulos K, Tschopp J. (2001). NF-kappaB signals induce the expression of c-FLIP. Mol Cell Biol. 21(16):5299-305. doi: 10.1128/MCB.21.16.5299-5305.2001.

Miller BJ, Cram P, Lynch CF, Buckwalter JA. (2013). Risk factors for metastatic disease at presentation with osteosarcoma: an analysis of the SEER database. J Bone Joint Surg Am. 95(13):e89. doi: 10.2106/JBJS.L.01189.

Miller DM, Thomas SD, Islam A, Muench D, Sedoris K. (2012). c-Myc and cancer metabolism. Clin Cancer Res. 18(20):5546-53. doi: 10.1158/1078-0432.CCR-12-0977.

Mortera R, Vivero-Escoto J, Slowing II, Garrone E, Onida B, Lin VS. (2009). Cell-induced intracellular controlled release of membrane impermeable cysteine from a mesoporous silica nanoparticle-based drug delivery system. Chem Commun (Camb). (22):3219-21. doi: 10.1039/b900559e.

Moubarak RS, Solé C, Pascual M, Gutierrez H, Llovera M, Pérez-García MJ, Gozzelino R, Segura MF, Iglesias-Guimarais V, Reix S, Soler RM, Davies AM, Soriano E, Yuste VJ, Comella JX. (2010). The death receptor antagonist FLIP-L interacts with Trk and is necessary for neurite outgrowth induced by neurotrophins. J Neurosci. 30(17):6094-105. doi: 10.1523/JNEUROSCI.0537-10.2010.

Muller PY, Milton MN. (2012). The determination and interpretation of the therapeutic index in drug development. Nat Rev Drug Discov. 11(10):751-61. doi: 10.1038/nrd3801.

Nagase M, Oto J, Sugiyama S, Yube K, Takaishi Y, Sakato N. (2003). Apoptosis induction in HL-60 cells and inhibition of topoisomerase II by triterpene celastrol. Biosci Biotechnol Biochem. 67(9):1883-7. doi: 10.1271/bbb.67.1883.

Nagata S. (2018). Apoptosis and Clearance of Apoptotic Cells. Annu Rev Immunol. 36:489-517. doi: 10.1146/annurev-immunol-042617-053010. doi: 10.1146/annurev-immunol-042617-053010.

Nakamura T, Yamada Y, Yano K. (2007). Direct synthesis of monodispersed thiol-functionalized nanoporous silica spheres and their application to a colloidal crystal embedded with gold nanoparticles. J Mater Chem 17: 3726–3732. doi: 10.1039/b705209j.

Nakanishi M, Shimada M, Niida H. (2006). Genetic instability in cancer cells by impaired cell cycle checkpoints. Cancer Sci. 97(10):984-9. doi: 10.1111/j.1349-7006.2006.00289.x.

Nam HY, Kwon SM, Chung H, Lee SY, Kwon SH, Jeon H, Kim Y, Park JH, Kim J, Her S, Oh YK, Kwon IC, Kim K, Jeong SY. (2009). Cellular uptake mechanism and intracellular fate of hydrophobically modified glycol chitosan nanoparticles. J Control Release. 135(3):259-67. doi: 10.1016/j.jconrel.2009.01.018.

Nat Methods. (2012). The quest for quantitative microscopy. 9(7):627. doi: 10.1038/nmeth.2102.

Nguyen DX, Bos PD, Massagué J. (2009). Metastasis: from dissemination to organ-specific colonization. Nat Rev Cancer. 9(4):274-84. doi: 10.1038/nrc2622.

Nicoletti I, Migliorati G, Pagliacci MC, Grignani F, Riccardi C. (1991). A rapid and simple method for measuring thymocyte apoptosis by propidium iodide staining and flow cytometry. J Immunol Meth. 139:271-279. doi: 10.1016/0022-1759(91)90198-O.

Nowak-Sliwinska P, Segura T, Iruela-Arispe ML. The chicken chorioallantoic membrane model in biology, medicine and bioengineering. Angiogenesis. 2014 Oct;17(4):779-804. doi: 10.1007/s10456-014-9440-7.

O'Brien ME, Borthwick A, Rigg A, Leary A, Assersohn L, Last K, Tan S, Milan S, Tait D, Smith IE. (2006). Mortality within 30 days of chemotherapy: a clinical governance benchmarking issue for oncology patients. Br J Cancer. 95(12):1632-6. doi: 10.1038/sj.bjc.6603498.

Oh N, Park JH. (2014). Endocytosis and exocytosis of nanoparticles in mammalian cells. Int J Nanomedicine. 9 Suppl 1:51-63. doi: 10.2147/IJN.S26592.

Orrenius S, Nicotera P, Zhivotovsky B. (2011). Cell Death Mechanisms and Their Implications in Toxicology. Toxicol Sci. 119(1):3-19. doi: 10.1093/toxsci/kfq268.

O'Shannessy DJ, Somers EB, Wang LC, Wang H, Hsu R. (2015). Expression of folate receptors alpha and beta in normal and cancerous gynecologic tissues: correlation of expression of the beta isoform with macrophage markers. J Ovarian Res. 8:29. doi: 10.1186/s13048-015-0156-0.

Ossowski L, Reich E. (1980). Experimental model for quantitative study of metastasis. Cancer Res. 40(7):2300-9.

Owens DE 3rd, Peppas NA. (2006). Opsonization, biodistribution, and pharmacokinetics of polymeric nanoparticles. Int J Pharm. 307(1):93-102. doi: 10.1016/j.ijpharm.2005.10.010.

Oxtoby NP, Alexander DC; EuroPOND consortium. (2017). Imaging plus X: multimodal models of neurodegenerative disease. Curr Opin Neurol. 30(4):371-379. doi: 10.1097/WCO.0000000000000460.

Ozaki T, Nakagawara A. (2011). Role of p53 in Cell Death and Human Cancers. Cancers (Basel). 3(1): 994–1013. doi: 10.3390/cancers3010994.

Paaby AB, Rockman MV. (2012). The many faces of pleiotropy. Trends Genet. 29(2):66-73. Chemical tuning enhances both potency toward nrf2 and in vitro therapeutic index of triterpenoids. Toxicol Sci. 140(2):462-9. doi: 10.1093/toxsci/kfu080.

Paatero I, Casals E, Niemi R, Özliseli E, Rosenholm JM, Sahlgren C. (2017). Analyses in zebrafish embryos reveal that nanotoxicity profiles are dependent on surface-functionalization controlled penetrance of biological membranes. Sci Rep. 7(1):8423. doi: 10.1038/s41598-017-09312-z.

Padma VV. (2015). An overview of targeted cancer therapy. Biomedicine (Taipei). 5(4):19. doi: 10.7603/s40681-015-0019-4.

Palumbo MO, Kavan P, Miller WH Jr, Panasci L, Assouline S, Johnson N, Cohen V, Patenaude F, Pollak M, Jagoe RT, Batist G. (2013). Systemic cancer therapy: achievements and challenges that lie ahead. Front Pharmacol. 4:57. doi: 10.3389/fphar.2013.00057.

Papaccio F, Paino F, Regad T, Papaccio G, Desiderio V, Tirino V. (2017). Concise Review: Cancer Cells, Cancer Stem Cells, and Mesenchymal Stem Cells: Influence in Cancer Development. Stem Cells Transl Med. 6(12):2115-2125. doi: 10.1002/sctm.17-0138.

Park J, Park J, Pei Y, Xu J, Yeo Y. (2016). Pharmacokinetics and biodistribution of recently-developed siRNA nanomedicines. Adv Drug Deliv Rev. 104:93-109. doi: 10.1016/j.addr.2015.12.

Parker N, Turk MJ, Westrick E, Lewis JD, Low PS, Leamon CP. (2005). Folate receptor expression in carcinomas and normal tissues determined by a quantitative radioligand binding assay. Anal Biochem. 338(2):284-93. doi: 10.1016/j.ab.2004.12.026.

Paulos CM, Reddy JA, Leamon CP, Turk MJ, Low PS. (2004). Ligand binding and kinetics of folate receptor recycling in vivo: impact on receptor-mediated drug delivery. Mol Pharmacol. 66(6):1406-14. doi: 10.1124/mol.104.003723.

Pernet C. (2016). Null hypothesis significance testing: a short tutorial. F1000Res. 4:621. doi: 10.12688/f1000research.6963.3

Perreault F, Popovic R, Dewez D. (2014). Different toxicity mechanisms between bare and polymer-coated copper oxide nanoparticles in Lemna gibba. Environ Pollut. 185:219-27. doi: 10.1016/j.envpol.2013.10.027.

Pillai G. (2014). Nanomedicines for Cancer Therapy: An Update of FDA Approved and Those under Various Stages of Development. SOJ Pharmacy & Pharmaceutical Sciences. 1. doi: 10.15226/2374-6866/1/2/00109.

Piras R, Piras MM. (1975). Changes in Microtubule Phosphorylation during Cell Cycle of HeLa Cells. Proc Natl Acad Sci U S A. 72(3):1161-5. doi: 10.1073/pnas.72.3.1161.

Popat A, Hartono SB, Stahr F, Liu J, Qiao SZ, Qing Max Lu G. (2011). Mesoporous silica nanoparticles for bioadsorption, enzyme immobilisation, and delivery carriers. Nanoscale. 3(7):2801-18. doi: 10.1039/c1nr10224a.

Popat A, Ross BP, Liu J, Jambhrunkar S, Kleitz F, Qiao SZ. (2012). Enzyme-responsive controlled release of covalently bound prodrug from functional mesoporous silica nanospheres. Angew Chem Int Ed Engl. 51(50):12486-9. doi: 10.1002/anie.201206416.

Porta F, Lamers GE, Morrhayim J, Chatzopoulou A, Schaaf M, den Dulk H, Backendorf C, Zink JI, Kros A. (2013). Folic acid-modified mesoporous silica nanoparticles for cellular and nuclear targeted drug delivery. Adv Healthc Mater. 2(2):281-6. doi: 10.1002/adhm.201200176.

Preissner S, Dunkel M, Hoffmann MF, Preissner SC, Genov N, Rong WW, Preissner R, Seeger K. (2012). Drug cocktail optimization in chemotherapy of cancer. PLoS One. 7(12):e51020. doi: 10.1371/journal.pone.0051020.

Ramirez LY, Huestis SE, Yap TY, Zyzanski S, Drotar D, Kodish E. (2009). Potential Chemotherapy Side Effects What Do Oncologists Tell Parents? Pediatr Blood Cancer. 52(4): 497–502. doi: 10.1002/pbc.21835.

Ray P, White RR. (2010). Aptamers for Targeted Drug Delivery. Pharmaceuticals (Basel). 3(6): 1761–1778. doi: 10.3390/ph3061761.

Ridler TW, Calvard S. (1978). Picture thresholding using an iterative selection method. IEEE Trans Syst. Man Cybern. 8, 630–632. doi: 10.1109/TSMC.1978.4310039.

Riihimäki M, Thomsen H, Hemminki A, Sundquist K, Hemminki K. (2013). Comparison of survival of patients with metastases from known versus unknown primaries: survival in metastatic cancer. BMC Cancer. 13:36. doi: 10.1186/1471-2407-13-36.

Rivera Gil P, Hühn D, del Mercato LL, Sasse D, Parak WJ. (2010). Nanopharmacy: Inorganic nanoscale devices as vectors and active compounds. Pharmacol Res. 62(2):115-25. doi: 10.1016/j.phrs.2010.01.009.

Robergs RA. (2017). Lessons from Popper for science, paradigm shifts, scientific revolutions and exercise physiology. BMJ Open Sport Exerc Med. 3(1):e000226. doi:10.1136/bmjsem-2017-000226.

Rosenholm JM, Penninkangas A, Lindén M. (2006). Amino-functionalization of large-pore mesoscopically ordered silica by a one-step hyperbranching polymerization of a surface-grown polyethyleneimine. Chem Commun (Camb). (37):3909-11. doi: 10.1039/b607886a.

Rosenholm JM, Lindén M. (2008a). Towards establishing structure-activity relationships for mesoporous silica in drug delivery applications. J Control Release. 128(2):157-64. doi: 10.1016/j.jconrel.2008.02.013.

Rosenholm JM, Duchanoy A, Lindén M. (2008b). Hyperbranching surface polymerization as a tool for preferential functionalization of the outer surface of mesoporous silica. Chem. Mater. 20:1126-33. doi: 10.1021/cm7021328.

Rosenholm JM, Meinander A, Peuhu E, Niemi R, Eriksson JE, Sahlgren C, Lindén M. (2009). Targeting of porous hybrid silica nanoparticles to cancer cells. ACS Nano. 3(1):197-206. doi: 10.1021/nn800781r.

Rosenholm J, Sahlgren C, Lindén M. (2010a). Cancer-Cell Targeting and Cell-Specific Delivery by Mesoporous Silica Nanoparticles. J Mater Chem. 20: 2707–13. doi: 10.1039/b920076b.

Rosenholm JM, Sahlgren C, Lindén M. (2010b). Towards Multifunctional, Targeted Drug Delivery Systems Using Mesoporous Silica Nanoparticles--Opportunities & Challenges. Nanoscale. 2(10):1870-83. doi: 10.1039/c0nr00156b.

Rueden CT, Schindelin J, Hiner MC, DeZonia BE, Walter AE, Arena ET, Eliceiri KW. (2017). ImageJ2: ImageJ for the next generation of scientific image data. BMC Bioinformatics. 18(1):529. doi: 10.1186/s12859-017-1934-z.

Safa AR. (2012). c-FLIP, a master anti-apoptotic regulator. Exp Oncol. 34(3):176-84.

Salminen A, Lehtonen M, Paimela T, Kaarniranta K. (2010). Celastrol: Molecular targets of Thunder God Vine. Biochem Biophys Res Commun. 394(3):439-42. doi: 10.1016/j.bbrc.2010.03.050.

Samadi Moghaddam M, Heiny M, Shastri VP. (2015). Enhanced Cellular Uptake of Nanoparticles by Increasing the Hydrophobicity of Poly(lactic Acid) through Copolymerization with Cell-Membrane-Lipid Components. Chem Commun (Camb). 51(78):14605-8. doi: 10.1039/c5cc06397c.

Sanberg PR, Gharib M, Harker PT, Kaler EW, Marchase RB, Sands TD, Arshadi N, Sarkara S. (2014). Changing the academic culture: Valuing patents and commercialization toward tenure and career advancement. Proc Natl Acad Sci U S A. 111(18): 6542–6547. doi: 10.1073/pnas.1404094111.

Sanhai WR, Sakamoto JH, Canady R, Ferrari M. (2008). Seven challenges for nanomedicine. Nat Nanotechnol. 3(5):242-4. doi: 10.1038/nnano.2008.114.

Savjani KT, Gajjar AK, Savjani JK. (2012). Drug solubility: importance and enhancement techniques. ISRN Pharm. 2012:195727. doi: 10.5402/2012/195727.

Schuhmacher A, Gassmann O, Hinder M. (2016). Changing R&D models in research-based pharmaceutical companies. J Transl Med. 14: 105. doi: 10.1186/s12967-016-0838-4.

Schulte PA, Salamanca-Buentello F. (2007). Ethical and scientific issues of nanotechnology in the workplace. Cien Saude Colet. 12(5):1319-32. doi: 10.1289/ehp.9456.

Seigneuric R, Markey L, Nuyten DS, Dubernet C, Evelo CT, Finot E, Garrido C. (2010). From nanotechnology to nanomedicine: applications to cancer research. Curr Mol Med. 10(7):640-52. doi: 10.2174/156652410792630634.

Seligmann J, Twelves C. (2013). Tubulin: an example of targeted chemotherapy. Future Med Chem. 5(3):339-52. doi: 10.4155/fmc.12.217.

Shang L, Nienhaus K, Nienhaus GU. (2014). Engineered nanoparticles interacting with cells: size matters. J Nanobiotechnology. 12:5. doi: 10.1186/1477-3155-12-5.

Shen J, Putt KS, Visscher DW, Murphy L, Cohen C, Singhal S, Sandusky G, Feng Y, Dimitrov DS, Low PS. (2015). Assessment of folate receptor-β expression in human neoplastic tissues. Oncotarget. 6(16): 14700–14709. doi: 10.18632/oncotarget.3739.

Shrader-Frechette K. (2007). Nanotoxicology and Ethical Conditions for Informed Consent. NanoEthics. 1(1):47-56. doi: 10.1007/s11569-007-0003-x.

Shuchman M. (2018). Obtaining funding an age-old problem for young researchers with novel ideas. CMAJ. 190(16): E516–E517. doi: 10.1503/cmaj.109-5583.

Sonoke S, Ueda T, Fujiwara K, Kuwabara K, Yano J. (2011). Galactose-Modified Cationic Liposomes as a Liver-Targeting Delivery System for Small Interfering RNA. Biol Pharm Bull. 34(8):1338-42. doi: 10.1248/bpb.34.1338.

Sotiriou S, Koletsas N, Koletsa T, Touloupidis S, Lambropoulou M. (2017). Thyroid transcription factor-1 expression in invasive and non-invasive urothelial carcinomas. Hippokratia. 21(3):154-157.

Souza TGF, V. S. T. Ciminelli VST, Mohallem NDS. (2016). A comparison of TEM and DLS methods to characterize size distribution of ceramic nanoparticles. J. Phys.: Conf. Ser. 733 012039. doi: 10.1088/1742-6596/733/1/012039.

Sriraman SK, Aryasomayajula B, Torchilin VP. (2014). Barriers to Drug Delivery in Solid Tumors. Tissue Barriers. 2:e29528. doi: 10.4161/tisb.29528.

Srivastava V, Gusain D, Sharma YC. (2015). Critical Review on the Toxicity of Some Widely Used Engineered Nanoparticles. Ind. Eng. Chem. Res. 54(24): 6209-33. doi: 10.1021/acs.iecr.5b01610.

Steichen SD, Caldorera-Moore M, Peppas NA. (2013). A review of current nanoparticle and targeting moieties for the delivery of cancer therapeutics. Eur J Pharm Sci. 48(3):416-27. doi: 10.1016/j.ejps.2012.12.006.

Stephan P. (2012a). How Economics Shapes Science. Boston, MA: Harvard University Press. doi: 10.1111/1475-4932.12480.

Stephan P. (2012b). Research efficiency: Perverse incentives. Nature. 484(7392):29-31. doi: 10.1038/484029a.

Sudhakar A. (2009). History of Cancer, Ancient and Modern Treatment Methods. J Cancer Sci Ther. 1(2): 1–4. doi: 10.4172/1948-5956.100000e2.

Sukumaran P, Löf C, Kemppainen K, Kankaanpää P, Pulli I, Näsman J, Viitanen T, Törnquist K. (2012). Canonical transient receptor potential channel 2 (TRPC2) as a major regulator of calcium homeostasis in rat thyroid FRTL-5 cells: importance of protein kinase C δ (PKCδ) and stromal interaction molecule 2 (STIM2). J Biol Chem. 287(53):44345-60. doi: 10.1074/jbc.M112.374348.

Sun J, Yu X1, Wang C, Yu C, Li Z, Nie W, Xu X, Miao X, Jin X. (2017a). RIP-1/c-FLIPL Induce Hepatic Cancer Cell Apoptosis Through Regulating Tumor Necrosis Factor-Related Apoptosis-Inducing Ligand (TRAIL). Med Sci Monit. 23:1190-1199. doi: 10.12659/msm.899727.

Sun J, Wei Q, Zhou Y, Wang J, Liu Q, Xu H. (2017b). A systematic analysis of FDA-approved anticancer drugs. BMC Syst Biol. 11(Suppl 5): 87. doi: 10.1186/s12918-017-0464-7.

Sun R, Wang W, Wen Y, Zhang X. (2015). Recent Advance on Mesoporous Silica Nanoparticles-Based Controlled Release System: Intelligent Switches Open up New Horizon. Nanomaterials (Basel). 5(4):2019-2053. doi: 10.3390/nano5042019.

Thomas M, Finnegan CE, Rogers KM, Purcell JW, Trimble A, Johnston PG, Boland MP. (2004). STAT1: a modulator of chemotherapy-induced apoptosis. Cancer Res. 64(22):8357-64. doi: 10.1158/0008-5472.CAN-04-1864.

Thorn CF, Oshiro C, Marsh S, Hernandez-Boussard T, McLeod H, Klein TE, Altman RB. (2011). Doxorubicin pathways: pharmacodynamics and adverse effects. Pharmacogenet Genomics. 21(7):440-6. doi: 10.1097/FPC.0b013e32833ffb56.

Tohme S, Simmons RL, Tsung A. (2017). Surgery for Cancer: A Trigger for Metastases. Cancer Res. 77(7):1548-1552. doi: 10.1158/0008-5472.CAN-16-1536.

Trott A, West JD, Klaić L, Westerheide SD, Silverman RB, Morimoto RI, Morano KA. (2008). Activation of heat shock and antioxidant responses by the natural product celastrol: transcriptional signatures of a thiol-targeted molecule. Mol Biol Cell. 19(3):1104-12. doi: 10.1091/mbc.e07-10-1004.

Tsai CP, Chen CY, Hung Y, Chang FH, Mou CY. (2009). Monoclonal Antibody-Functionalized Mesoporous Silica Nanoparticles (MSN) for Selective Targeting Breast Cancer Cells. J Mater Chem. 19: 5737–43. doi: 10.1039/b905158a.

Underwood S, Gorham JM. (2017). Challenges and approaches for particle size analysis on micrographs of nanoparticles loaded onto textile surfaces. Special Publication (NIST SP) - 1200-22. doi: 10.6028/NIST.SP.1200-22.

Upla P, Marjomäki V, Kankaanpää P, Ivaska J, Hyypiä T, Van Der Goot FG, Heino J. (2004). Clustering induces a lateral redistribution of alpha 2 beta 1 integrin from membrane rafts to caveolae and subsequent protein kinase C-dependent internalization. Mol Biol Cell. 15(2):625-36. doi: 10.1091/mbc.e03-08-0588.

Urbano PC, Soccol VT, Azevedo VF. (2014). Apoptosis and the FLIP and NF-kappa B proteins as pharmacodynamic criteria for biosimilar TNF-alpha antagonists. Biologics. 8:211-20. doi: 10.2147/BTT.S57253.

Vallet-Regí M, Balas F, Arcos D. (2007). Mesoporous materials for drug delivery. Angew Chem Int Ed Engl. 46(40):7548-58. doi: 10.1002/anie.200604488.

Vallet-Regí M, Colilla M, Izquierdo-Barba I, Manzano M. (2017). Mesoporous Silica Nanoparticles for Drug Delivery: Current Insights. Molecules. 23(1). pii: E47. doi: 10.3390/molecules23010047.

Van Grinsven MJ, van Ginneken B, Hoyng CB, Theelen T, Sanchez CI. (2016). Fast Convolutional Neural Network Training Using Selective Data Sampling: Application to Hemorrhage Detection in Color Fundus Images. IEEE Trans Med Imaging. 35(5):1273-1284. doi: 10.1109/TMI.2016.2526689.

Venditto VJ, Szoka FC Jr. (2013). Cancer nanomedicines: so many papers and so few drugs!. Adv Drug Deliv Rev. 65(1):80-8. doi: 10.1016/j.addr.2012.09.038.

Verma A, Stellacci F. (2010). Effect of Surface Properties on Nanoparticle–Cell Interactions. Small. 6(1):12-21. doi: 10.1002/smll.200901158.

Vivero-Escoto JL, Slowing II, Trewyn BG, Lin VS. (2010). Mesoporous silica nanoparticles for intracellular controlled drug delivery. Small. 6(18):1952-67. doi: 10.1002/smll.200901789.

von Haartman E, Lindberg D, Prabhakar N, Rosenholm JM. (2016). On the intracellular release mechanism of hydrophobic cargo and its relation to the biodegradation behavior of mesoporous silica nanocarriers. Eur J Pharm Sci. 95:17-27. doi: 10.1016/j.ejps.2016.06.001.

Wagner V, Dullaart A, Bock AK, Zweck A. (2006). The emerging nanomedicine landscape. Nat Biotechnol. 24(10):1211-7. doi: 10.1038/nbt1006-1211.

Wan Y, Zhao D. (2007). On the Controllable Soft-Templating Approach to Mesoporous Silicates. Chem Rev. 107(7):2821-60. doi: 10.1021/cr068020s.

Wang S. (2009). Ordered Mesoporous Materials for Drug Delivery. Microporous Mesoporous Mater. 117: 1–9. doi: 10.1016/j.micromeso.2008.07.002.

Wang X, Chen W, Zeng W, Bai L, Tesfaigzi Y, Belinsky SA, Lin Y. (2008). Akt-mediated eminent expression of c-FLIP and Mcl-1 confers acquired resistance to TRAIL-induced cytotoxicity to lung cancer cells. Mol Cancer Ther. 7(5):1156-63. doi: 10.1158/1535-7163.

Wang Y, Huang HY, Yang L, Zhang Z, Ji H. (2016). Cetuximab-Modified Mesoporous Silica Nano-Medicine Specifically Targets EGFR-Mutant Lung Cancer and Overcomes Drug Resistance. Sci Rep. 6:25468. doi: 10.1038/srep25468.

Weber CJ, Müller S, Safley SA, Gordon KB, Amancha P, Villinger F, Camp VM, Lipowska M, Sharma J, Müller C, Schibli R, Low PS, Leamon CP, Halkar RK. (2013). Expression of functional folate receptors by human parathyroid cells. Surgery. 154(6):1385-93; discussion 1393. doi: 10.1016/j.surg.2013.06.045.

Weibel D, Jovanovic ZR, Gálvez E, Steinfeld A. (2014). Mechanism of Zn Particle Oxidation by H2O and CO2 in the Presence of ZnO. Chem Mater. 26(22): 6486–6495. doi: 10.1021/cm503064f.

Westerheide SD, Bosman JD, Mbadugha BN, Kawahara TL, Matsumoto G, Kim S, Gu W, Devlin JP, Silverman RB, Morimoto RI. (2004). Celastrols as Inducers of the Heat Chock Response and Cytoprotection. J Biol Chem. 279(53):56053-60. doi: 10.1074/jbc.M409267200.

Wicki A, Witzigmann D, Balasubramanian V, Huwyler J. (2015). Nanomedicine in cancer therapy: challenges, opportunities, and clinical applications. J Control Release. 200:138-57. doi: 10.1016/j.jconrel.2014.12.030.

Wilbrandt W. (1935). THE SIGNIFICANCE OF THE STRUCTURE OF A MEMBRANE FOR ITS SELECTIVE PERMEABILITY. J Gen Physiol. 18(6): 933–965. doi:10.1085/jgp.18.6.933.

Wong PT, Choi SK. (2015). Mechanisms and implications of dual-acting methotrexate in folate-targeted nanotherapeutic delivery. Int J Mol Sci. 16(1):1772-90. doi: 10.3390/ijms16011772.

Xiao D, Jia HZ, Zhang J, Liu CW, Zhuo RX, Zhang XZ. (2014). A dual-responsive mesoporous silica nanoparticle for tumor-triggered targeting drug delivery. Small. 10(3):591-8. doi: 10.1002/smll.201301926.

Yamashiro M, Hasegawa H, Matsuda A, Kinoshita M, Matsumura O, Isoda K, Mitarai T. (2013). A case of water intoxication with prolonged hyponatremia caused by excessive water drinking and secondary SIADH. Case Rep Nephrol Urol. 3(2):147-52. doi: 10.1159/000357667.

Yan L, Rosen N, Arteaga C. (2011). Targeted cancer therapies. Chin J Cancer. 30(1): 1–4. doi: 10.5732/cjc.010.10553

Yeh WC, Itie A, Elia AJ, Ng M, Shu HB, Wakeham A, Mirtsos C, Suzuki N, Bonnard M, Goeddel DV, Mak TW. (2000). Requirement for Casper (c-FLIP) in regulation of death receptor-induced apoptosis and embryonic development. Immunity. 12(6):633-42. doi: 10.1016/S1074-7613(00)80214-9.

Yu X, Trase I, Ren M, Duval K, Guo X, Chen Z. (2016). Design of Nanoparticle-Based Carriers for Targeted Drug Delivery. J Nanomater. 2016:1087250. doi: 10.1155/2016/1087250.

Yuan L, Chen W, Hu J, Zhang JZ, Yang D. (2013). Mechanistic study of the covalent loading of paclitaxel via disulfide linkers for controlled drug release. Langmuir. 29(2):734-43. doi: 10.1021/la304324r.

Yue ZG, Wei W, Lv PP, Yue H, Wang LY, Su ZG, Ma GH. (2011). Surface Charge Affects Cellular Uptake and Intracellular Trafficking of Chitosan-Based Nanoparticles. Biomacromolecules. 12(7):2440-6. doi: 10.1021/bm101482r.

Zeisser-Labouèbe M, Delie F, Gurny R, Lange N. (2009). Screening of nanoparticulate delivery systems for the photodetection of cancer in a simple and cost-effective model. Nanomedicine (Lond). 4(2):135-43. doi: 10.2217/17435889.4.2.135.

Zhang F, Stephan SB, Ene CI, Smith TT, Holland EC, Stephan MT. (2018). Nanoparticles That Reshape the Tumor Milieu Create a Therapeutic Window for Effective T-cell Therapy in Solid Malignancies. Cancer Res. 78(13):3718-3730. doi: 10.1158/0008-5472.CAN-18-0306.

Zhang Y, Yang JM. (2013). Altered energy metabolism in cancer: a unique opportunity for therapeutic intervention. Cancer Biol Ther. 14(2):81-9. doi: 10.4161/cbt.22958.

Zhou Y, Quan G, Wu Q, Zhang X, Niu B1, Wu B1, Huang Y, Pan X1, Wu C. (2018). Mesoporous silica nanoparticles for drug and gene delivery. Acta Pharm Sin B. 8(2):165-177. doi: 10.1016/j.apsb.2018.01.007.

Zhu X, Zhu L, Chen Y, Tian S. (2008). Acute toxicities of six manufactured nanomaterial suspensions to Daphnia magna. J. Nanopart. Res. 11(1):67-75. doi: 10.1007/s11051-008-9426-8.

Zhu X, Wang J, Zhang X, Chang Y, Chen Y. (2010). Trophic transfer of TiO2 nanoparticles from daphnia to zebrafish in a simplified freshwater food chain. Chemosphere. 79(9):928-33. doi: 10.1016/j.chemosphere.2010.03.022.

Zijlstra A, Mellor R, Panzarella G, Aimes RT, Hooper JD, Marchenko ND, Quigley JP. (2002). A quantitative analysis of rate-limiting steps in the metastatic cascade using human-specific real-time polymerase chain reaction. Cancer Res. 62:7083–7092.

Erik Niemelä

Nanoparticles as Targeting System for Cancer Treatment

– From idea towards reality –

This thesis focuses on the development of innovative drug delivery systems that could be used in the future to fight cancer. This is done in conjunction with developing imaging modalities for detecting the drug efficacy in the target cells. By exploiting the increased metabolism of cancer cells and their high replication rate, it was possible to design mesoporous silica nanoparticles (MSNs) for targeted drug delivery. This thesis reports successful targeting of cancer cells utilizing glucose motifs and folic acid as targeting ligands on the carrier system, which was loaded with a potent natural compound named celastrol. Sugar decorated celastrol-loaded MSNs could be used as a first line of defense against cancers, as most of the human tumors has an increased metabolic rate compared to healthy tissues and would therefore specifically internalize our proposed particles in higher amounts gaining enhanced drug efficacy. In addition, this thesis shows the potential use of a multi-drug loaded MSNs for achieving synergistic anti-cancerous and anti-invasive efficacy in thyroid cancer cells with lower off-target effects compared to the freely administered drug cocktail. Taken together, these findings function as an academic proof of concept demonstrating that it is possible for targeted drug delivery and enhanced drug efficacy utilizing functionalized mesoporous silica nanoparticles that could be used for further development.

Åbo Akademi University Press | ISBN 978-952-12-3854-3